

# **Effect of Short Chain Fatty Acids and Sodium Chloride on Immune Cell-mediated Cardiovascular Health**

Inaugural thesis presented to the Faculty of Mathematics and Natural Sciences of Heinrich Heine University Düsseldorf for the degree of Doctor of Natural Sciences

**Mina Gadelrab Botros Yakoub**

From Luxor Qena, Egypt. 31/01/1990

Düsseldorf, July 2020

From the Department of Nephrology, University Hospital of Düsseldorf  
at the Heinrich Heine University Düsseldorf

Published by permission of the  
Faculty of Mathematics and Natural Sciences at  
Heinrich Heine University Düsseldorf

Supervisor: PD Dr Johannes Stegbauer  
Co-supervisor: Prof. Dr Jürgen Scheller

Date of the oral examination:

## **Statutory Declaration**

I declare under oath that I have produced my thesis independently and without any undue assistance by third parties under consideration of the 'Principles for the Safeguarding of Good Scientific Practice at Heinrich Heine University Düsseldorf'

Düsseldorf,

Mina Yakoub

# Table of Content

<b>Abbreviations</b> .....	<b>7</b>
<b>1 Summary</b> .....	<b>10</b>
<b>2 Introduction</b> .....	<b>12</b>
Cardiovascular diseases .....	12
Impact of immune cells on CVD .....	13
Atherosclerosis.....	16
Aortic abdominal aneurysm (AAA) .....	18
Role of Angiotensin II (Ang II) in atherosclerosis and aneurysm .....	19
Cardiovascular diseases and diet .....	19
Part I: Short chain fatty acid (SCFA) .....	20
Part II: Salt intake .....	22
The aim of the study .....	22
<b>3 Materials and Methods</b> .....	<b>23</b>
Experimental mice .....	23
Animal models .....	23
Osmotic minipumps preparation and implantation .....	24
Assessment of the AAA and inflammation by MRI .....	25
PFCs formation, administration and F signal assessment.....	27
Blood pressure measurements.....	28
Blood samples withdrawal and dissection of the aorta, the aortic arch, and other organs .....	28
Tissue fixation and Paraffin embedding .....	28
Paraffin removal and dewaxing .....	29
Immunohistochemistry of brachiocephalic artery.....	29
Movat staining: .....	29
CD3 and F4/80 staining:.....	30
Sirius red/Fast green staining of heart sections: .....	30
Oil Red O staining (ORO) for the aortas:.....	31
Flow cytometry .....	31
Plasma Cholesterols and Triglycerides measurements .....	36
Isolation of murine splenic naïve CD8 T-cells and their stimulation for differentiation .....	36
mRNA quantification and assessment by qPCR.....	37
Isolated kidney perfusion.....	40
Assessment of vascular stiffness by Single cell atomic Spectroscopy .....	40

Computational analysis.....	41
Statistical analysis .....	41
<b>4 Results .....</b>	<b>42</b>
Part I: Effect of short chain fatty acids on Atherosclerosis.....	42
C3 increased significantly the survival rate of the Ang II infused mice .....	42
C3 did not change the body weight or the lipid profile .....	42
C3 reduced the deposition of atherosclerosis in the aortas.....	43
C3 reduced the stenosis in the brachiocephalic artery. ....	44
Immune cells infiltration and distribution in the aorta were confirmed by immunohistochemical imaging of the brachiocephalic artery .....	45
C3 decreased the number of immune cells infiltrated in the aortas.....	46
C3 modulated the splenic immune cells signature .....	47
C3 reduced cardiac hypertrophy and fibrosis.....	49
C3 improved Ang II-induced heart damage .....	50
C3 decreased the induced hypertension .....	51
C3 induced vasorelaxation in the isolated perfused kidneys .....	52
Short term treatment of C3 decreases aortic stiffness.....	52
Part II: Effect of high salt intake on Abdominal Aortic Aneurysm .....	53
Salt intake decreased the survival of the ApoE -/- mice after Ang II infusion .....	53
MRI scans were established to visualize aneurysm .....	53
Salt pre-treatment increased the incidence of AAA.....	54
Salt pre-treatment exacerbated the pathological status of AAA.....	55
ApoE-/- mice which had an aneurysm in the salt pre-treated group showed higher 19F signal than the corresponding mice in the control group .....	57
Salt pre-treatment increased the inflammatory cytokines in the aortic tissue.....	58
Salt pre-treatment increased the number of T-cells embedded in the aortic tissue and the surrounding Perivascular adipose tissue (PVAT) .....	59
Salt pre-treatment increased the number of splenic IL17/INF $\gamma$ double producing CD8 T-cells in vivo but not other T-cells in the salt pre-treated mice .....	61
Salt pre-treatment induced polarization of splenic CD8 naïve T-cells <i>in vitro</i> .....	62
The abdominal aortas of the salt pre-treated mice had a higher number of macrophages compared to the control group. ....	62
Salt pre-treatment increased the number of neutrophils infiltrated in the abdominal aorta of salt pre-treated mice .....	63
Neutrophil elastase but not metalloprotease relative expression was higher in the aortas of the salt pre-treated mice .....	63
Salt pre-treatment increased the breakdown of the elastic fibers in the aorta.....	64

<b>5 Discussion</b> .....	<b>66</b>
Part I: Effect of short chain fatty acids on Atherosclerosis.....	66
Part II: Effect of high salt intake on Abdominal Aortic Aneurysm .....	71
<b>6 Conclusion</b> .....	<b>77</b>
<b>7 References</b> .....	<b>78</b>
<b>8 Acknowledgment</b> .....	<b>97</b>

# Abbreviations

AAA: Abdominal Aortic Aneurysm

AFM: Atomic Force Microscopy

Ang II: Angiotensin II

ANP: Atrial Natriuretic Peptide

APC: Antigen Presenting Cell

ApoE<sup>-/-</sup>: Apolipoprotein knock-out

BNP: Brain Natriuretic Peptide

C3: Propionate

cDNA: Complementary Deoxyribonucleic Acid

CT: Threshold Cycle

CVD: Cardiovascular diseases

DNA: Deoxyribonucleic acid

ECM: Extracellular Matrix

FCS: Fetal Calf Serum

FFPE: Formalin-Fixed Paraffin-Embedded

GAPDH: Glyceraldehyde 3-phosphate dehydrogenase

gDNA: Genomic Deoxyribonucleic Acid

HBSS: Hank's Balanced Salt Solution

HDAC: Histone Deacetylase

HDL: High Density Lipoprotein

I.V.: Intravenous

IFN $\gamma$ : Interferon gamma

IL17: Interleukin 17

IVC: Inferior Vena Cava  
LDL: Low density Lipoprotein  
MEM: Minimum Essential Medium  
MHC: Major Histocompatibility Complex  
MRI: Magnetic Resonance Imaging  
mRNA: messenger Ribonucleic acid  
NaCl: Sodium Chloride, salt  
NADH: Nicotinamide Adenine Dinucleotide Hydrogen  
NEAA: Non-Essential Amino Acid  
NK: Natural killer  
OD: Optical Density  
ORO: Oil Red O  
PBS: Phosphate Buffer Solution  
PCR: Polymerase Chain Reaction  
PEEK: Polyether Ether Ketone  
PFA: Paraformaldehyde  
PFC: Perfluorocarbon  
PVAT: Perivascular Adipose Tissue  
RARE: Rapid Acquisition with Relaxation Enhancement  
RNA: Ribonucleic Acid  
ROS: Reactive Oxygen Species  
RT: Room Temperature  
SBP: Systolic Blood pressure  
SCFA: Short Chain Fatty Acid  
SMC: Smooth muscle cell  
TGF $\beta$ : Transforming Growth Factor Beta  
TNF $\alpha$ : Tumour Necrosis Factor Alpha

T<sub>reg</sub>: Regulatory T-cells

VEGF: Vascular endothelial growth factor

VSMC: Vascular Smooth Muscle Cell

WHO: World Health Organization

# 1 Summary

Cardiovascular diseases such as atherosclerosis and aneurysm remain to be the leading cause of morbidity and mortality worldwide. The main risk factors for the development of atherosclerosis and aneurysm are hypertension and hyperlipidemia causing vascular injury. In this context, vascular injury is largely mediated by immune cells. Thus, either a hypertensive stimulus like angiotensin II (Ang II) or hyperlipidemia causes activation of proinflammatory T cells and macrophages infiltrating into the vasculature and the perivascular fat to cause endothelial dysfunction, inflammation, apoptosis, remodeling, extracellular matrix degeneration, and atherosclerotic plaque development. Nutrition factors have shown to influence the microbiome of the gut and thereby vascular diseases by modulating the immune response. Thus, the composition and production of bacterial metabolites resorbed and distributed in the circulation can affect the immune system and cardiovascular function. Here, we studied the immune-mediated effect of short chain fatty acids (SCFA) and salt, two important nutrition factors on vascular disease.

In part I, we investigated the effect of propionate (C3), one of the most important SCFAs, on Ang II-induced atherosclerosis. SCFA are produced by the gut microbiome as a result of fiber fermentation and have been shown to affect the immune response of the host. Here, we demonstrated that chronic C3 treatment has a pronounced anti-atherosclerotic effect in Ang II-infused (500ng/kg/min) ApoE<sup>-/-</sup> mice as it reduces significantly the development of atherosclerotic plaques in the aorta and the brachiocephalic artery compared to sham-treated mice. This effect was mainly immune-mediated. Immune cell infiltration into the vasculature was significantly reduced. Moreover, chronic C3 treatment shifted the immune response to an anti-inflammatory phenotype by reducing Th17 and CD4 effector memory cells and increasing CD4 naïve T-cells. Besides the immune-mediated effect, we showed that C3 improved endothelial dysfunction and reduced blood pressure. In addition, C3 attenuates Ang II-induced cardiac fibrosis and cardiac hypertrophy demonstrating an additional cardio-protective effect of C3.

In part II, we studied the effect of high salt intake on Ang II-induced abdominal aortic aneurysm (AAA). Chronic high salt intake is a major risk factor for cardiovascular diseases. Recent studies showed that excessive chronic salt intake affects the immune response. However, it remains unclear how salt accelerates vascular damage via an immune cell-mediated mechanism. To answer this question, we pre-treated ApoE<sup>-/-</sup> mice with high salt (1% salt via drinking water) for two weeks. One week after switching to normal salt intake, AAA was induced by chronic Ang II infusion (1000ng/kg/min). AAA and aortic inflammation were assessed by a newly established magnetic resonance imaging (MRI) protocol. Compared to sham pre-treated mice, salt pre-treatment increased the incidence of AAA and worsened the

outcome in ApoE<sup>-/-</sup> mice. This detrimental outcome was accompanied by accelerated vascular inflammation detected *in vivo* by MRI in salt-pre-treated mice. Further analysis revealed that cytokines characterizing a T-cell or macrophage dependent immune response were significantly increased in aortas of salt pre-treated mice. Beside an aggravated increase in effector and central memory CD4 T-cells, salt pre-treatment induced an increase in the pro-inflammatory CD8 T-cell subsets in the aorta and spleen. The effect of salt on CD8 differentiation was confirmed by *in vitro* experiments. Our study highlights the role of CD8 T-cells on the salt-mediated vascular injury. In addition, frequencies of neutrophils and neutrophil elastase expression was significantly increased in aortas of salt pre-treated ApoE<sup>-/-</sup> mice suggesting a direct effect of salt pre-treatment on neutrophil function and thereby on AAA formation. Notably, pro-inflammatory M1 macrophages seem to be more abundant in the salt pre-treated mice. Here, we showed that salt exacerbates AAA via an immune cell-mediated mechanism. T-cells, neutrophils, and macrophages were demonstrated to be the key players in the salt-mediated vascular injury.

In this study, we demonstrated that C3 and salt modulated the immune response in the Ang II-infused ApoE<sup>-/-</sup> mice differently and in turn affected the vascular injury. C3 and other SCFAs are produced as a result of fiber intake. Fibers and salt are main nutrition components. Changing food habits such as increased fiber intake and reduced salt intake will decrease significantly the cardiovascular disease within the populations.

## 2 Introduction

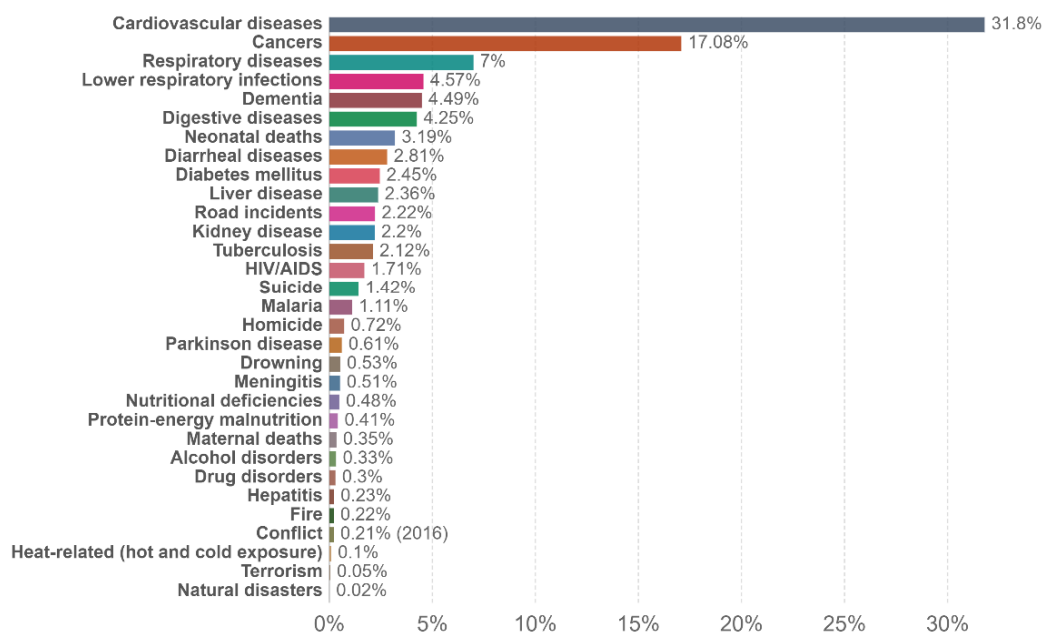
### Cardiovascular diseases

Cardiovascular diseases (CVD) are still the leading cause of death worldwide (Lozano *et al.* 2012, Lancet) as shown in figure 1. According to the World Health Organization (WHO), 17.9 million people died in 2016 because of an underlying CVD which represents 31% of all global deaths. The percentage of mortalities as a result of an underlying CVD has increased steeply in the last decades (Global Burden of Disease, GBD; figure 2). CVD are a group of versatile diseases that affect heart and vessels. There are several risk factors for CVD which can be comprised of two groups: modifiable risk factors (behavioral factors) such as unhealthy diet, smoking, physical inactivity and obesity, and non-modifiable risk factors. Non-modifiable risk factors are factors that are caused due to the presence of another underlying physiological condition, pathophysiological condition or genetic reasons such as hypertension, hyperlipidemia, family history, age, race, and gender. There are a wide range of CVD therapeutic agents, but many CVD still have no medications and can be treated only by surgical intervention. The main therapeutic strategies are directed to lower blood pressure (antihypertensive agents) or reduce lipid concentration in plasma (Stewart *et al.* 2017. JRSM Cardiovasc Dis).

Figure 1

#### Share of deaths by cause, World, 2017

Data refers to the specific cause of death, which is distinguished from risk factors for death, such as air pollution, diet and other lifestyle factors. This is shown by cause of death as the percentage of total deaths.



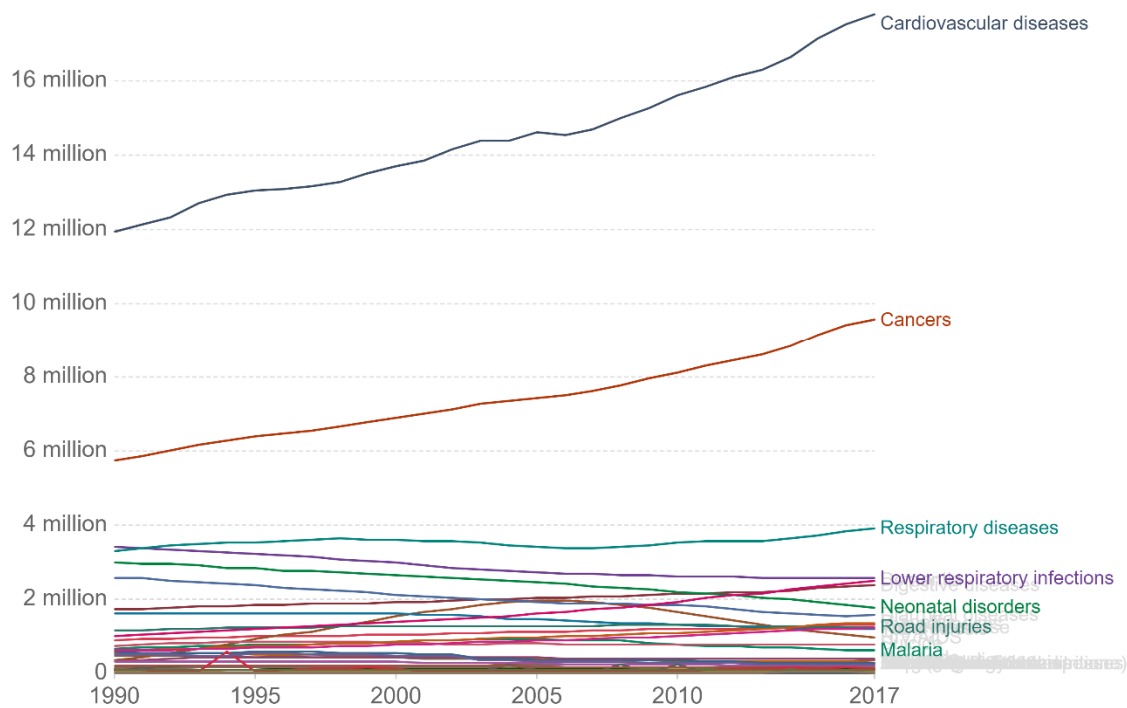
Source: IHME, Global Burden of Disease

CC BY

Fig.1: Worldwide share of death by cause in 2017. Source: Global Burden of Disease Collaborative Network. Global Burden of Disease Study 2017 (GBD 2017) Results. Seattle, United States: Institute for Health Metrics and Evaluation (IHME), 2018. Represented by: ourworldindata.org

Figure 2

### Number of deaths by cause, World, 1990 to 2017



Source: IHME, Global Burden of Disease

OurWorldInData.org/causes-of-death • CC BY

Fig. 2: Change in the worldwide share of death by cause from 1990 through 2017. Source: Global Burden of Disease Collaborative Network. Global Burden of Disease Study 2017 (GBD 2017) Results. Seattle, United States: Institute for Health Metrics and Evaluation (IHME), 2018. Represented by: ourworldindata.org

### Impact of immune cells on CVD

Leucocytes are diverse and versatile heterogeneous types of cells. Despite that each type of cell is unique and has a specific role; the intercommunication between immune cells is tremendous. The immune system can be split between innate and adaptive responses. The innate system represents the initial immediate response of the host to the invaders while the adaptive system develops as a specific response to an individual pathogen, toxin or allergen. Innate immune cells include basophils, dendritic cells, eosinophils, monocytes and macrophages, neutrophils and natural killer (NK) cells. Phagocytes such as neutrophils, macrophages, and monocytes cells exert their effect by engulfing the pathogen, foreign particles or toxins. Neutrophils

and macrophages release cytotoxic compounds such as reactive oxygen species. On the other hand, adaptive immune cells consist of lymphocytes, namely B-cells and T-cells. B-cells are crucial for antibody production. There are 2 subsets of T-cells; T helper cells which are characterized by expression of CD4<sup>+</sup> marker, and cytotoxic T-cells which is characterized by the expression of CD8<sup>+</sup> marker. In order to mediate a cellular immune response, T-cells require the processing and presenting of antigen by Antigen-presenting cells (APC). APC are a group of heterogeneous cells such as dendritic cells, macrophages, Langerhans cells and B cells. CD4<sup>+</sup> and CD8<sup>+</sup> T-cells can be in different forms such as naïve cells, effector cells, central and effector memory cells, as well as other forms. The elevated frequencies of effector, effector memory, and central memory T-cells is a sign of activation of pro-inflammatory response. CD4<sup>+</sup> effector T-cells are subdivided into further subsets such as Th1, Th2, Th9, and Th17 while CD8<sup>+</sup> effector T-cells are subdivided Tc1, Tc2, Tc9, and Tc17. Th1 is identified by the expression of T-bet transcription factor and Th7 is identified by the expression of RORγt. A portion of CD4<sup>+</sup> cells is regulatory T-cells (T<sub>reg</sub>). T<sub>reg</sub> play an important role in the modulation of immune responses. T<sub>reg</sub> are identified by CD25<sup>+</sup> and FoxP3<sup>+</sup> markers. The adaptive response is an enduring response that can persist in a dormant state but re-exhibit rapidly defensive actions after another encounter with their specific antigen (Chaplin. 2006. *J Allergy Clin Immunol*; Alam. 1998. *Prim Care*; Mittrücker *et al.* 2014. *Arch Immunol Ther Exp*; Cronkite *et al.* 2018. *J Immunol Res*). Cytokines are a big group of heterogeneous polypeptides produced by many leucocytes. Cytokines are polyfunctional. They maintain the intercommunication and coordination between immune cells, trigger, and cease inflammation. Cytokines can exert pro-inflammatory, anti-inflammatory or dual functions (Holtmann *et al.* 1995. *Naturwissenschaften*; Cavillon. 2001. *Cell Mol Biol*). Specific T-cell subsets have a distinctive signature for cytokines secretion. Th1 secretes predominantly IFNγ and TNFα whereas Th17 produces IL17. Tc1 is distinguished by producing IFNγ. A novel cytotoxic subset of Tc1 has been identified which produces both IL17 and IFNγ (Tajima *et al.* 2011. *Int Immunol*). IL17, IFNγ, and TNFα are known for their pro-inflammatory characteristics. T<sub>reg</sub> counterbalance Th17 by producing the anti-inflammatory IL10 (Chaudhry *et al.* 2011. *Immunity*)

Immune cells have a huge impact on CVD. The underlying mechanism of many CVD such as atherosclerosis and aneurysm is widely accepted to be due to vascular inflammation (Fernández-Ruiz. 2016. *Nat Rev Cardiol*). Some immune cells were shown to exacerbate CVD, while others are known to induce healing and recovery in the heart and the vasculature. The balance and homeostasis between pro-inflammatory and anti-inflammatory immune cells are fundamental. Any shift in the balance would lead to a shift in the effect of the immune system on CVD. The higher abundance of anti-inflammatory cells leads to a protective effect and improvement of CVD while the prevalence of pro-inflammatory cells leads to the progression of diseases. Such a balance axis can be seen between M1 (Pro-inflammatory) and M2 (anti-inflammatory) Macrophages and between Th1, Th17 (Pro-inflammatory) and

T<sub>reg</sub> (Kvakan *et al.* 2009. *Circulation*; Madhur *et al.* 2010. *Hypertension*; Mills. 2012. *Crit Rev Immunol*). Clinical trials were carried out on humans for anti-inflammatory approaches such as CANTOS (Canakinumab Anti-inflammatory Thrombosis Outcome Study) and COLCOT (Colchicine Cardiovascular Outcomes Trial) showed a beneficial effect on reducing cardiovascular diseases, shedding a light on the potency of modulation of immune cells of cardiovascular health outcomes.

**Figure 3**

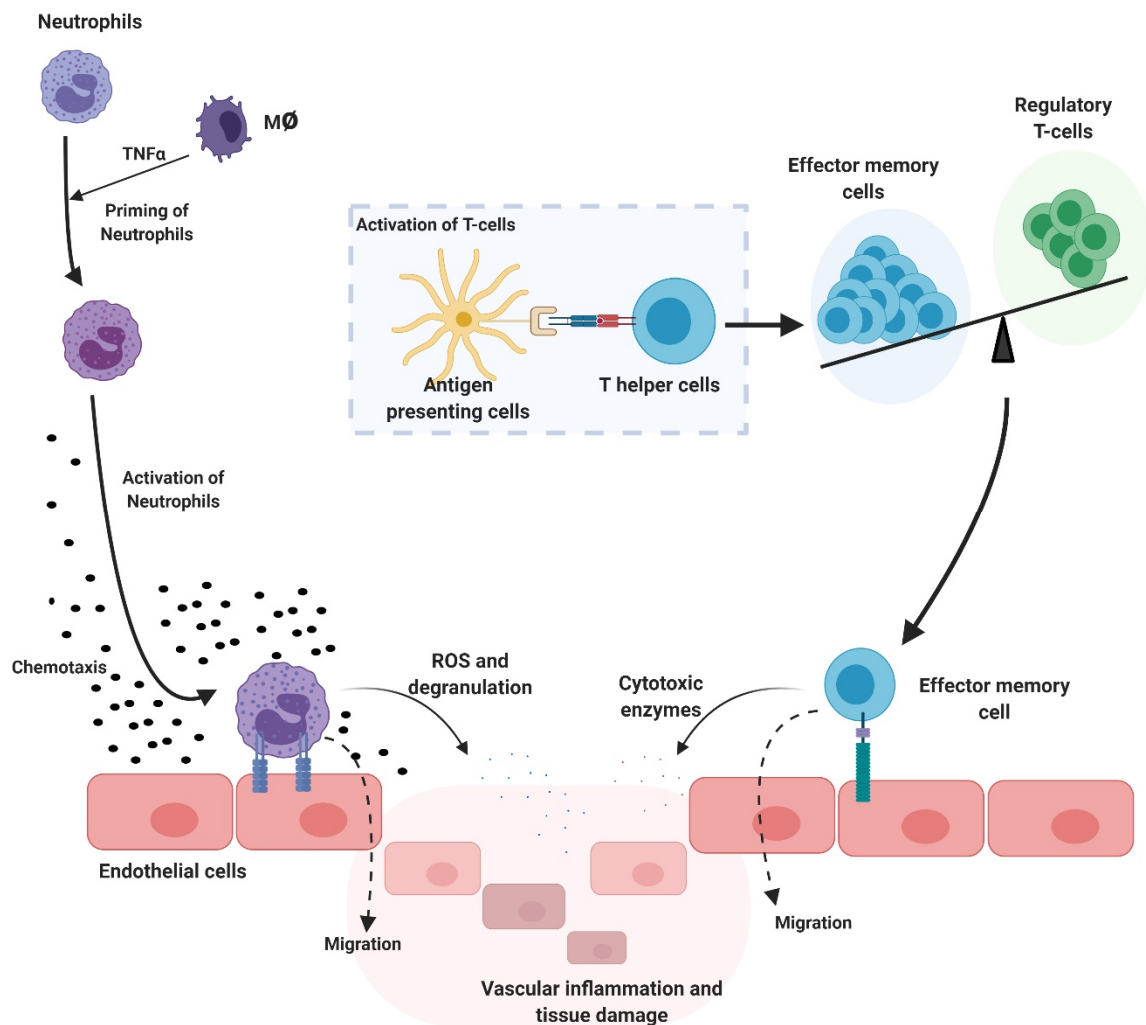


Fig. 3: An illustration showing some examples for the effect of different innate and adaptive immune subsets on vascular injury. Different T-cell subsets have distinctive role in vascular injury. Excreted cytokines from T-cells lead to the recruitment of other immune cells. The dysbalance between pro-inflammatory cells (e.g.: effector memory) and anti-inflammatory cells (e.g.: Treg) contribute to the progress of vascular injury. Activated neutrophils release Ros and modulate the ECM. The illustration was drawn using Biorender application and adapted from Lintermans *et al.* 2014 *Front Immunol*

## **Atherosclerosis**

Atherosclerosis is a global burden (Herrington *et al.* 2019. *Circ Res*; Ross. 1993. *Nature*). Atherosclerosis is a chronic disease that occurs due to the building up of atherosclerotic plaques on the arterial walls leading to narrowing of the lumen of the arteries and hindrance of the normal blood flow. Furthermore, atherosclerotic plaques may rupture, leading to infarctions and death. Atherosclerosis shares the same causes and risk factors as many other CVD risk factors. Atherosclerosis is predominantly asymptomatic; nevertheless, complications of atherosclerosis are likely to occur such as triggering secondary CVD, for instance, coronary artery disease, and heart failure (Dayton *et al.* 1969. *Am J Med*; National Research Council US Committee on Diet and Health. 1989).

Lipid profile plays a crucial role in the pathogenesis of atherosclerosis. Lipid transport is done by lipoproteins, mainly High-density lipoprotein (HDL) and Low-density lipoprotein (LDL). HDL "Good cholesterol" carries lipid from the body cells into the blood while the LDL "Bad cholesterol" carries lipid to the body cells from the blood, thus contributing in the accumulation of fat cells on the vascular walls. Hypercholesterolemia, in particular high concentration of LDL, is a major trigger to the pathophysiology of atherosclerosis. Elevated LDL concentration in the plasma leads to increase permeability of arterial endothelium to lipid which give rise to lipid retention in the arteries. Lipid particles are modified and oxidized into pro-inflammatory particles. The modified lipid droplets are antigenic, so they get engulfed by phagocytes (mainly macrophages) forming "foam cells". The building up of foam cells leads to the production of a "fatty streak". Vascular smooth muscle cells (SMC) migrate from the media of the vessel to the intima. Foam cells bind to the endothelial layer of the vessel (which expresses adhesion molecules, such as vascular adhesion molecule 1) and the SMC. Vascular injury and turbulent blood movement caused by the development of the fatty streak accelerates the development of atherosclerosis. The end result is a sequela of vascular modifications, such as pathological intimal thickening, fibrous capping and plaque formation which eventually result in thrombosis formation and plaque rupture. (Lu H *et al.* 2016. *Arterioscler Thromb Vasc*; Bergheanu SC *et al.* 2017. *Neth Heart J*; Insull W Jr. 2009. *Am J Med*; Rader *et al.* 2008 *Nature*). Statins as Cholesterol-lowering drugs remain to be the primary treatment strategy against atherosclerosis.

**Figure 4**

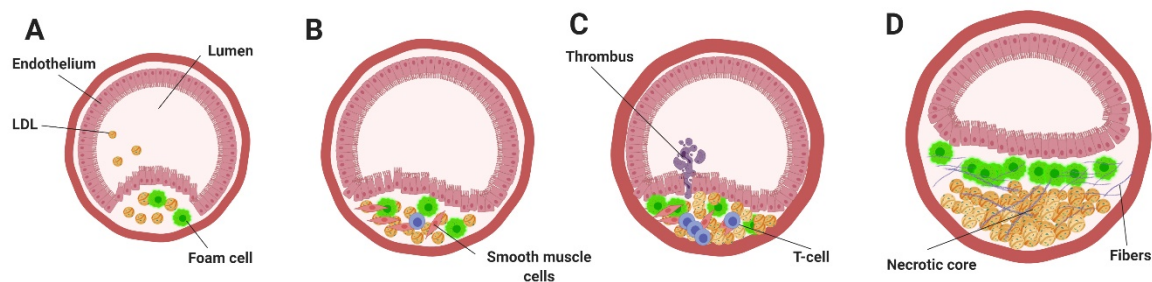


Fig. 4: The figure shows the sequential process of atherosclerosis pathogenesis. A: Oxidation of LDL in the vessels and the formation of foam cells. B: Migration of smooth muscle cells C: Thrombus formation. D: Fibrosis and capsulation of atherosclerotic plaque. The illustration was drawn using Biorender application and adapted from Rader *et al.* 2008 Nature

Several innate and adaptive immune cells contribute to the development of atherosclerosis, but macrophages and T-cells seem to be the main players in the pathogenesis. Macrophages actively participate in the ingestion of lipoproteins to produce foam cells. The ability of macrophages to migrate is reduced significantly as a result of lipoproteins phagocytosis, which leads to further progression of inflammation (Randolph. 2014. *Circ Res*). During this stage, macrophages produce many pro-inflammatory cytokines (such as  $\text{TNF}\alpha$ ) and reactive oxygen species. The pro-inflammatory M1 macrophages have higher abundance compared to the anti-inflammatory M2 macrophages (Chistiakov *et al.* 2015. *Int J Cardiol*). Macrophages interact and activate T-cells through many mechanisms, one of which is antigen-presenting via MHC class II (Underhill *et al.* 1999. *J Exp Med*).

T-cells (CD3) are the second most abundant immune cells after macrophages in atherosclerotic lesions. T-cells consist of mainly T helper cells (CD4) and cytotoxic cells (CD8). Both CD4 and CD8 T-cells play a role in the pathogenesis of atherosclerosis. The depletion of CD8 T-cells was shown to ameliorate atherosclerosis (Kyaw *et al.* 2013. *Circulation*). Besides, it has been shown that the adoptive transfer of CD4 T-cells aggravates atherosclerosis in immunodeficient apolipoprotein E knockout ( $\text{ApoE}^{-/-}$ ) mice (Zhou *et al.* 2000. *Circulation*). Different subsets of CD4 T-cells mediate a different effect on the development. Th17 and Th1 are pro-inflammatory subsets that promote atherosclerosis through the production of IL17 and  $\text{IFN}\gamma$  respectively (Erbel *et al.* 2009. *J Immunol*; Gupta *et al.* 1997. *J Clin Invest*). In contrast, regulatory T-cells ( $\text{T}_{\text{reg}}$ ) have anti-atherosclerotic activity (Didion *et al.* 2009. *Hypertension*)

## **Aortic abdominal aneurysm (AAA)**

Aortic abdominal aneurysm (AAA) is the 13<sup>th</sup> leading cause of death in men over 55 years in the United States according to Centers for Disease Control and Prevention. AAA is dilation in the infrarenal aorta in the form of a bulge. Blood flow may split the layers of the aortic walls resulting in dissection aneurysm which is a special type of AAA. The bulge may rupture leading to death. Typically, AAA is asymptomatic, or the symptoms are subclinical. (Sakalihasan *et al.* 2018. *Nat Rev Dis Primers*; van Beek *et al.* 2014 *Eur J Vasc Endovasc Surg*) Despite the known risk factors such as being hyperlipidemia, hypertension, male gender, smoking, and alcohol consumption (Forsdahl *et al.* 2009. *Circulation*), AAA remains a public health issue.

The actual mechanism of action of the pathophysiology of AAA is still unclear, however, some features characterize AAA such as degradation of the extracellular matrix (ECM), immune cell infiltration and increased oxidative stress in the aortic wall. Metalloproteases 2 and 9 (MMP2, MMP9), as well as elastases, play a key role in the development of AAA. MMP2, MMP9, and elastases are matrix-degrading enzymes released into the aortic wall resulting in the degradation of collagen and elastin, two main components of the extracellular matrix (Busuttill *et al.* 1982. *J Surg Res*; Guo *et al.* 2006. *Ann N Y Acad Sci*). Several immune cells contribute to the pathogenesis of AAA. For instance, macrophages exacerbate AAA by promoting the degradation of ECM and inducing inflammation by producing cytokines (Raffort *et al.* 2017. *Nat Rev Cardiol*). Neutrophils release neutrophil elastase which breakdown the elastic fibre of the aortas (Cohen *et al.* *J Invest Surg.* 1991). Furthermore, neutrophil extracellular traps (NETs) was shown to promote AAA (Meher *et al.* 2018. *Arterioscler Thromb Vasc Biol*). T-cells are predominant population in AAA. Studies showed that all CD4 T-cell subsets were present in aneurysmal lesions in humans (Téo *et al.* 2018. *Mediators Inflamm*). Similarly, it has been shown that CD8 promotes the development of aneurysm via IFN $\gamma$  production (Zhou *et al.* 2013. *J Immunol*).

No pharmacological therapy is shown to be effective for the treatment of AAA (Robertson *et al.* 2014. *Cochrane Database Syst Rev*) and surgical intervention remains to be the only mean of treatment.  $\beta$ -blockers, angiotensin-converting enzyme inhibitors, angiotensin receptor blockers, statins are suggestive for the management of AAA (Castellano *et al.* 2012. *Ann N Y Acad Sci*).

## **Role of Angiotensin II (Ang II) in atherosclerosis and aneurysm**

Ang II is one component of the renin angiotensin system. The precursor of Ang II is angiotensinogen. Angiotensinogen converts to angiotensin I by renin. Angiotensin I can be degraded into several metabolite peptides, one of which is Ang II by the effect of angiotensin-converting enzyme (ACE). Ang II activates two types of receptors: AT1R and AT2R (Burnier *et al.* 2000. Lancet)

Ang II is a major trigger in the pathophysiology of atherosclerosis and aneurysm. Ang II induces vascular injury through several mechanisms. Ang II induces vascular inflammation and promotes the infiltration of immune cells into the vascular tissues. Ang II promotes the polarization of macrophages and stimulates the expression of monocytes/macrophages chemoattractant proteins (Ruiz-Ortega *et al.* 2000. Kidney Int). Furthermore, Ang II increased the expression of CD69 (an early activation marker) as well as TNF $\alpha$  production in T-cells (Guzik *et al.* 2007. J Exp Med). Ang II was shown to increase vascular permeability, allowing more immune cells to participate. Moreover, Ang II induces remodeling the extracellular matrix (such as increasing the expression of vascular cell adhesion molecule-1 and selectins) which in turn helps immune cells to adhere to the vascular tissues. Ang II stimulates the release of growth factors such as vascular endothelial cell growth factor (VEGF) and transforming growth factor beta (TGF $\beta$ ). Ang II stimulates the production of reactive oxygen species (ROS) by inducing a vascular NADH oxidase. ROS initiates the oxidation of LDL and their accumulation. Apart from that, Ang II induces hypertension which is a primary risk factor for CVD. All these factors exacerbate the development of vascular injuries such as atherosclerosis and aneurysms. After injury, vascular repair takes place. Vascular repair is accompanied by fibrosis and collagen accumulation in the heart and the vessels. In addition, stimulation of angiotensin receptor 1 (AT1R) by Ang II induces cardiac hyperplasia or hypertrophy (Touyz. 2005. Curr Opin Nephrol Hypertens). In both of our models, the mice were infused with Ang II to induce and atherosclerosis and aneurysm.

## **Cardiovascular diseases and diet**

An unhealthy diet is one of the major risk factors for CVD. No doubt changing diet is the first step to decrease the risk and the susceptibility to CVD. Specific diet components have distinctive impact on immune cells priming and differentiation (Childs *et al.* 2019 Nutrients). Thus, the ingestion of specific food components affects CVD -at least in part- via modulation of the immune system. Recently, several studies showed that the effect of diet on immune cells is mediated by gut microbiome (Brestoff *et al.* 2013. Nat Immunol). Such effect is mediated by changing the composition of different commensal bacteria in the gut which in turn changes the secretion of metabolites. For example, salt was shown to drive the differentiation of T-cells into the pro-inflammatory Th17 phenotype in the gut by depleting lactobacillus. The depletion of lactobacillus resulted in lowering the production of tryptophan metabolites which is linked to the differentiation of T-cells (Wilck *et al.*

2017. Nature). The gut microbiota shapes many physiological and pathological processes in humans. Gut microbiome differs from one person to another and it is sensitive to diet, lifestyle, and socioeconomic status (Spor *et al.* 2011. Nat Rev Microbiol).

A diet such as 'Prudent' dietary pattern, Mediterranean, or 'DASH compliant' was shown to have a positive impact on the reduction of CVD risk. In contrast, diet such as 'Western' was shown to be adversely related to CVD (Jacobs *et al.* 2015. Curr Opin Lipidol; Williams *et al.* 2013. Proc Nutr Soc). According to the suggested diet patterns, the optimal diet for preventing CVD should include high fiber sources, low salt, high potassium, low sugar, low fat, and balanced macro and micronutrients. In this study, we investigated the immune-mediated effect of one product of fiber digestion (short chain fatty acids; part I) and salt intake (part II) on CVD.

### **Part I: Short chain fatty acid (SCFA)**

Fiber intake was shown to help in the prevention of CVD and to reduce the mortality from CVD (Threapleton *et al.* 2013. BMJ; Hartley *et al.* 2016. Cochrane Database Syst Rev; Kim *et al.* 2016. Arch Cardiovasc Dis). SCFA are the end product of the bacterial flora – namely Clostridium clusters – while fermenting of indigestible carbohydrates and fibers, such as cellulose (Topping *et al.* 2001. Physiol Rev).

SCFA are carboxylic acids defined by the presence of an aliphatic tail of two to six carbons. The major SCFA produced are acetate (C2), propionate (C3), and butyrate (C4). The majority of SCFA are absorbed from the gut by diffusion through the epithelium to the lamina propria while the rest is taken directly by the epithelial cells (Fleming *et al.* 1991. J Nutr). SCFA enter the bloodstream and taken by the portal vein to the liver in which the majority get metabolized (Peters *et al.* 1992. Gut). SCFA are mainly metabolized via the Krebs's cycle into Acetyl coA in the hepatocytes (Gill *et al.* 2018. Aliment Pharmacol Ther; Bugaut. 1987. Comp Biochem Physiol B). The importance of SCFA to human health became of interest after it was found that the reduction of SCFA concentration was linked to cancer and inflammatory diseases (Sivaprakasam *et al.* 2016. Pharmacol Ther).

SCFA are specific ligands for G protein-coupled receptor 41 (GPR41; called Free fatty acid receptor 3 or FFAR3), G protein-coupled receptor 43 (GPR43; or Free fatty acid receptor 2, FFAR2), G protein-coupled receptor-109A; GPR109A and Olfactory receptor-78; Olfr78 (Priyadarshini *et al.* 2018. Compr Physiol; Le Poulet *et al.* 2003. J Biol Chem). GPR41 and GPR43 are expressed on immune cells, adipose tissue and intestinal cells (Sivaprakasam *et al.* 2016. Pharmacol Ther). GPR41 was found to be localized in the vascular endothelium (Natarajan *et al.* 2016. Physiol Genomics). Moreover, SCFA was found to inhibit Histone deacetylase which in turn leads to hyperacetylation of histones. This is one of the mechanisms of action of SCFA which

should be taken into consideration along with activation of GPR41 and GPR43 (Davie. 2003. J Nutr).

Several studies showed that SCFA influence the priming and differentiation of immune cells (Sivaprakasam *et al.* 2016. Pharmacol Ther; Vinolo *et al.* 2011. Nutrients). SCFA was shown to promote the differentiation of T<sub>reg</sub> (Smith *et al.* 2013. Science; Arpaia *et al.* 2013. Nature). Treatment of mice with Propionate (C3) ameliorated experimental autoimmune encephalomyelitis (EAE) via the stimulation of T<sub>reg</sub> (Haghikia *et al.* 2015. Immunity). Studies showed that SCFA suppressed autoimmune diseases by modulation of immune cells and suppression of IL-17A production (Luu *et al.* 2019. Nat Commun). Immune-mediated effects of SCFAs have been demonstrated in several other disease models, such as colitis, and airway disease (Koh *et al.* 2016. Cell), as explained in figure 5.

Figure 5

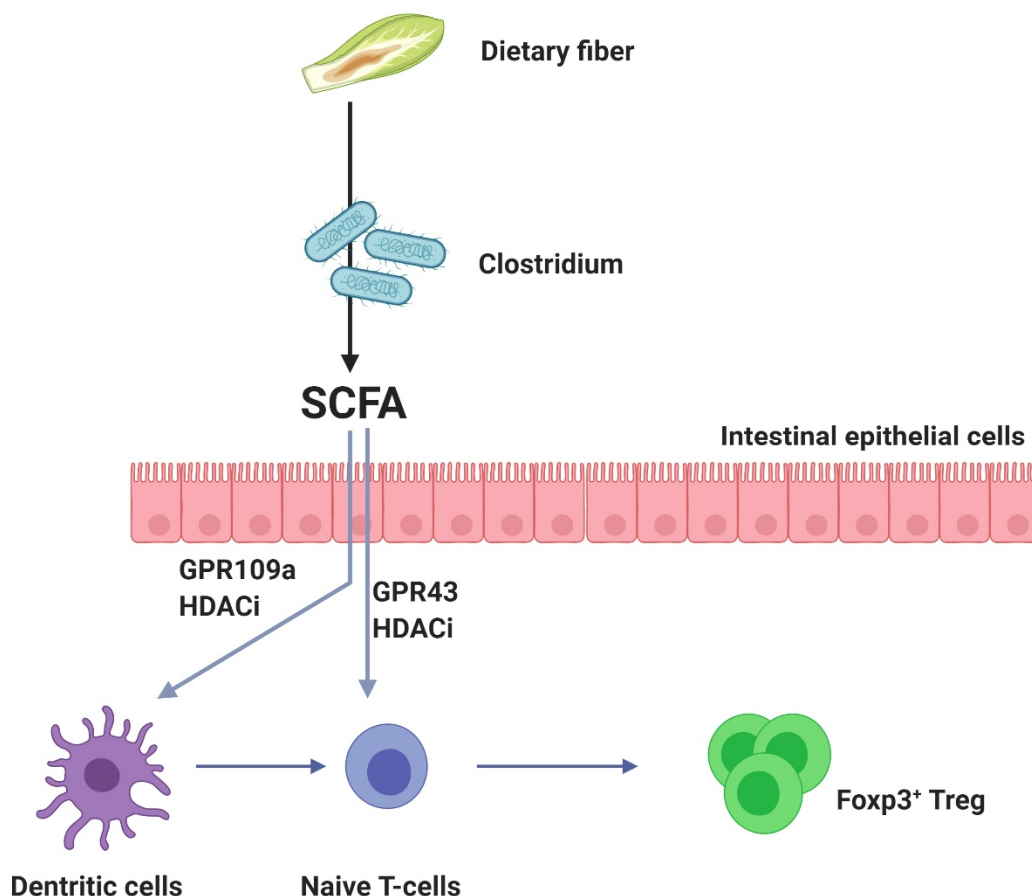


Fig. 5: An illustration of the effect of SCFA on immune cells modulation. SCFA induces the production of Treg. SCFA are produced as a result of fermentation of gut microbiome to the indigestible fibers. The illustration was drawn using Biorender application and adapted from Honda *et al.* 2016. Nature.

## **Part II: Salt intake**

The major source of sodium in our diet is the table salt (NaCl) but other forms of sodium in food such as sodium glutamate (preservative) also contribute to the total sodium intake. High salt intake is widely accepted as a global burden, regardless of the socio-economical level. According to the WHO guidelines, the daily recommended salt intake for adults is less than 5 g salt per day. In Germany, the averaged salt intake is 8–10 gm/day (Strohm *et al.* 2016. Ernährungs Umschau). High salt intake was shown to exacerbate CVD. Several studies showed a direct correlation between excessive salt intake and hypertension (Frisoli *et al.* 2012. Am J Med; He *et al.* 2002. J Hum Hypertens) as well as stroke, heart failure and other cardiovascular diseases (Strazzullo *et al.* 2019. BMJ).

High salt intake has a huge impact on immune cells (Afsar *al.* 2018. Hypertension). Salt was shown to trigger the priming of T-cells into Th17 cells in many studies. It has been demonstrated that salt intake induces Th17 CD4 T-cell response thereby aggravates the development of experimental autoimmune encephalomyelitis in mice (Kleinewietfeld *et al.* 2013. Nature). The upregulation of Th17 CD4 T-cells was reported in the salt mediated lupus nephritis (Yang *et al.* 2015. Int Immunopharmacol). In addition, to the effect of salt of Th17 cell, salt was found to suppresses T<sub>reg</sub> functions in humans and *in vitro* (Hernandez *et al.* 2015. J Clin Invest). Moreover, salt induces M1 macrophages and suppresses M2 anti-inflammatory type macrophages (Zhang. 2015. J Clin Invest; Binger 2015. J Clin Invest). Salt was shown to promote the production of some pro-inflammatory cytokines, for instance, TNF $\alpha$  and Interleukin-6 (IL6) (Hashmat *et al.* 2016. Am J Physiol Renal Physiol). The exact mechanism of salt on immune cells is not fully understood and more investigations must be carried out.

## **The aim of the study**

Nutrition factors have been shown to affect vascular diseases by modulating the immune response. These nutrition factors are consumed by populations on a daily base. In our study, we aimed to investigate the immune-mediated effect of two nutrition factors on two models of vascular injury. In part I, we investigated the effect of SCFA on an atherosclerosis model while in part II, we studied the role of high salt intake on abdominal aortic aneurysm (AAA) model. We generated mouse models for atherosclerosis and AAA in which we used ApoE<sup>-/-</sup> mice and induced vascular injury by Ang II infusion. In both parts, we assessed the Ang II-induced vascular injury, immune cells and cytokines modulation and whether there are direct effects on the heart and vasculature as a result of treating the mice with either SCFAs or salt.

### 3 Materials and Methods

#### Experimental mice

Apolipoprotein E knock-out (ApoE<sup>-/-</sup>) mice were backcrossed on a C57BL/6 background at least 10 times. Experiments were approved by the responsible federal state authority (Landesamt fuer Natur-, Umwelt-, und Verbraucherschutz Nordrhein-Westfalen) and performed in accordance to the guidelines from the Directive 2010/63/EU of the European Parliament on the protection of animals used for scientific purposes. Mice were bred and maintained at the animal facility of the University Hospital Düsseldorf (animal protocol G301/18). ApoE<sup>-/-</sup> mice were chosen because of their susceptibility to vascular inflammatory diseases like atherosclerosis and aneurysm. Mice were kept under appropriate conditions with food and water *ad libitum*. Light to dark cycle was 12:12 hrs.

#### Animal models

##### Part I: Effect of short chain fatty acids on Atherosclerosis

6 to 8 weeks old ApoE<sup>-/-</sup> mice were supplied with 200mM sodium propionate (C3) (P1880, Sigma, Steinheim, Germany) in the drinking water during the whole experimental period. Treatment with C3 was started 5 days before implantation of osmotic minipumps (Model 1004, Alzet, Durcet, California, USA) filled with Angiotensin II (Ang II) (A9525-10MG, Sigma, Steinheim, Germany) at a dose of 500 ng/kg/min. After 4 weeks of Ang II infusion, the mice were euthanized for the assessment of atherosclerosis, vascular function, and immune responses. Control mice were supplied with 200mM sodium chloride (NaCl) (VWR chemical, Louvain-la-Neuve, Belgium) in the drinking water instead of sodium propionate and underwent the same procedures.

Figure 6

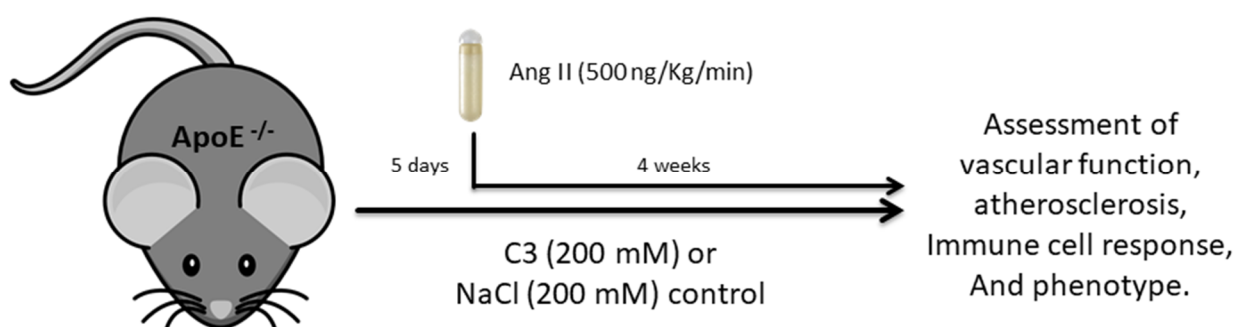


Fig. 6: ApoE<sup>-/-</sup> mice were supplied with drinking water containing 200 mM C3 or 200 mM NaCl (control). The treatment started 5 days prior to Ang II (500 ng/kg/min) infusion and continued until the end of the experiment. After 4 weeks of Ang II the mice were sacrificed.

## Part II: Effect of high salt intake on Abdominal Aortic Aneurysm

6 to 8 weeks old ApoE<sup>-/-</sup> mice were supplied with 1 % Salt (NaCl, Sodium Chloride, VWR chemical, Louvain-la-Neuve, Belgium) in the drinking water for 2 weeks and then returned to normal tap water as a wash-out period. After 1 week of salt discontinuation, ApoE<sup>-/-</sup> mice were implanted with osmotic minipumps (Model 1004, Alzet, Durcet, California, USA) filled with a high dose of (Ang II) (1000 ng/kg/min). Ang II was used to induce the development of abdominal aortic aneurysm (AAA) for 10 days. During the 10 days of Ang II infusion, magnetic resonance imaging (MRI) scans were performed on the mice at different time points. After 10 days of Ang II infusion, the mice were euthanized for further assessment of inflammatory responses and vascular function. Control mice underwent the same procedures except for pre-treatment with Salt.

Figure 7

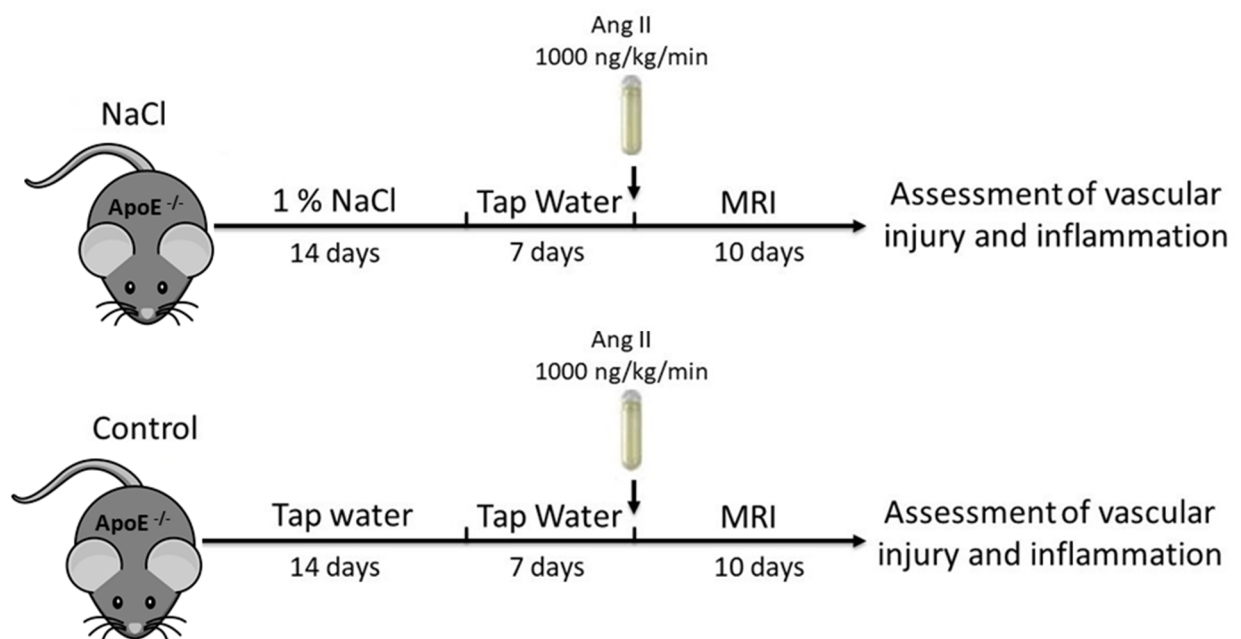


Fig. 7: ApoE<sup>-/-</sup> mice were supplied with 1 % NaCl in the drinking water (or tap water; control) for 2 weeks and then NaCl was discontinued. 1 week after discontinuation of NaCl supplementation, minipumps containing Ang II (1000 ng/kg/min) were implanted to induce AAA for 10 days. Afterwards, the mice were euthanized.

### Osmotic minipumps preparation and implantation

Ang II solution was prepared at a concentration so that the release rate from the minipumps is 500 or 1000 ng/kg/min. Ang II solution was prepared by diluting the lyophilized powder of Ang II with saline solution (Fresenius Kabi, Bad Homburg, Germany). In case of MRI investigation are planned to be performed, the metal tips

of the minipump were replaced by PEEK (polyetheretherketone) (0002612, Alzet, Durcet, California, USA) tips. PEEK tips were washed with 1 % Human Serum Albumin (HSA)(Albutein, Grifols, Frankfurt, Germany) in Phosphate buffer solution Dulbecco without Ca<sup>2+</sup> without Mg <sup>2+</sup> (PBS)(Biochrome, Berlin, Germany) before use to prevent the adherence of Ang II to the tips. The weight of the minipumps was measured before and after filling to ensure that the minipumps were completely filled. Filled minipumps were incubated in tubes containing saline solution at 37°C overnight to promote a direct release of Ang II after implantation.

To implant the minipumps, mice were anesthetized with 1.5 % Isoflurane (Piramal, Hallbergmoss, Germany) or mix of Ketamine (100 mg/kg, i.p.) (Ketaset, Zoetis, New Jersey, United States) and Xylazine (5 mg/kg, i.p.) (Rompun, Bayer, Leverkusen, Germany). Ophthalmological cream was applied to the eyes of the mice to prevent dehydration of the mice. The fur of the mice was shaved at the back of the neck region and then skin with disinfected. A small cut was made at the shaved part. A subcutaneous pocket was made with scissors at the flanks of the mice. The minipumps were inserted in the pocket in an upright position. Single knots stitches were done to close the surgical opening. Buprenorphine (Buprenovet, Bayer, Leverkusen, Germany) as a potent analgesic was injected subcutaneously in a dose of 0.02 mL per mice. The mice were observed the following days until complete recovery.

### **Assessment of the AAA and inflammation by MRI**

Assessment of AAA and inflammation was done in collaboration with Dr Sebastian Temme, Department of Molecular Cardiology, University of Düsseldorf. MRI assessments were done as described previously (Temme et al. 2015. Circulation). Mice were anesthetized using 1.5 % Isoflurane and placed into a 25-mm quadrature resonator tunable to <sup>1</sup>H and <sup>19</sup>F (figure 8). The temperature was adjusted for the mice to be at 37°C during the whole measurements. Experiments were performed at a vertical 9.4 T Bruker AVANCEIII Wide Bore NMR spectrometer (Bruker, Rheinstetten, Germany) operating at frequencies of 400.21 MHz for <sup>1</sup>H and 376.54 MHz for <sup>19</sup>F measurements using a Bruker microimaging unit Micro 2.5 with actively shielded gradient sets (1.5 T/m). Morphological <sup>1</sup>H scans (axial and sagittal) were performed to obtain an anatomical overview of the area from the kidneys to the lungs. Furthermore, MR angiography of the same area conducted to visualize the blood flow in the abdominal aorta and the inferior vein. Afterwards, the resonator was tuned to <sup>19</sup>F to obtain anatomically matching <sup>19</sup>F images. <sup>1</sup>H and <sup>19</sup>F Scans were merged with an in-house developed software module to produce a complete overview of the abdominal region and localize inflammation. The two kidneys were used for the orientation of the scans.

<sup>1</sup>H MR reference images were done using a rapid acquisition and relaxation enhancement sequence (RARE; field of view (FOV) = 2.56 × 2.56 cm<sup>2</sup>, matrix 256 × 256, 0.1 × 0.1 mm<sup>2</sup> in-plane resolution, 1 mm slice thickness; TR = 3000 ms; RARE

factor = 32, 6 averages, Time = 4-5 minutes).  $^{19}\text{F}$  images were performed at the same FOV with a  $^{19}\text{F}$  RARE sequence (matrix  $64 \times 64$ ,  $0.4 \times 0.4 \text{ mm}^2$  in-plane resolution, 1 mm slice thickness; TR = 40000 ms, TE = 3.45 ms, RARE factor = 32, 256 averages, Time = 34 min).

**Figure 8**

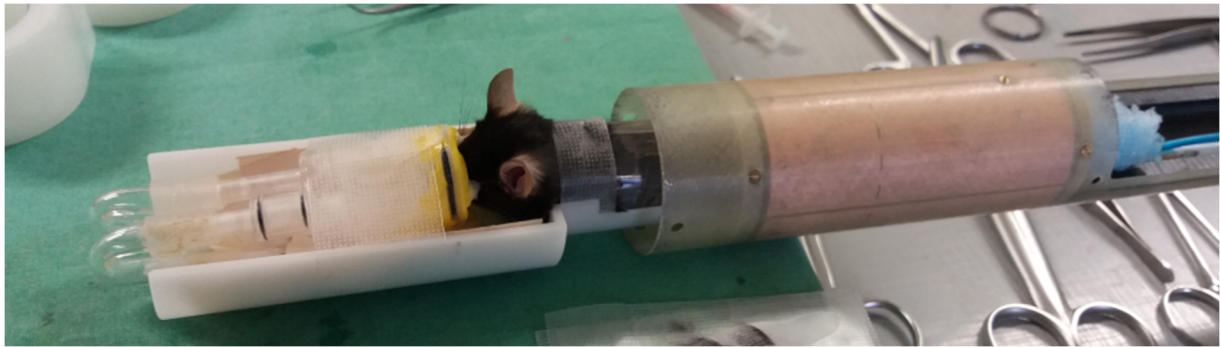


Fig. 8: ApoE<sup>-/-</sup> mice anaesthetized using isoflurane inhalation and placed in a coil for MRI assessment.

$^1\text{H}$  Scans were performed at day 0 (baseline measurement), day 2, day 4, day 7 and day 10 after osmotic pump implantations while  $^{19}\text{F}$  Scans were performed on day 2, day 4, day 7 and day 10 as shown in figure 9.

**Figure 9**

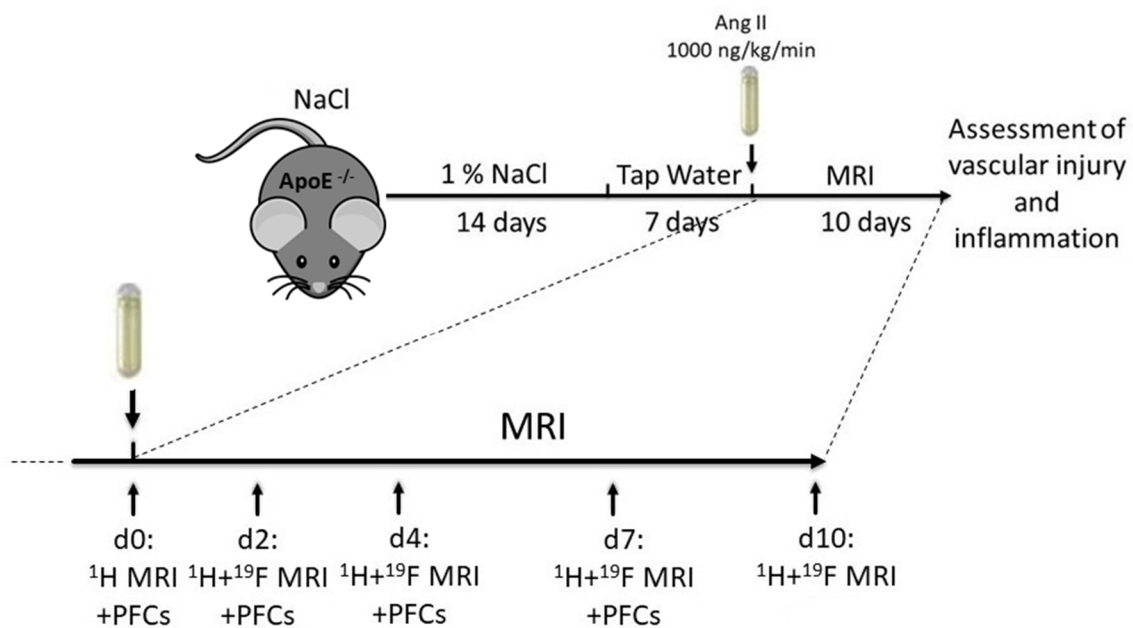


Fig. 9: MRI  $^1\text{H}$  and  $^{19}\text{F}$  RARE scans were performed on ApoE<sup>-/-</sup> mice at different time point before and after minipumps implantation filled with Ang II (10000 ng/kg/min). PFCs were injected before minipumps implantation and then at day 2, day 4, and day 7 after implantations of minipumps.

Abdominal aortic aneurysm (AAA) was identified as a 1.5-fold increase in the maximum diameter of the aorta or 2.25-fold increase in the maximum area. The area and diameter of the aorta were inspected using the anatomical and angiographic views. Both the anatomical and angiographic views were used to consider aneurysm cases in which the bloodstream was not dilated while the aortic wall was dilated.

### **PFCs formation, administration and F signal assessment**

20 % emulsion of Perfluorocarbons (PFCs) was developed in house at the department of molecular cardiology of the University of Düsseldorf as described elsewhere (Grapentin et al. 2014, Nanomedicine). In brief, 2.4% (w/w) phospholipid (Lipoid S75, Lipoid AG, Ludwigshafen, Germany) was diluted in with 10 mM phosphate buffer (isotonized with glycerol). 20% (w/w) perfluoro-15- crown-5 ether (ABCR, Karlsruhe, Germany) was added to the dispersion. A crude emulsion was formed by high shear mixing (Ultra Turrax TP 18/10; IKA-Werke, Staufen, Germany). High-pressure homogenization was performed in 10 cycles at 1000 bar (Avestin Emulsiflex C5, AVESTIN Europe, Mannheim, Germany). PFCs were heat-sterilized in glass vials under standard conditions (121 °C, 2 bar, 20 min.).

PFCs were injected to experimental mice intravenously via the tail at day 0, day 2, day 4, and day7 after implantations of osmotic pumps which leads to the cellular uptake of the administered PFCs by circulating monocytes (Flögel et al. 2008; figure 10). <sup>19</sup>F MRI measurements were conducted after 24-48h to verify the adequate accumulation of PFC-loaded cells in the inflamed area (Flögel et al. 2008; Circulation). The <sup>19</sup>F signal was recorded as the total cumulative signal acquired from the vessel wall of the abdominal aorta by manual drawing regions of interest to select the vessel wall which was assessed by the anatomical <sup>1</sup>H scans.

**Figure 10**

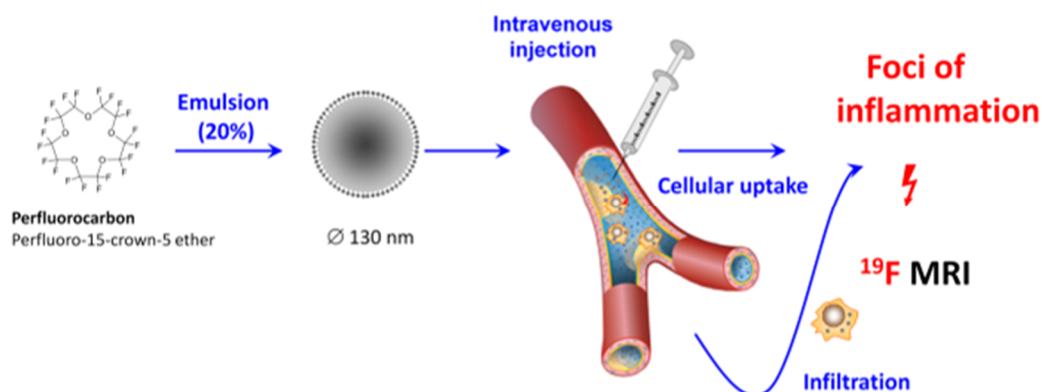


Fig. 10: 20 % PFCs emulsion was injected intravenously via the tail at different time points and leads to cellular uptake by phagocytes.

## **Blood pressure measurements**

Systolic blood pressure (SBP) was measured in conscious mice by tail-cuff plethysmography (BP-98A; Softron) as described (Stegbauer et al. 2017. JCI Insight). The mice were put in a restrainer while being conscious to ensure their immobility. The restrainer with the mice was placed in a climatic coil which was adjusted at 37°C to provide heating. The cuff was placed at the proximal end of the tail of the mice. Ten measurements per mouse were recorded daily. For habituation, mice were trained daily for 5 consecutive days before Ang II pump implantation. Systolic blood pressure was calculated as the mean of all measured values for each day per mouse.

## **Blood samples withdrawal and dissection of the aorta, the aortic arch, and other organs**

The mice were anesthetized with Ketamine and Xylazine. The peritoneal cavity of the mice was opened. The left renal vein was cut, and the blood was withdrawn. Cervical dislocation was performed to ensure the mouse was euthanized. The circulation system was flushed using ice-cold 100 U/ml Heparin (B. Braun, Melsungen, Germany) in PBS solution. The aorta with the perivascular adipose tissue (PVAT) was dissected by creating a gap between the aorta and the vertebral column in the thoracic region and then the gap was extended to dissect the aorta completely. The PVAT tissue was removed from the aorta if necessary. For histochemical analysis, the brachiocephalic artery was cut from the aortic arch and fixed. The heart, kidney, and spleen were dissected for further analysis and stored in RNAlater® solution (Qiagen, Hilden, Germany), All tissue protector® (Qiagen, Hilden, Germany), or in ice-cold PBS solution for mRNA, protein or FACS analysis respectively. Minipumps were disposed and the mice were returned to the animal facility for incineration.

## **Tissue fixation and Paraffin embedding**

After dissection, fixation of organs and tissues were carried out. For fixation, organs such as heart, kidney, and spleen were put in 10 % Formalin solution while aorta and brachiocephalic artery were put in 4 % Paraformaldehyde (PFA) overnight. Tissues were washed briefly in PBS solution. To dehydrate the tissues, tissues were immersed in a serial dilution of ethanol followed by xylol and paraffin. Finally, tissues were embedded in paraffin blocks. The blocks were stored at room temperature.

## **Paraffin removal and dewaxing**

Formalin-fixed paraffin-embedded (FFPE) blocks were cut using a sharp blade in a convenient thickness and placed over coated glass slides. For dewaxing, slides were immersed in xylol twice for 5 minutes each, and then in absolute ethanol twice afterwards in 96 % ethanol, 80 % ethanol, and 70 % ethanol for 3 minutes each step. Slides were then washed in distilled water twice for 5 minutes.

## **Immunohistochemistry of brachiocephalic artery**

The brachiocephalic artery was separated from the aortic arch, fixed in formalin, and embedded in paraffin blocks. Finally, the paraffin blocks were cut into 7µm thin sections. Different histochemical approaches were applied such as Movat, CD3 and F4/80 staining.

### **Movat staining:**

Microscopical slides were fixed in Bouin's solution for 10 minutes at 50°C, immersed in 5 % sodium thiosulfate for 5 minutes, 1 % Alcian blue for 15 minutes, and then alkaline alcohol for 10 minutes at 60°C. Movat Weigert's solution was prepared out of 2 % alcohol hematoxylin, ferric chloride stock solution and Iodine stock solution in a ratio of 3:2:1. Tissues were stained in Weigert's solution for 20 mins. Crocein Scarlet Acid/ Fuchsin working solution (3:1) was composed and used for staining the slides for 2 mins. Slides then were put in 5 % phosphotungstic acid for 5 minutes and then transferred immediately in 1% acetic acid for 5 minutes. Washing with water was done between each step. Dehydration was done in 95% ethanol, then twice for 1 minute in 100% ethanol. Slides were immersed in alcohol saffron for 8 minutes, twice in 100% ethanol for 1min, and then twice in xylol for 5 minutes. Finally, tissues were mounted in mounting medium (Roti©-Mount HP68.1, Karlsruhe, Germany) and covered by coverslips. Chemicals were purchased from Sigma, Chempur, Microm, and Carl-Roth. Movat staining is a multi-chromic approach by which we can evaluate atherosclerotic plaques and stenosis in the brachiocephalic artery. The area of the maximum stenosis was calculated as a percentage of the total area of the transverse section of the brachiocephalic artery. The calculation was done using ImageJ software. (Movat. 1955. AMA Arch Pathol)

### **CD3 and F4/80 staining:**

For CD3 staining, slides were incubated in antigen retrieval buffer pH 9 (S2367, Dako, Carpinteria, CA, USA) for 20 minutes at 98 °C and then for 30 mins at room temperature. For F4/80 staining, slides were incubated with Proteinase K (S3020, Dako, Glostrup, Denmark) for 2.5 to 3 minutes. Afterwards, all slides were loaded with 3 % H<sub>2</sub>O<sub>2</sub> for 10 minutes and then with horse serum (Vector, MP-7401 Burlingame, CA, USA) for 20 minutes. Without rinsing, slides were incubated with the "ready to use" polyclonal rabbit anti-CD3-antibody (No dilution; IS503, Dako, Glostrup, Denmark) or monoclonal rat F4/80 antibody (1:100, MCA497RT, Bio-Rad, Oxford, UK) overnight at 4 °C. After extensively washing with washing buffer (Dako, S0809, Glostrup, Denmark), slides were incubated with ImmPRESS anti-rabbit IgG HRP (No dilution, Vector, MP-7401, Burlingame, CA, USA) for 30 minutes at room temperature. The staining was visualized using DAB stain (DM827, Agilent, Ratingen, Germany). Slides were immersed in Hematoxylin solution for 45 seconds to stain the nuclei of the cells. After washing with tap water for 10 minutes, slides were dried, mounted (Roti©-Mount HP68.1, Karlsruhe, Germany) and covered by coverslips. The number of CD3+ or F4/80+ cells was calculated per transverse section in the brachiocephalic artery at the maximum stenosis.

### **Sirius red/Fast green staining of heart sections:**

Hearts were fixed and embedded in paraffin blocks. Sections (10 µm thick) were stained with picosirius red stain for detecting total collagen (Chondrex™, Redmond, Washington, USA) as described previously (Zhang et al. 2014. JCI). In brief, tissue slides were incubated with one drop (0.2 - 0.3 ml) of Sirius red/Fast green collagen staining kit solution (Chondrex™) for 30 minutes at room temperature. For collagen calculation using a spectrophotometer (Nanodrop 2000c, Thermo, USA), the stain was removed using a 1 ml extraction buffer. The eluted dye solution was taken and the OD values at 540 nm and 605 nm were measured. To determine the amount of collagen, we used this equation: Collagen (µg/section) = [OD<sub>540</sub> value – (OD<sub>605</sub> value x 0.291)] / 0.0378.

To obtain representative images, slide were stained with Sirius red/Fast green kit and then rinsed with 0.5 ml distilled water. Slides were mounted (Roti©-Mount HP68.1, Karlsruhe, Germany) and covered by coverslips. Microscopical images were made from the stained slides. An alternative method to quantify collage in the tissues using the images was established. The percentage of collagen was calculated by determining the number of red color pixels (representing the collagen) in the picture of the stained heart transverse sections and divided by the number to other pixels (representing the non-collagen tissues). The calculation of pixels was done using Photoshop CS5.

### **Oil Red O staining (ORO) for the aortas:**

ORO staining was performed as described by us before (Yang et al. 2018. Pflugers Arch). After 4 weeks of Ang II infusion, mice were sacrificed. Aortas were dissected from the aortic arch to the femoral bifurcation and incubated in 4 % PFA at 4 °C overnight. After removal of adventitia, aortas were stained with Oil red O solution (Oil Red O, Sigma-Aldrich Chemie GmbH, Steinheim, Germany) as described previously (Guang et al, 2018 Pflugers Arch). In brief, the Oil red O (ORO) solution was prepared by dissolving 0.4 g ORO powder dissolved in 80 ml methanol. ORO staining solution was freshly prepared by mixing 1 M sodium hydroxide (JT Baker, Fischer Scientific, Thermo) with ORO solution in the ratio of 2:7. Aortas were incubated in 78% methanol (VWR chemical, Louvain-la-Neuve, Belgium) for 5 minutes, then in ORO staining solution for 90 minutes and finally in 78% methanol for 10 minutes. All incubations were done at room temperature. Aortas were preserved in PBS. To obtain photographs, aortas were opened vertically to expose the inner surface, pinned and photographed under the microscope (Leica MZ6, Wetzlar, Germany) using a digital camera (Coopix 4500, Nikon, Tokyo, Japan, Carl Zeiss, Jena, Germany). For atherosclerosis assessment in the stained aortas, the area of the atherosclerotic plaques was calculated as the area percentage of the total area of the aorta. Measurement of the area was done using ImageJ.

### **Flow cytometry**

Flow cytometric analysis of the aortic tissues was performed directly after sacrificing the mice. In part I, we were interested in atherosclerosis, so we used the whole aorta from the aortic arch through the bifurcation of the aorta for the analysis. On the other hand, in part II we were interested in aortic abdominal aneurysm (AAA), so we dissected the abdominal aorta (starting from the diaphragm through the bifurcation of the aorta) accompanied by the perivascular adipose tissue (PVAT). A modified protocol of Butcher *et al.* (Butcher et al. 2012. Circ Res) was used to obtain a single-cell suspension. Briefly, the aorta was digested using a collagenase-containing digestion solution (600 U/ml Collagenase type II, 60 U/ml DNase I, in HBSS). After centrifugation, the pellet was resuspended in RPMI medium (Life technologies™, Thermo Fischer Scientific, Waltham, USA) and cells were incubated at 37°C for 30 minutes. Finally, the single cells were resuspended in FACS buffer (PBS supplemented with 0.5% BSA and 2mM EDTA) and stained with the following antibodies against CD45, F4/80, CD3, CD4, CD8a, CD44, CD62L, CD69, CD11b, Ly6G, and Ly6C. All antibodies were purchased from Biolegend (San Diego, USA), Miltenyi Biotec (Bergisch Gladbach, Germany), and Becton Dickinson (Franklin Lakes, NJ, USA). To exclude dead cells DAPI stain was used.

For spleen FACS analysis, spleens were cut into smaller pieces, then fragmented and passed through 100 µm filter (EASYstrainer™, Greiner bio-one, Solingen, Germany) using 0.5 HSA% in PBS solution as a vehicle. To investigate extracellular

markers, single cells were washed with FACS buffer. Cells were centrifuged (300 g, 10 minutes, 4°C), resuspended in RPMI 1640 medium (FG1415, Biochrome, Berlin, Germany), and incubated for 30 minutes at 37 °C. Cells were stained with the same antibody panel as the aorta. DAPI stain was used to differentiate between live and dead cells. To investigate intracellular markers (such as cytokines), cells were restimulated. For restimulation, 100 µL RPMI 1640 containing 10% FCS, 1% Penicillin/Streptomycin solution (Biochrome, Berlin, Germany), 50 ng/mL PMA (Sigma), 750 ng/mL Ionomycin (Sigma) and 0.75 µL/mL Monesin (GolgiStop Protein transport inhibitor, BD Bioscience, Ney Jersey, USA) were added to each 1 million cells. The cells were incubated for 4 hours at 37 °C. After incubation, cells were washed twice with 200 µL FACS buffer. 50 µL of LIVE/DEAD® Fixable Aqua Dead Cell Stain (Invitrogen™Life Technologies Corporation, Carlsbad, USA) were added at a concentration of 1:1000 to mark the dead cells. Cells were incubated for 15 min at 4°C in dark and washed twice. Cells were suspended in 100 µL Perm solution (Invitrogen) for permeabilization and fixation, then incubated for 30 min on ice and in dark. 150 µL of Perm buffer (Invitrogen) were added and cells were incubated overnight in dark at 4°C. Cells were centrifuged and the supernatant was discarded. Cells were stained with antibodies against CD3, CD4, CD8, IL17, IFN $\gamma$ , TNFa, and Foxp3 for 30 min at 4°C in dark. Cells were washed twice with 200 µL Perm buffer and then suspended in 250 µL.

Flow cytometric measurements were done using Canto II™ Flow Cytometer (BD Biosciences, San Jose, USA). Kaluza® Flow Analysis Software (Beckman Coulter Inc., Krefeld, Germany) was used for data analysis. Flow cytometry gating strategy for aortas of ApoE<sup>-/-</sup> mice treated with C3 or control was illustrated in figure 11. Gating strategy for the abdominal aortas and spleens of ApoE<sup>-/-</sup> mice in the salt pre-treated and control group to evaluate T-cells was shown in figure 12 and to evaluate monocytes, macrophages and neutrophils was shown in figure 13.

Figure 11

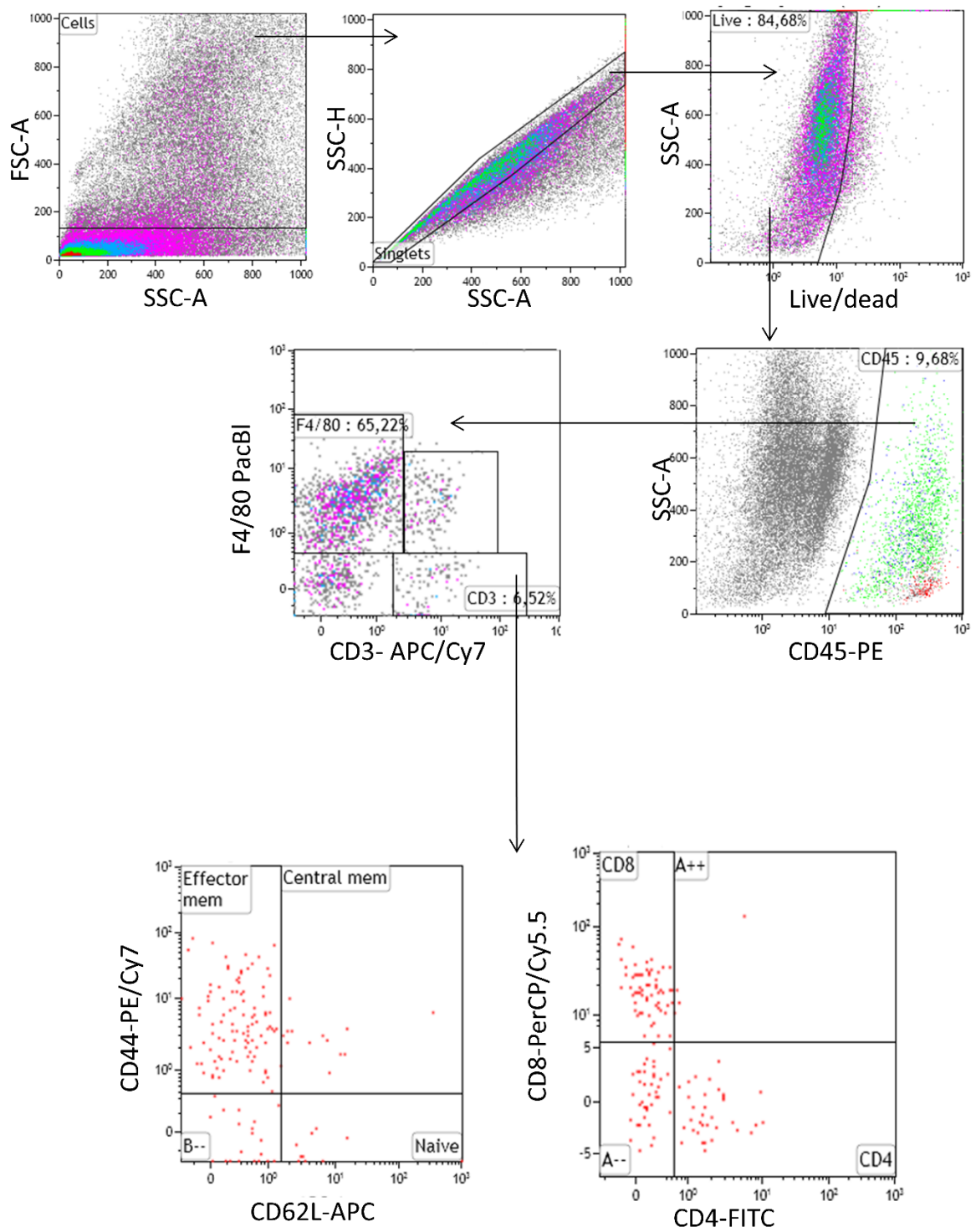


Fig. 11: Flow cytometry gating strategy for the abdominal aortas and spleens of ApoE<sup>-/-</sup> mice in the Salt pre-treated and control group control for T-cells assessment.

Figure 12

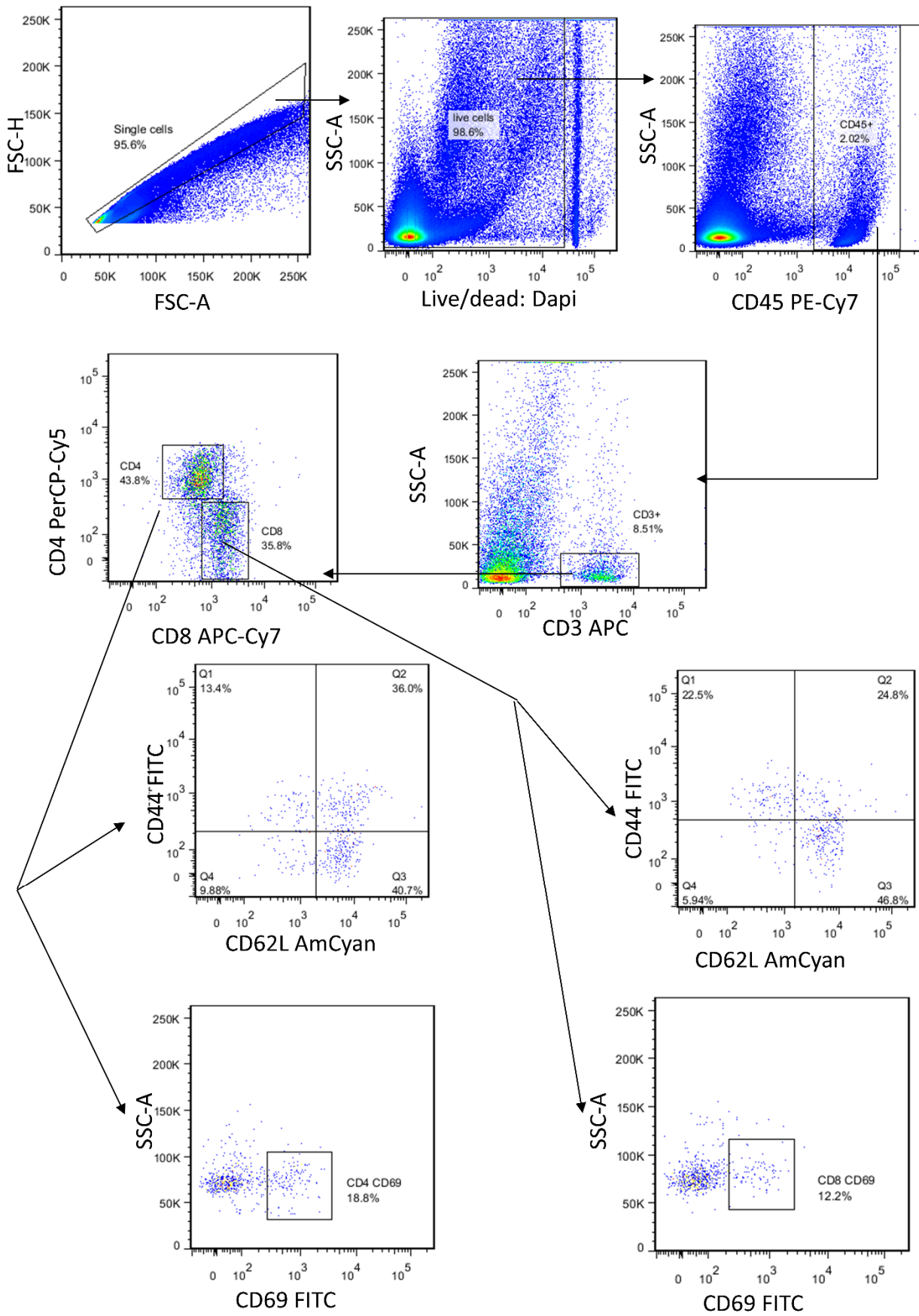


Fig. 12: Flow cytometry gating strategy for aortas of ApoE<sup>-/-</sup> mice treated with C3 or control for T-cells assessment.

Figure 13

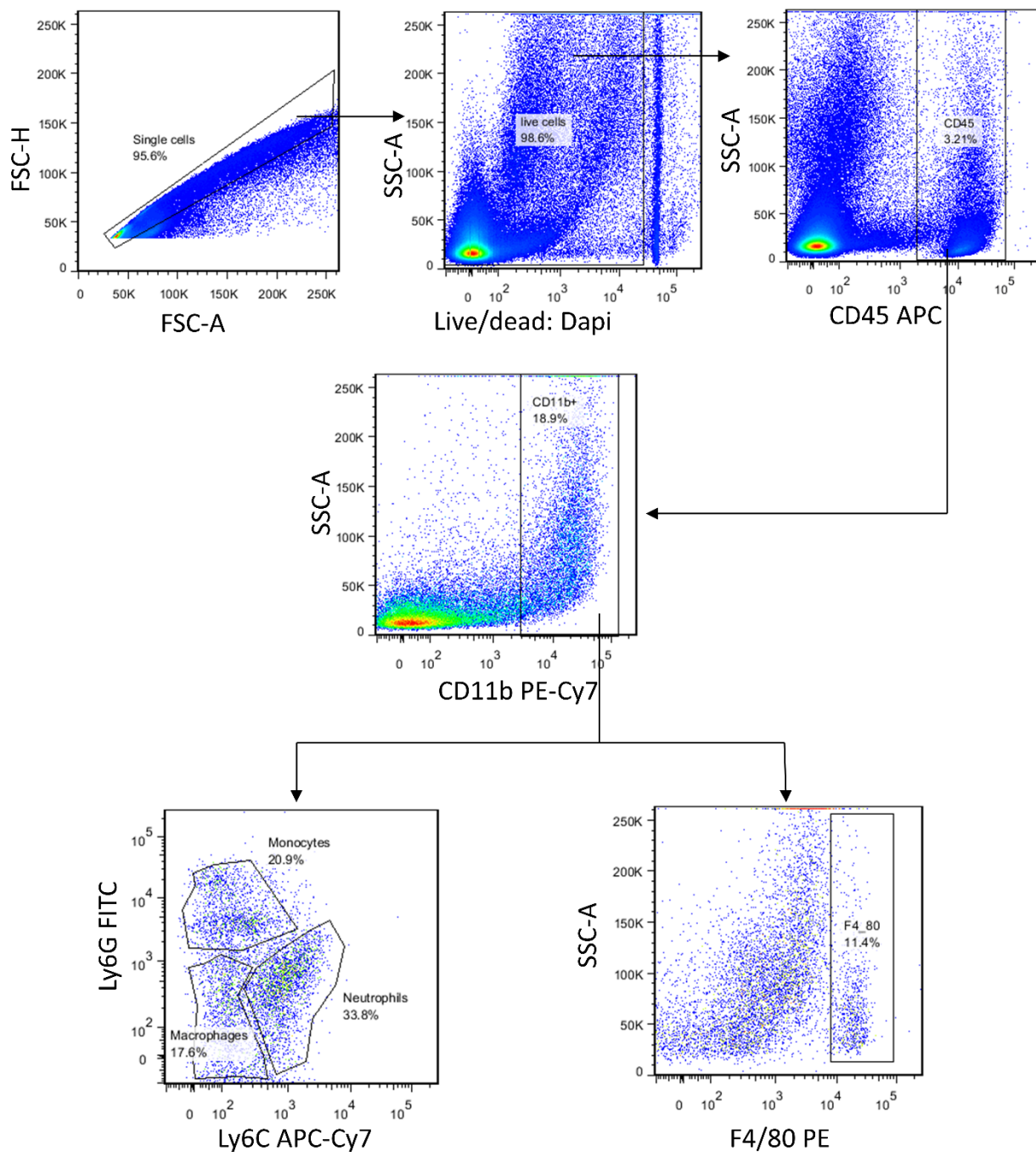


Fig. 13: Flow cytometry gating strategy for the abdominal aortas and spleens of ApoE<sup>-/-</sup> mice in the Salt pre-treated and control group control for macrophages, neutrophils and monocytes assessment.

## **Plasma Cholesterols and Triglycerides measurements**

The plasma concentrations of total circulating cholesterol, low-density lipoprotein (LDL), high-density lipoprotein (HDL) and triglycerides were analyzed spectrophotometrically (Cobas ® 8000 modular analyzer series, Roche, USA) in an in-house facility using the following enzymatic kits; Cholesterol Gen.2, LDL-Cholesterol Gen.3, HDL-Cholesterol Gen.4 and TRIGL (Roche diagnostic, Mannheim, Germany).

## **Isolation of murine splenic naïve CD8 T-cells and their stimulation for differentiation**

To assess the effect of high salt on the differentiation of naïve T-cell, splenic naïve CD8 T-cells were isolated and stimulated to be differentiated into effector CD8 cells. C57BL/6 mice were euthanized and the spleens were dissected and placed in RPMI 1640 (Thermo Fisher, Waltham, MA, USA). The spleen was cut into small pieces then fragmented and passed through 100 µm filter (EASYstrainer™, Greiner bio-one, Solingen, Germany). 5 mL of RPMI 1640 were passed through the filter to ensure the collection of all the cells. Splenic cells were centrifuged (300g, 10 mins, 4°C), resuspended in RPMI medium and incubated for 30 minutes at 37 °C.

Isolation of naïve T-cells was done using naïve CD8+ T-Cell Isolation mouse Kit™ (Miltenyi Biotec, Bergisch Gladbach, Germany) according to producer's protocol. In brief, the splenic cell number was determined using a hemocytometer. Cells were centrifuged (300g, 10 mins, 4°C) and the supernatant was discarded. For each 10<sup>7</sup> total cells, the following procedures were carried out. The cell pellet was resuspended in 40 µL of FACS buffer and then 10 µL of Biotin-Antibody Cocktail were added. The cells were mixed well and incubated for 5 minutes in the refrigerator (2–8 °C). 20 µL of FACS buffer were added, followed by adding 20 µL of Anti-Biotin MicroBeads and then 10 µL of CD44 MicroBeads. The cells were well mixed and incubated for 10 minutes in the refrigerator (2–8 °C). LS Column™ was placed in the magnetic field of a suitable MACS Separator. LS column was prepared by rinsing with 3 mL of FACS buffer. The cell suspension was applied into the column while attached to the magnetic field separator and the flow-through (representing the unlabeled enriched naïve CD8+ T-cells) was collected.

A specific RPMI 1640 medium deprived of Na<sup>+</sup> and K<sup>+</sup> was purchased from cell culture technologies (Ticino, Switzerland) and reconstituted according to the manufacturer's protocol. After reconstitution, 10% FCS, 1% Penicillin/Streptomycin solution, 1% L-Glutamine (Sigma), 1% Non-essential amino acids (NEAA)(Sigma), 1% sodium pyruvate (Sigma) and 50 µM b-Mercaptoethanol (Gibco) were added to the medium. Furthermore, the medium was supplied with different NaCl (VWR chemical, Louvain-la-Neuve, Belgium) and KCl (Sigma) concentrations depending on the experimental design. The reconstituted medium was used throughout the whole experiment.

96 well-plate was coated overnight with aCD3 (BD Pharmingen, BD Biosciences) in a concentration of 2 µg/ml (50 µl per well), and then rinsed 3 times with PBS.

For each well in the 96 well-plate, the following were added:

- 50 µl of plain medium
- 50 µl of 2 µg/ml aCD28 in medium (BD Pharmingen, BD Biosciences)
- 50 µl of medium containing different NaCl concentration
- 50 µl of medium containing 100.000 cells of naive CD8+ T-cells.

Cells were incubated in the 96 well-plate for 4 days at 37 °C and afterwards, the supernatant was collected. To determine the relative percentage of naïve cells which were polarized into CD8 effector cells, IFN $\gamma$  concentration was evaluated in the supernatant of the cells. IFN $\gamma$  was used as a marker for CD8+ effector cells (T<sub>c</sub>) development. IFN $\gamma$  concentration was determined using mouse IFN $\gamma$  Quantikine ELISA kit (R&D Systems). Quantikine ELISA kits were used according to the manufacturer's protocol. In brief, a serial dilution of the standard was prepared. The supernatant was diluted with assay diluent. Standard, ELISA control, and supernatant samples were applied in a readily antibody-coated well-plate. Wells were washed several times and a colorant conjugate was added to the wells. The reaction was stopped after 25 min and the plate was placed in a plate reader (Multimode Detector DTX 880, Beckman Coulter, California, USA) to measure the absorbance of each well. A concentration to absorbance correlation curve was established for the standard. The relative concentration of cytokines in the supernatant was deduced from the standard curve.

### **mRNA quantification and assessment by qPCR**

qPCR measurements were carried out to determine the relative abundance of the expressed mRNA. RNA content in the tissue was isolated using RNeasy® plus mini kit. The manufacturer's protocol was followed. In brief, tissues were transferred to RLT solution with 10%  $\beta$ -mercaptoethanol and then ruptured for 30-40 seconds. The ruptured tissue in the solution was centrifuged for 3 mins at 21000 g. The supernatant was taken and placed in genomic DNA (gDNA) eliminator column and shortly centrifuged at 8000 g to get rid of genomic content. gDNA column was discarded and then 70 % ethanol was added to the eluted and mixed. The mixture was transferred into an RNA column and centrifuged shortly at 8000 g. The eluent was discarded, and the RNA column was washed twice with 350 µL of RW1 buffer for carbohydrates protein and other impurities removal. DNase enzyme was added to the column and the column was incubated at room temperature for 15 minutes to make sure all gDNA is broken down. The column was washed twice with 500 µl RPE buffer to remove salt impurities. The column was centrifuged twice for 2 min at the maximum speed to get rid of any liquid. 50 µl of RNase free water was put into the

column and centrifuged for 1 minute to obtain the purified RNA content. The amount of RNA was quantified spectrophotometrically.

In order to obtain the complementary DNA (cDNA), QuantiTect® Reverse Transcription kit was used. Isolated RNA of similar concentration was incubated with 2 µL of gDNA wipeout buffer at 42°C for 2 min to remove any remaining genomic DNA. 0.5 µL of the isolated RNA from each sample was taken to be checked with polymerase chain reaction (PCR). A master mix of Quantiscript reverse transcriptase, Quantiscript RT buffer and RT primer was made. The master mix was added to the isolated RNA samples and incubated at 42°C for 2 min and then at 95° C for 3 minutes to acquire the cDNA. Glyceraldehyde phosphate 3-dehydrogenase (GAPDH) primer was used as a control during PCR.

For qPCR, a master mix was made. The master mix includes 10 µL/well sybr green master mix, 0.1 µL/well forward and 0.1 µL/well reverse primers and 8.8 µL/well RNase free water. The master mix was pipetted into a 96 well plate followed by 1 µL/well cDNA. Proper mixing of all components in the well was carried out. The plate was sealed, and qPCR run was done with 7300 Real-time PCR system (Thermofisher, Waltham, USA)

The thermal cycles of qPCR were conducted as followed:

Stage	Repetitions	Temperature	Time
1	1	95.0 °C	15:00
2	40	95.0 °C	00:15
		58.0 °C	00:30
		72.0 °C	00:30
		76.0 °C	00:34
3 (Dissociation)	1	95.0 °C	00:15
		60.0 °C	01:00
		95.0 °C	00:15
		60.0 °C	00:15

The quantification of mRNA was based on the fluorescence threshold (Threshold cycle, CT value). The CT value is the cycle of PCR at which the reporter fluorescence significantly exceeds background fluorescence. The expression of the target mRNA was normalized with the housekeeping gene GAPDH to calculate the relative expression of the mRNA. Relative expression of mRNA is measured in arbitrary units. Further normalization with the control group was done to get more relevant comparative analysis.

qPCR Primers (Eurofins genomics, Germany) used were as the following:

- GAPDH:  
Forward:GTGTTCCCTACCCCAATGTGT  
Reverse: GTCCTCAGTGTAGCCCAAGATG
- ANP:  
Forward: CTGGGCTTCTTCCTCGTCTT  
Reverse: CCTCATCTTCTACCGGCATCT
- BNP:  
Forward: AAGGTGCTGTCCCAGATGATT  
Reverse: CCATTTCTCCGACTTTTCTC
- FN:  
Forward: CGAGGTGACAGAGACCACAA  
Reverse: CTGGAGTCAAGCCAGACACA
- $\beta$ MHC  
Forward: GGCAGAGCAGGACAACCTC  
Reverse: AGGTCCGCGTTCACCTCCT
- Coll-1:  
Forward: ATCTCCTGGTGCTGATGGAC  
Reverse: ACCTTGTTTGCCAGGTTTCCAC
- TNF $\alpha$ :  
Forward: ATGTCTCAGCCTCTTCTCATTC  
Reverse: GTCTGGGCCATAGAACTGATGA
- TGF $\beta$ :  
Forward: GCTGCGCTTGCAGAGATTAAAA  
Reverse: CGTCAAAGACAGCCACTCA
- IL-6:  
Forward: CAGAGGATACCACTCCCAACA  
Reverse: GCCATTGCACAACTCTTTTCTC
- IL17a:  
Forward: GGCCCTCAGACTACCTCAACC  
Reverse: TGAGCTTCCCAGATCACAGAG
- IL1b:  
Forward: GGATGAGGACATGAGCACCTT  
Reverse: CTAATGGGAACGTCACACACC

## **Isolated kidney perfusion**

Isolated kidney perfusion experiments were performed to test the direct effect of propionate on vascular function. C3 treated and control ApoE<sup>-/-</sup> were euthanized after 28 days chronic Ang II (500 ng/kg/min) infusion. Aorta was exposed and the blood flow was partially blocked by making a knot above the renal artery using surgical sutures and clamping the rear lower end of the aorta. A small incision was made in the abdominal aorta, a cannula was inserted, and the knot was tightened around the cannula. The cannula was connected to the flowing system with Krebs solution as a vehicle and the left renal vein was ruptured. Krebs solution was pushed through to flush the kidney. Fat, kidney capsule and other tissues were carefully removed from the kidney and the renal arteries. Two catheters were inserted in the renal arteries and tied firmly using sutures. The catheter with the kidney was dissected and connected to the perfusion circuit. Krebs–Henseleit solution was constituted in-house and used as the running buffer. Pressure resistance to the Krebs–Henseleit solution was recorded. Norepinephrine (1µM; Sigma Aldrich) was used to induce pre-contraction.

In order to test the direct effect of Propionate (C3) on endothelial functions, the kidneys from Ang II-infused ApoE<sup>-/-</sup> mice treated with C3 and control were isolated and perfused. Afterwards, pre-contraction of the kidneys with norepinephrine was done, and kidneys were subjected to an incremental concentration of carbachol. Vasorelaxation percentage of norepinephrine mediated pre-contraction was assessed for the kidneys of the 2 groups. Experiments were done in cooperation with Dr. Sascha Höges

## **Assessment of vascular stiffness by Single cell atomic Spectroscopy**

Assessment of vascular stiffness were carried out in cooperation with Prof. Dr. Kristina Kusche-Vihrog and Dr. Martina Maase (Schierke et al. 2017. Sci Rep). Determination of the cortical stiffness (as an indicator for vascular function) was done by assessment of mechanical stiffness and thickness of the endothelium. ApoE<sup>-/-</sup> mice were treated with 200mM sodium propionate (C3) in the drinking water or normal tap water for 5 days. Afterwards, the mice were anesthetized by isoflurane inhalation and then they were euthanized by cervical dislocation. The thorax was opened, and the thoracic aorta was dissected. PVAT and connective tissue were removed. Aortas samples were glued on coverslips using Cell-Tak™ (BD Biosciences, San Jose, USA) and then cultured at 37 °C and 5% CO<sub>2</sub> in minimal essential medium (MEM, Invitrogen, Carlsbad, USA) containing 1% MEM vitamins (Biochrom, Berlin, Germany), penicillin G (10,000 U/mL), streptomycin (10,000 µg/mL) and 1% MEM non-essential amino acids (MEM NEAA, Gibco, Thermo Fischer, Waltham, USA).

For assessment of vascular stiffness, analysis of the force-distance curves of single endothelial cells was performed. A scanning probe microscope (MultiMode® SPM, Bruker, Karlsruhe, Germany) with a feedback-controlled heating device (Bruker) was used to appraise the endothelium of the aorta. The aortas were immersed in HEPES-buffered solution (standard composition in mM: 135 NaCl, 5 KCl, 1 MgCl<sub>2</sub>, 1 CaCl<sub>2</sub>, 10 HEPES (N-2-hydroxyethylpiperazine-N' -2-ethanesulfonicacid) during measurement. AFM nano-indentation measurements were done using soft cantilevers (spring constant: < 20 pN/nm; Novascan, Ames, IA, USA) with a polystyrene sphere as the tip (diameter: 10 μ m). A maximal loading force of 2 nN was applied. Obtained AFM data were collected with NanoScope softwares 5.31 and V8.10 (Bruker). Stiffness and thickness values were calculated from force-distance curves using the Protein Unfolding and Nano-Indentation Analysis Software PUNIAS.

## **Computational analysis**

ImageJ software was used for measuring the length, area or pixels from microscopical images. Measurements were used to compare subjects from different groups. ImageJ is open-source software developed by the National Institutes of Health and the Laboratory for Optical and Computational Instrumentation (Schneider CA et al. 2012, Nat Methods).

## **Statistical analysis**

To obtain comparative analysis between groups, a one-tailed unpaired t-test or one-tailed Mann-Whitney test was used. Unpaired t-test was used when a Gaussian distribution was assumed while Mann Whitney test was considered when a non-Gaussian distribution was assumed. Depicted data were calculated as median ± standard deviation or as mean ± SEM. Outliers were excluded when necessary. Outliers were identified by Grubbs' test. Normalization of the raw data was done in some experiments to obtain more statistically meaningful comparisons. Exact n-numbers are shown in the respective figures. The survival of the mice was visualized by Kaplan-Meier curves and statistically compared by using a one-tailed Log-rank test. A significant difference was considered when p-value <0.05. The significant difference was represented by an asterisk (\*). Statistical analysis and graphical representation were done by GraphPad Prism 6.

## 4 Results

### **Part I: Effect of short chain fatty acids on Atherosclerosis**

To investigate the effect of short chain fatty acids (SCFA) on atherosclerosis, ApoE<sup>-/-</sup> mice were treated with the SCFA, propionate (C3) (200 mM in the drinking water) or NaCl (control) (200 mM in the drinking water) for the whole experimental period. After 5 days of C3 or NaCl treatment, minipumps containing Ang II (500 ng/Kg/min) were implanted. After 28 days, the mice were sacrificed for the assessment of atherosclerosis, vascular function, and immune responses.

### **C3 increased significantly the survival rate of the Ang II infused mice**

The survival rate of Ang II infused ApoE<sup>-/-</sup> mice which were treated with C3 was significantly higher than the control group. During chronic Ang II infusion, none of the mice which were treated with C3 died while 64 % of the control group died (figure 14). The survival rate of C3 group suggests a protective effect of C3.

Figure 14

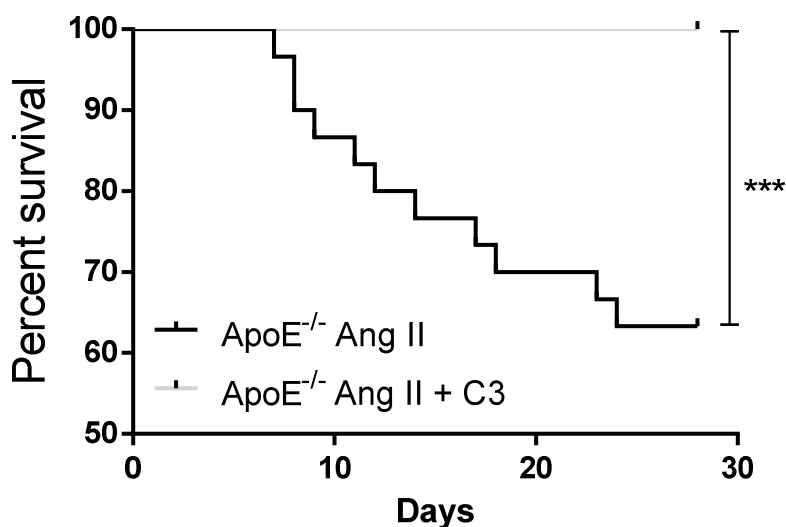


Fig. 14: The cumulative survival rate of C3 treated mice and control after Ang II minipumps implantation. n=30 per group. \*\*\*P<0.001, by log-rank test

### **C3 did not change the body weight or the lipid profile**

The bodyweight of C3 treated and control mice was evaluated after chronic Ang II infusion. No differences between the two groups were found (figure 15). Moreover, the lipid profile of the mice in the two groups including HDL, LDL, and triglycerides was assessed. No differences were noticed in the lipid profile between Ang II-infused mice in the two groups (table 1). This observation implies that chronic C3 treatment was well tolerated and did not influence the lipid deposition in mice.

**Figure 15**

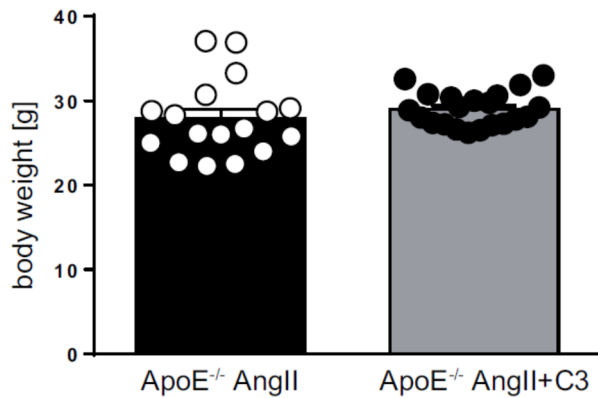


Fig. 15: Body weights of Ang II-infused ApoE<sup>-/-</sup> mice treated with C3 or control, ApoE<sup>-/-</sup> Ang II n=17, ApoE<sup>-/-</sup> Ang II +C3 n=21.

**Table 1**

		ApoE <sup>-/-</sup> Ang II	ApoE <sup>-/-</sup> Ang II + C3	p-value
Total cholesterol	(mg/dL)	379,4 ± 44,97	432,6 ± 54,13	0.4938
Triglycerides	(mg/dL)	92,60 ± 14,94	136,7 ± 35,82	0.3473
HDL	(mg/dL)	80,60 ± 4,007	85,57 ± 5,246	0.5007
LDL	(mg/dL)	265,6 ± 45,62	299,7 ± 45,90	0.6206

Table 1: Serum levels of total cholesterol, HDL cholesterol, LDL cholesterol and triglycerides were measured in Ang II-infused ApoE<sup>-/-</sup> mice treated with C3 (n=7) or control (n=5).

### **C3 reduced the deposition of atherosclerosis in the aortas**

To determine whether C3 affects atherosclerosis, we performed *en face* Oil Red O staining on whole aortas of Ang II infused ApoE<sup>-/-</sup> mice from the C3 group and control group. Aortas of C3 treated mice had significantly fewer atherosclerotic plaques compared to the aortas of the mice of the control group as shown in figure 16. Furthermore, the aortas of C3 treated mice had significantly smaller diameter compared to the control mice (1.013 mm ± 0.052 n=9 vs 1.389 mm ± 0.1775 n=7, p<0.05).

Figure 16

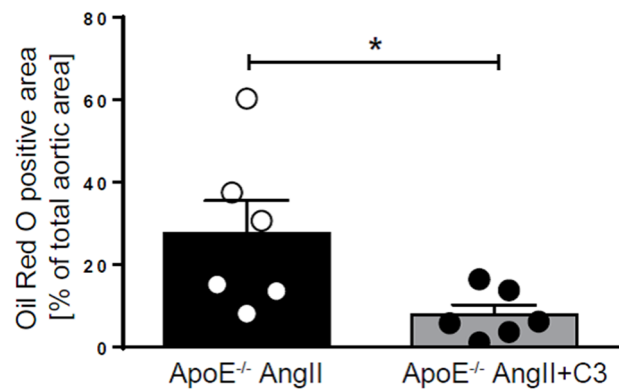
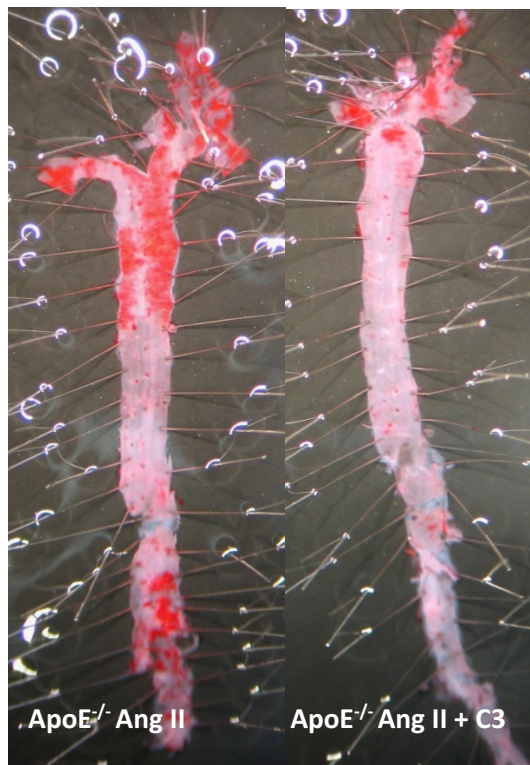


Fig. 16: En face Oil Red O staining of whole aortas for the quantification of atherosclerotic lesion burden. A: Representative images of the aortas of C3 treated and control mice. B: Quantification of the atherosclerotic plaques. n=6 per group. \*P<0.05, by 1-tailed t test.

### C3 reduced the stenosis in the brachiocephalic artery.

To validate the effect of C3 on the reduction of atherosclerosis, assessment of stenosis in the brachiocephalic artery was carried out. After 28 days of Ang II infusion, the brachiocephalic arteries from the ApoE<sup>-/-</sup> mice in the C3 group and the control group were collected, fixed, paraffinized and cut in transverse sections. Movat staining revealed that the maximum stenosis was significantly lower in the C3 treated mice compared to the control group as shown in figure 17. These results show that chronic C3 treatment reduces the development of atherosclerosis.

Figure 17

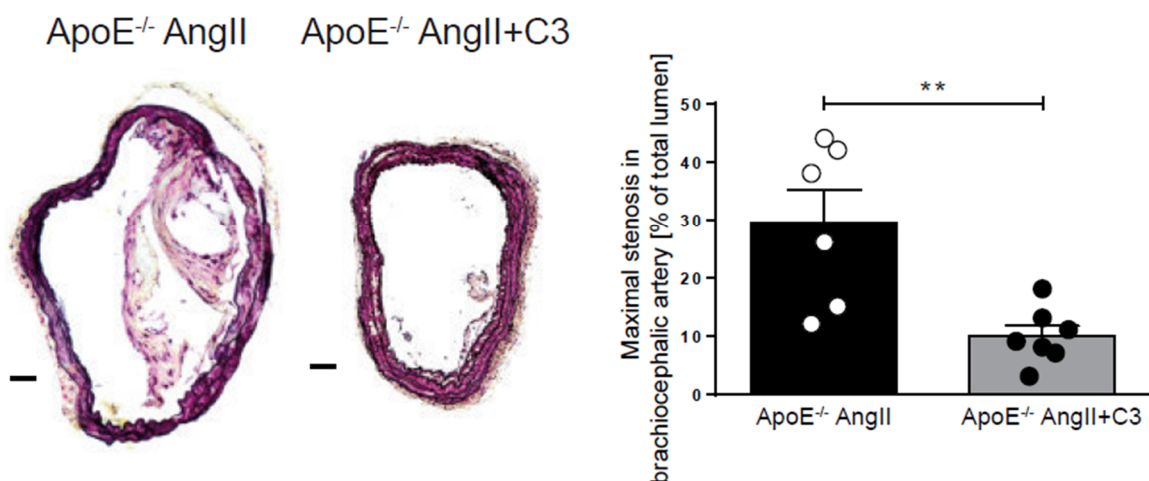


Fig. 17: The degree of stenosis in the brachiocephalic artery was determined in Movat-stained cross-sections. A: Representative sections (scale bar=100  $\mu$ m) from the brachiocephalic artery of C3 treated and control mice. B: Quantification of maximal stenosis, ApoE<sup>-/-</sup>-Ang II n=6, ApoE<sup>-/-</sup>-Ang II+C3 n=8. \*\*P<0.01, by 1-tailed t test. scale bar=100  $\mu$ m

## Immune cells infiltration and distribution in the aorta were confirmed by immunohistochemical imaging of the brachiocephalic artery

Since CD3+ T-cells and F4/80+ macrophages play a key role in the formation of atherosclerosis (Gisterå et al. 2017. Nat Rev Nephrol), we performed immunohistochemical staining on the brachiocephalic artery using antibodies against CD3 and F4/80. As shown in figures 18 and 19, CD3+ and F4/80+ cells were less in the atherosclerotic plaques and the vascular tissue of brachiocephalic arteries of C3 treated mice versus the control group after Ang II infusion. This observation indicates that C3 reduces inflammation in the vascular tissue.

**Figure 18**

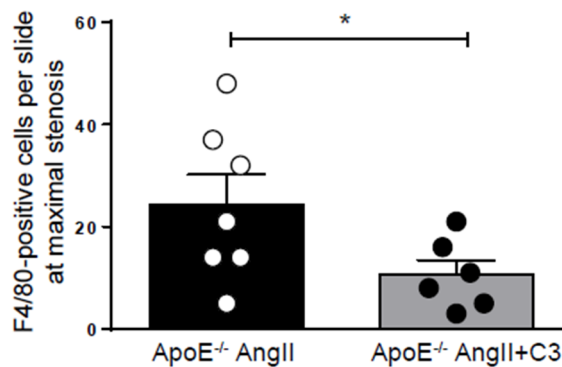
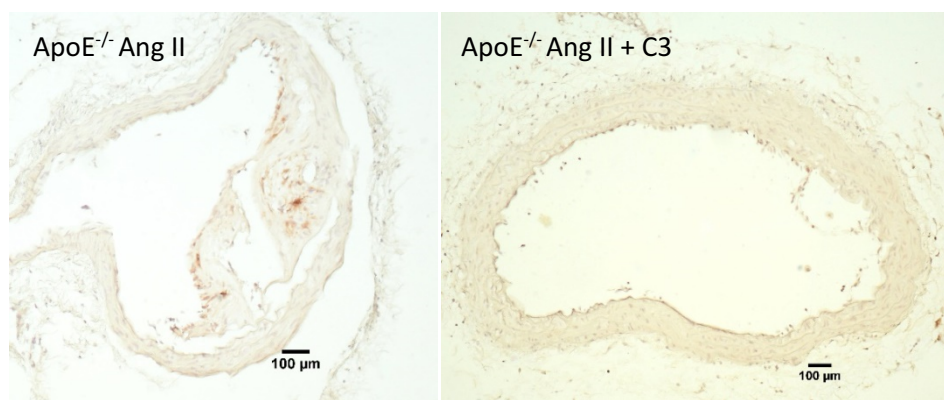
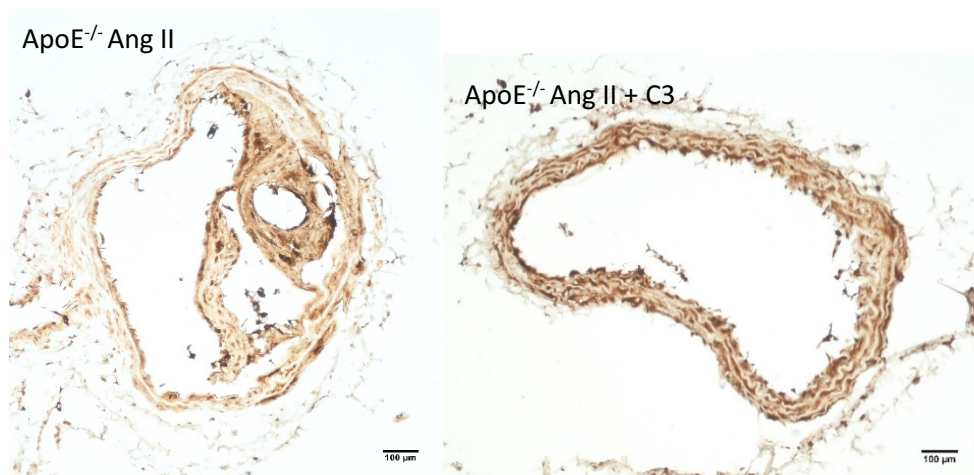


Fig. 18: Histochemical quantification of F4/80+ in sections of the brachiocephalic artery of C3 treated and control mice. ApoE<sup>-/-</sup>Ang II n=7, ApoE<sup>-/-</sup> Ang II+C3 n=6. \*P<0.05 by 1-tailed t test. scale bar=100 µm

**Figure 19**



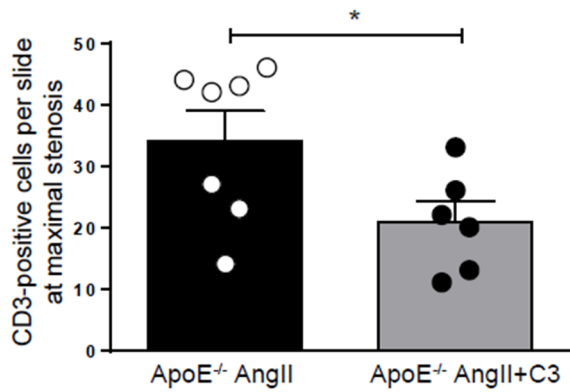


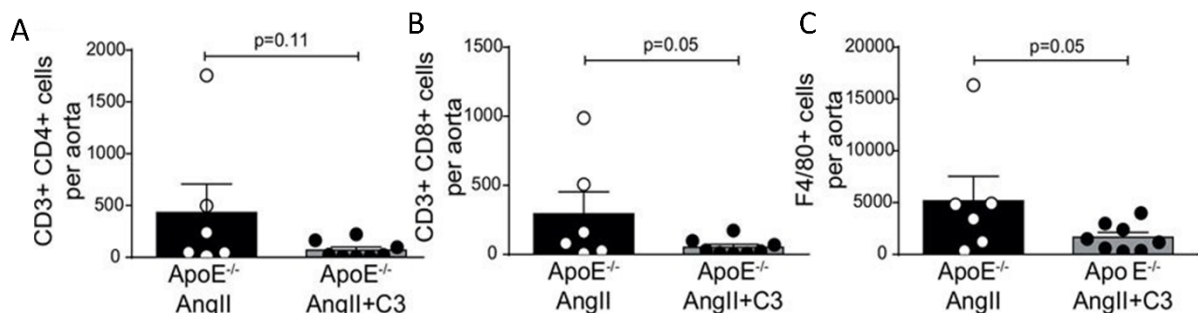
Fig. 19: Histochemical quantification of CD3+ in sections of the brachiocephalic artery of C3 treated and control mice. ApoE<sup>-/-</sup>-Ang II n=7, ApoE<sup>-/-</sup>- Ang II+C3 n=6. \*P<0.05, by 1-tailed t test. scale bar=100  $\mu$ m

### C3 decreased the number of immune cells infiltrated in the aortas

To further analyze the effect of C3 treatment on T-cells and macrophages infiltration into the vasculature, we performed flow cytometric analysis on the aortas of Ang II-infused C3 and control mice. F4/80+ macrophages in the aortas were less in the C3 treated mice compared to the control group as shown in figure 20. Flow cytometry assessment also showed a decrease in the number of CD3+ T-cells (in particular CD4+ and CD8+ T-cells) in the aortas of the C3 treated group compared to the control group. CD4 T-cells subpopulations were further investigated. The aortas of the mice in the C3 group have significantly less CD4 effector memory T-cells (CD44+ CD62L-) and significantly more CD4 naïve T-cells (CD44- CD62L+) in comparison to the control group (figure 20). No change was observed in CD4 central memory T-cells (CD44+ CD62L+) subpopulation between the two groups (figure 20). Although CD8 T-cells were less in the aortas of the C3 treated mice compared to the control group, no differences were noticed in CD8 subsets frequencies between the two groups (figure 20).

Combining the flow cytometry with the immunohistochemical analysis, the present results suggest a sustained anti-inflammatory effect of C3 in atherosclerosis.

Figure 20



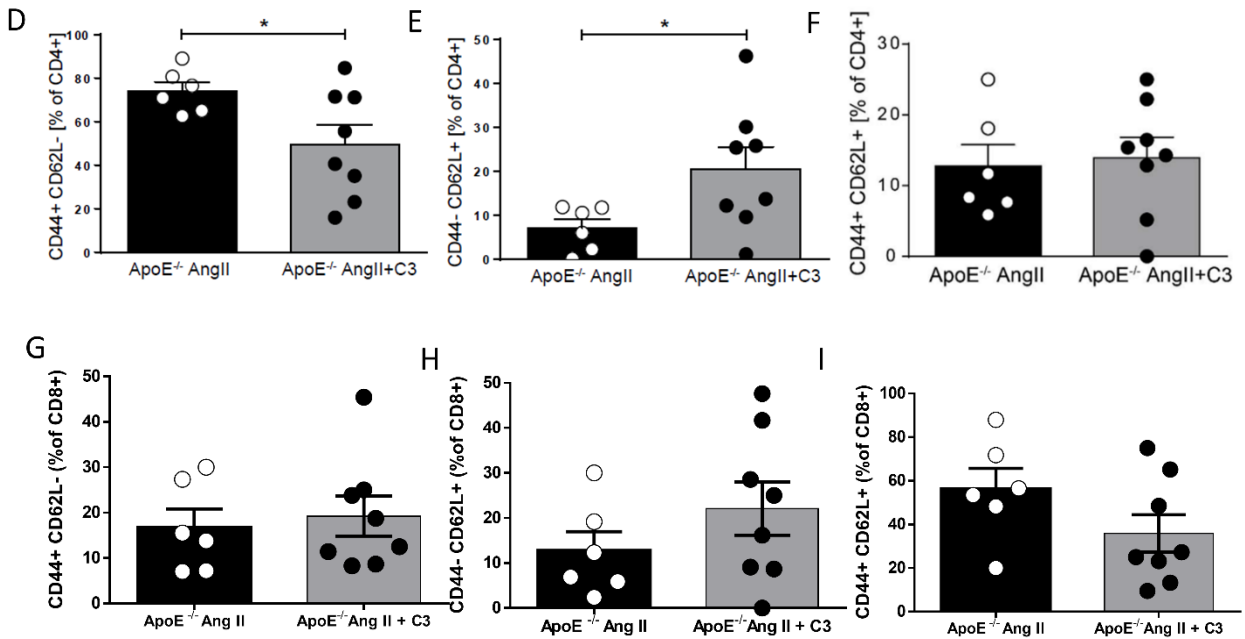


Fig. 20: Flow cytometric quantification of the aortas of ApoE<sup>-/-</sup> mice treated with C3 or control for T helper (CD3+CD4<sup>+</sup>)(A), cytotoxic T cells (CD3+CD8<sup>+</sup>)(B), and macrophages (F4/80<sup>+</sup>)(C). Further cytometric analysis was carried out for effector memory (CD44<sup>+</sup> CD62L<sup>-</sup>)(D & G), central memory (CD44<sup>+</sup> CD62L<sup>+</sup>)(F & I) and naïve (CD44<sup>-</sup> CD62L<sup>+</sup>) (E & H) of both CD4<sup>+</sup> and CD8<sup>+</sup> T-cell frequencies in the aortas of C3 treated and control mice. ApoE<sup>-/-</sup> Ang II n=6, ApoE<sup>-/-</sup> Ang II+C3 n=8. \*P<0.05, by 1-tailed t test.

### C3 modulated the splenic immune cells signature

Th17 and regulatory T-cell (T<sub>reg</sub>) are subsets of CD4 T-cells that are involved in atherosclerosis (Xie et al. 2010. Cytokine). Due to the relatively low number of immune cells infiltrated in the aorta compared to the spleen, the possibility to assess all immune subsets was limited. In order to verify the results obtained from flow cytometry analysis of the aorta and further investigate the effect of C3 on the T-cell subsets (such as Th17, Th1, and T<sub>reg</sub>), we did flow cytometric analysis on spleens of Ang II-infused C3 and control mice.

Flow cytometric analysis carried out on the spleen showed the same pattern observed in the aorta. After 28 days of Ang II infusion, C3 significantly decreased the CD4 effector memory T-cells (CD44<sup>+</sup> CD62L<sup>-</sup>) and increased the production of CD4 naïve T-cells (CD44<sup>-</sup>CD62L<sup>+</sup>) in comparison to the control group as shown in figure 21. No difference in the percentage of splenic CD4 central memory T-cells (CD44<sup>+</sup> CD62L<sup>+</sup>) out of CD4<sup>+</sup> T-cells was found between the C3 treated and control mice. Furthermore, flow cytometric analysis of splenic CD8 T-cells showed no

differences in the subpopulations of CD8 T-cells between the 2 groups (figure 21). In addition, C3 treated mice showed significantly lower proportions of splenic FoxP3-ROR $\gamma$ t+ Th17 cells compared to control groups. No significant differences in the T<sub>regs</sub> or Tbet+ Th1 T-cells were observed between the two groups (figure 22)

**Figure 21**

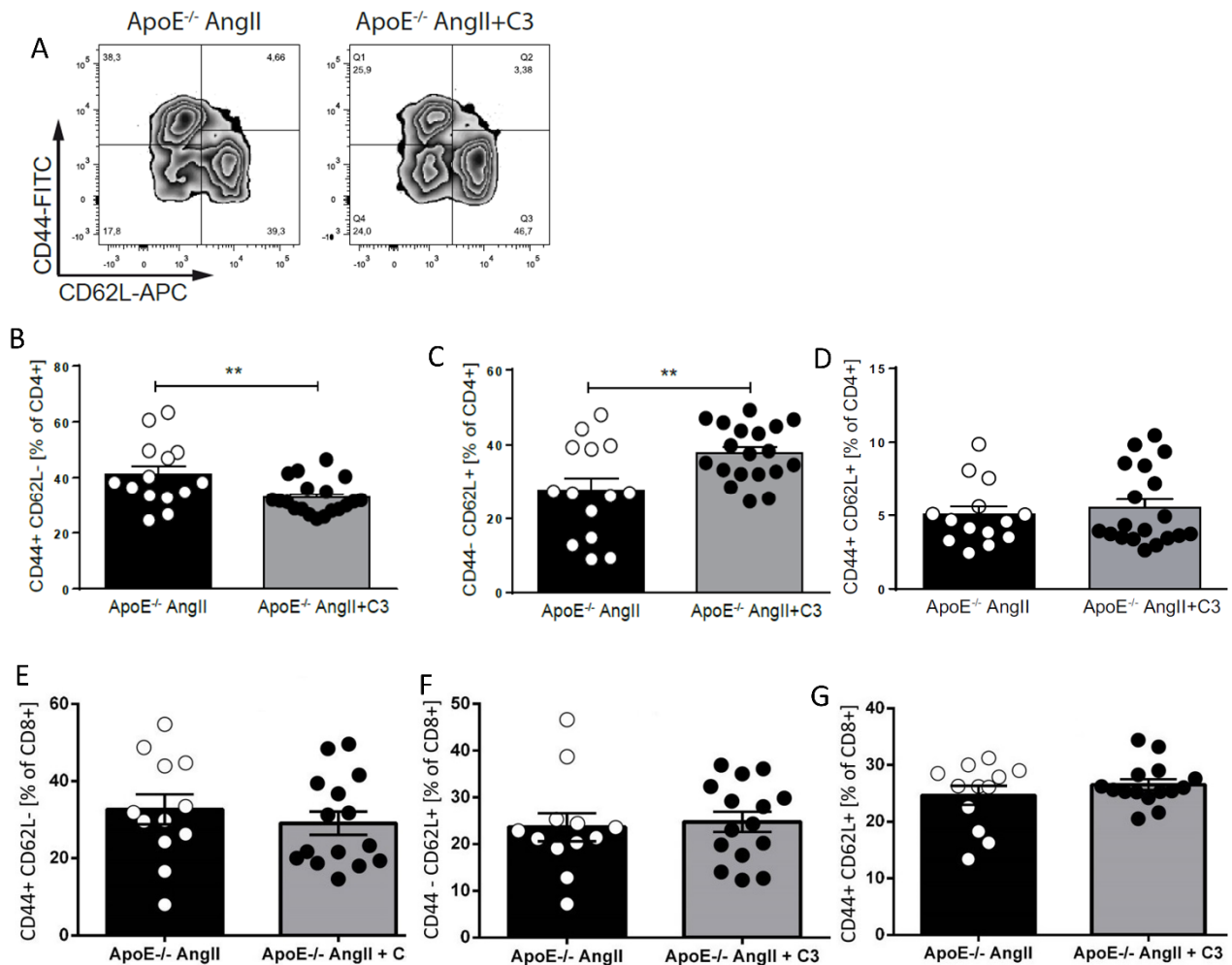


Fig. 21: After Ang II infusion, splenocytes were analysed for effector memory (CD44+CD62L-)(B &E), central memory (CD44+CD62L+) (D &G) and naive (CD44-CD62L+) (C & F) frequencies of CD4 and CD8 subsets. A: Representative flow cytometry plots. ApoE<sup>-/-</sup> Ang II n=12, ApoE<sup>-/-</sup> Ang II+C3 n=15. \*\*P<0.01, by 1-tailed t test.

**Figure 22**

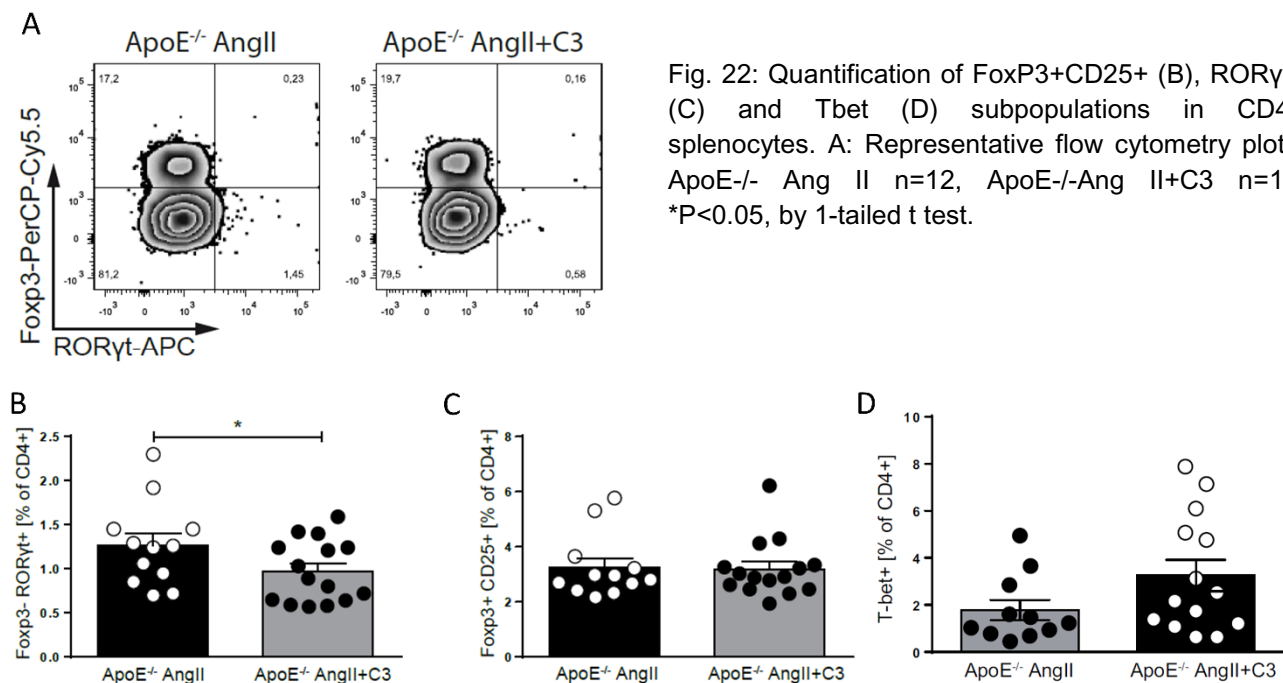


Fig. 22: Quantification of FoxP3+CD25+ (B), RORγt+ (C) and Tbet (D) subpopulations in CD4+ splenocytes. A: Representative flow cytometry plots. ApoE<sup>-/-</sup> Ang II n=12, ApoE<sup>-/-</sup>Ang II+C3 n=15. \*P<0.05, by 1-tailed t test.

### C3 reduced cardiac hypertrophy and fibrosis

To assess whether C3 ameliorates Ang II-induced cardiac hypertrophy, heart to bodyweight index of Ang II-infused ApoE<sup>-/-</sup> mice from C3 and control group was evaluated. Cardiac hypertrophy was significantly lower in C3 treated mice compared to the mice from the control group as shown in figure 23.

Cardiac fibrosis is a parameter of cardiac disease. To evaluate the influence of chronic C3 treatment on the hearts of the Ang II-infused mice, cardiac fibrosis was assessed in C3 treated and control mice. Hearts from C3 mice have significantly less collagen content in comparison to the hearts of the control group (figure 24), suggesting that C3 treatment reduced cardiac fibrosis.

**Figure 23**

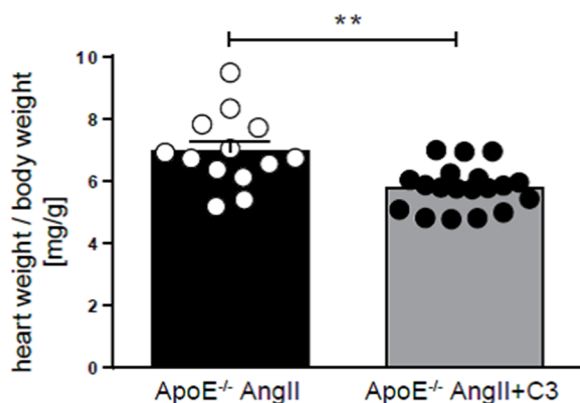
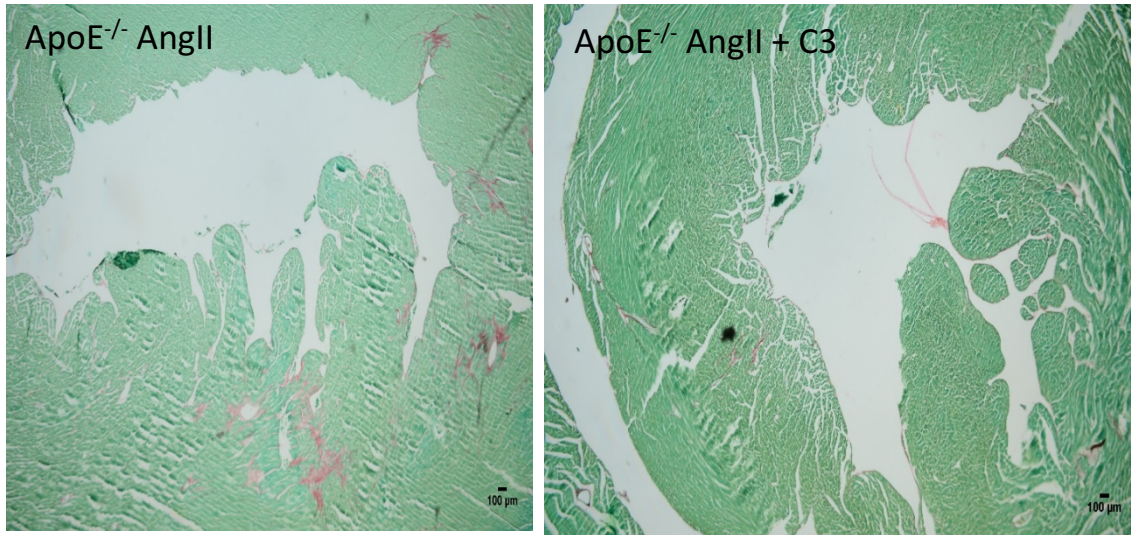


Fig. 23: Cardiac hypertrophy index (heart weight [mg]/body weight [g]) of Ang II-infused ApoE<sup>-/-</sup> mice treated with C3 or control was assessed. ApoE<sup>-/-</sup> Ang II n=16, ApoE<sup>-/-</sup> Ang II+C3 n=21. \*\*P<0.01, by 1-tailed t test.



**Figure 24**

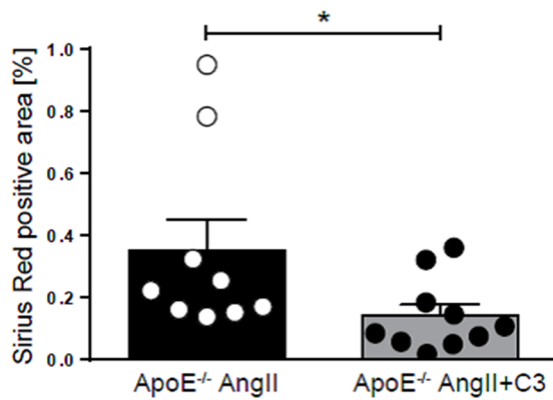


Fig. 24: Left ventricular cardiac fibrosis analysed by Sirius red staining for C3 treated and control mice. A: Representative photomicrographs (scale bar=100 µm). B: Quantification of collagen percentage to non-collagen area. ApoE<sup>-/-</sup> Ang II n=9, ApoE<sup>-/-</sup> Ang II+C3 n=10. \*P<0.05, by Mann-Whitney test

### **C3 improved Ang II-induced heart damage**

Relative mRNA expression of cardiac injury markers was assessed in cardiac tissue of ApoE<sup>-/-</sup> mice of the C3 treated and control group. The relative expression of ANP, BNP, and BMHC was significantly lower in the hearts of C3 treated mice compared to the control mice, as shown in figure 25.

Figure 25

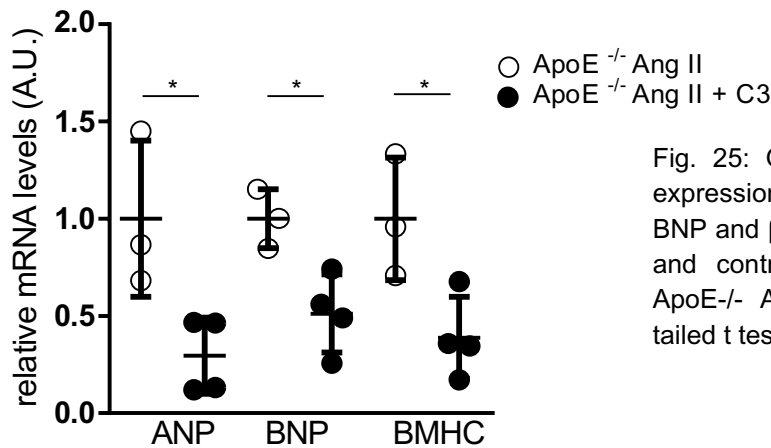


Fig. 25: Quantification of relative mRNA expression of the cardiac markers ANP, BNP and  $\beta$ MHC in the hearts of C3 treated and control mice. ApoE<sup>-/-</sup> Ang II n=3, ApoE<sup>-/-</sup> Ang II+C3 n=4. \*P<0.05, by 1-tailed t test.

### C3 decreased the induced hypertension

Recently, it was described that SCFA has direct blood pressure-lowering effects (Pluznick. 2017. Curr Hypertens), therefore we wanted to assess the blood pressure-lowering effect of C3 on Ang II infused ApoE<sup>-/-</sup> mice. Blood pressure was measured by using the cuff tail method during the fourth week after the implantation of the Ang II minipumps. The Ang II-induced hypertension was attenuated in C3 treated mice compared to control mice (figure 26).

Figure 26

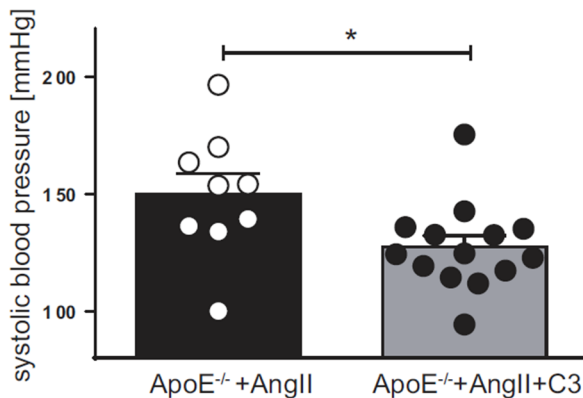


Fig. 26: Systolic blood pressure assessment via tail cuff method of C3 treated and control mice. ApoE<sup>-/-</sup> Ang II n=9, ApoE<sup>-/-</sup> Ang II+C3 n=14. \*P<0.05, by 1-tailed t test.

### C3 induced vasorelaxation in the isolated perfused kidneys

To test the direct effect of C3 on endothelial functions, kidneys from Ang II infused ApoE<sup>-/-</sup> mice treated with C3 or control were isolated and perfused. Chronic C3 treatment improved endothelial-dependent renal vasorelaxation significantly (figure 27).

Figure 27

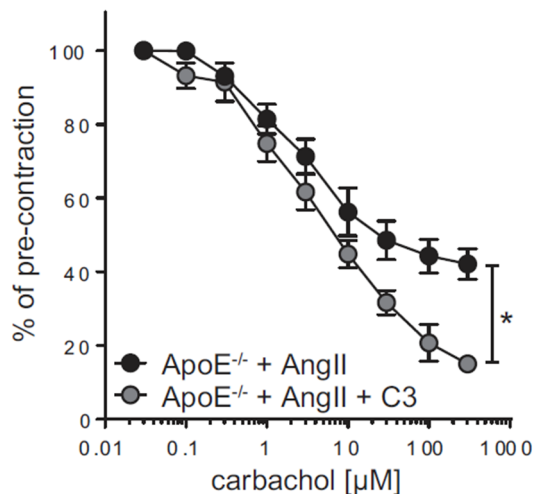


Fig. 27: Response of isolated perfused kidney from C3 treated and control mice to incremental doses of carbachol after pre-contraction with norepinephrine. \*P<0.05, by 1-tailed t test.

### Short term treatment of C3 decreases aortic stiffness

To further analyze the protective effects of C3 on vascular function, we performed atomic force microscopy on the aortas of C3 treated and control mice. To assess aortic stiffness, atomic force microscopy-based nanoindentation measurements were performed on the cortex of aortic endothelial cells of mice which were treated with C3 (or NaCl; control) for 5 days. None of the mice in this experiment was infused with Ang II. 5 days of C3 treatment significantly softened the endothelial cells compared to control treatment, as shown in figure 28.

Figure 28

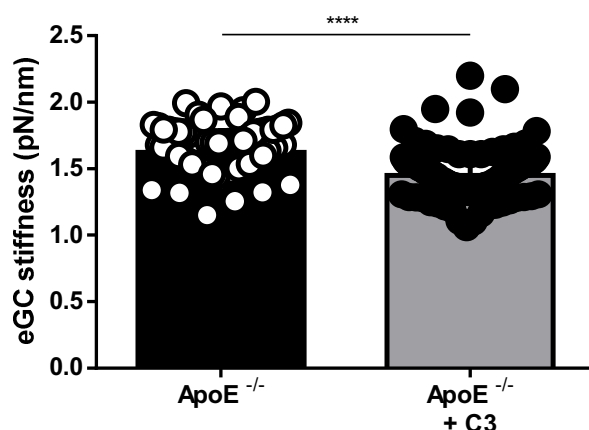


Fig. 28: Atomic force microscopy was performed on the endothelial cortex of the aortas of ApoE<sup>-/-</sup> mice and ApoE<sup>-/-</sup> mice supplied with C3 for 5 days. n=5 for each group and 20 measurement per mouse was carried out. \*\*\*\*P<0.0001, by 1-tailed t test.

## **Part II: Effect of high salt intake on Abdominal Aortic Aneurysm**

To study salt-mediated effects on Ang II-induced abdominal aortic aneurysm (AAA), ApoE<sup>-/-</sup> mice were supplied with 1 % salt in the drinking water for two weeks and then returned to normal tap water. One week after salt discontinuation, the mice were implanted with osmotic minipumps filled with Ang II (1000 ng/kg/min). MRI scans were performed at different time points at baseline and after implantation of the minipumps. After 10 days of Ang II infusion, mice were euthanized, and the assessment of inflammatory responses was carried out. Control mice underwent the same procedures except for pre-treatment with salt.

### **Salt intake decreased the survival of the ApoE<sup>-/-</sup> mice after Ang II infusion**

Survival was recorded in the salt pre-treated and the control group after starting Ang II infusion. A significantly higher number of salt pre-treated mice died compared to the control mice (84.4 % vs 66.7%) as shown in figure 29. The most common reason for death was either thoracic or abdominal aortic ruptures.

Figure 29

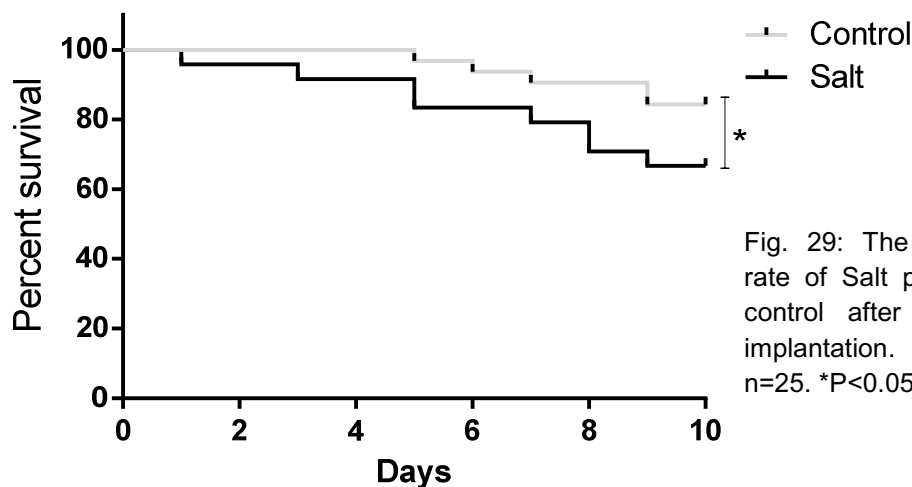


Fig. 29: The cumulative survival rate of Salt pre-treated mice and control after Ang II minipumps implantation. Control n=32, Salt n=25. \*P<0.05, by log-rank test

### **MRI scans were established to visualize aneurysm**

To evaluate AAA and vascular inflammation using a non-invasive technique, an MRI protocol was established using <sup>1</sup>H/<sup>19</sup>F scans (in cooperation with Dr rer nat Sebastian Temme). The MRI protocol was shown to visualize the different organs (using <sup>1</sup>H anatomical scans) as well as the big vessels such as the aorta, inferior vena cava (IVC) and other vessels (through the <sup>1</sup>H angiographic scans). Furthermore, <sup>19</sup>F scans were able to detect and visualize inflammation by the localization of the perfluorocarbons. By overlaying different scans, we could measure the aortic diameter (to assess AAA) and evaluate vascular inflammation (figure 30).

Figure 30

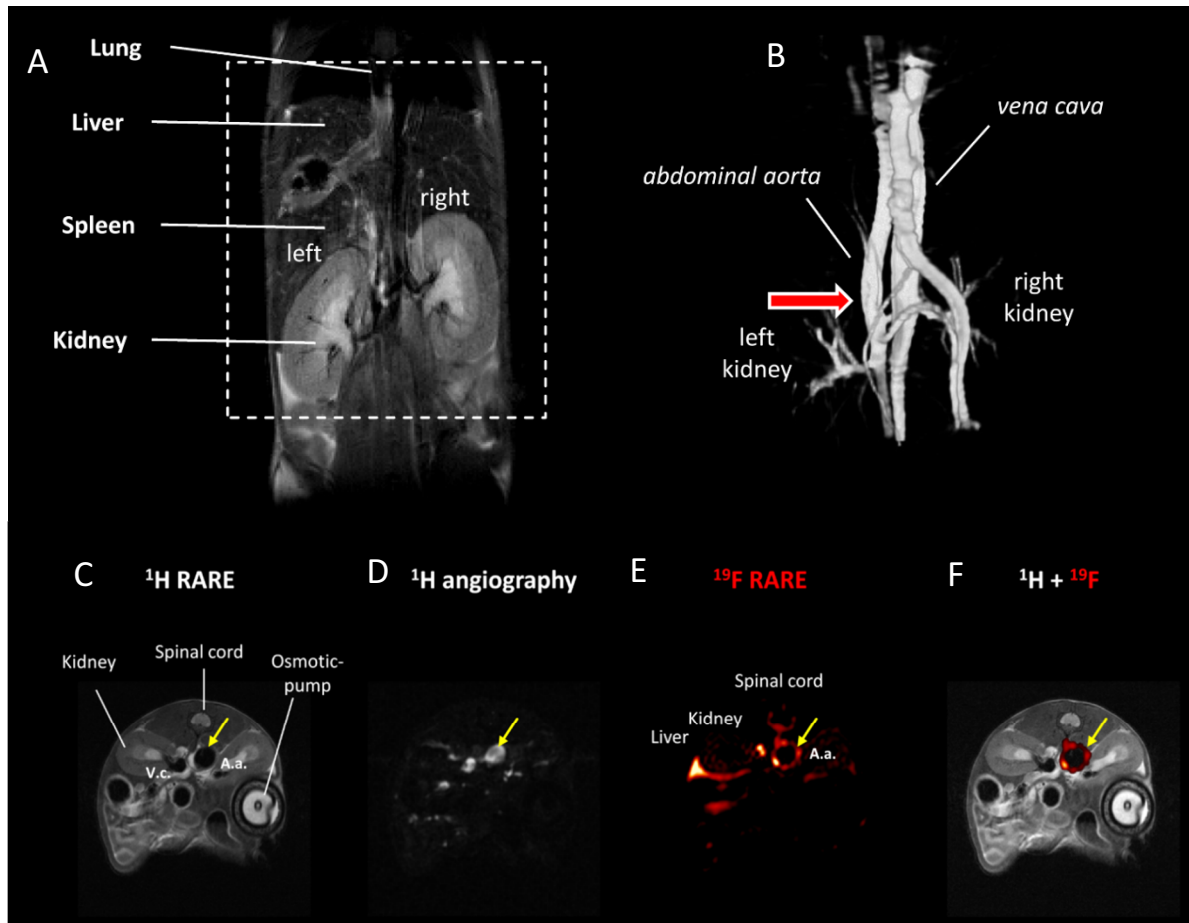


Fig. 30: A: Morphological  $^1\text{H}$  scans (axial and sagittal) were performed to obtain an anatomical overview of the area from the kidneys to the lungs for orientation. B and D:  $^1\text{H}$  angiographic scans to visualize big vessels. C: Representative image of  $^1\text{H}$  RARE scans. E: Representative image of  $^{19}\text{F}$  RARE scans. F: Overlay of matching  $^1\text{H}$  and  $^{19}\text{F}$  images. MRI was performed in cooperation with Dr Sebastian Temme, Department of Molecular Cardiology, Heinrich Heine University.

### Salt pre-treatment increased the incidence of AAA

$^1\text{H}$  anatomical and angiographic MRI scans were performed in the ApoE<sup>-/-</sup> mice at day 0 (baseline), 2, 4, 7 and 10 after implanting the Ang II osmotic pumps. AAA incidence was identified as a 1.5-fold increase in the maximum outer diameter of the aortas compared to the baseline measurement. The cumulative incidence of AAA in the two groups was recorded over the course of 10 days. MRI scans revealed that salt pre-treatment increased the incidence of AAA as shown in figure 31. 62% of mice had AAA in the salt pre-treated group while 31% of the mice had AAA in the control group. These results suggest that salt pre-treatment increased the incidence of AAA.

Figure 31

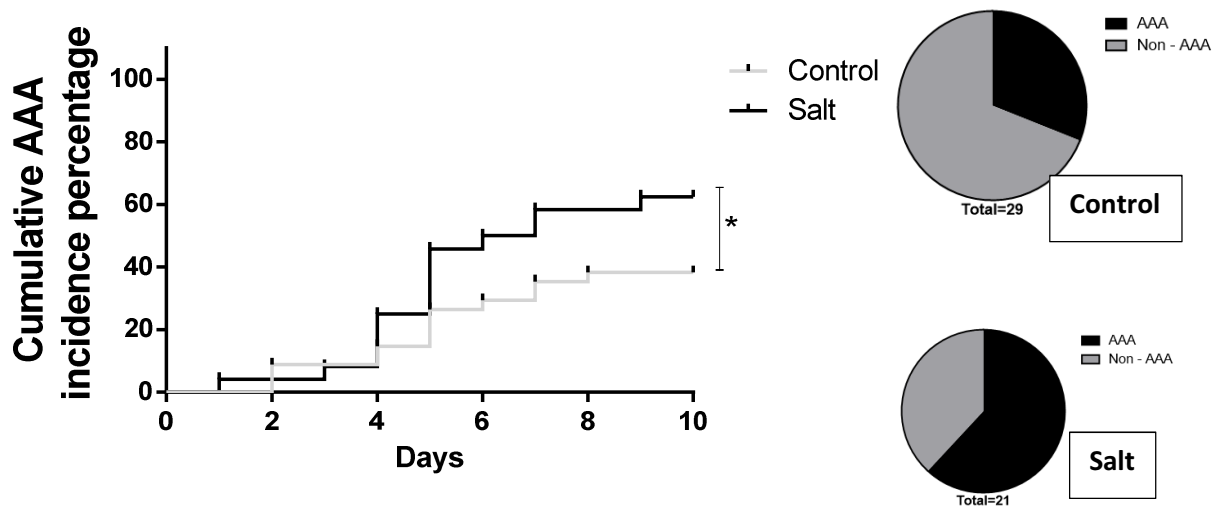


Fig. 31: Cumulative incidence of AAA in the ApoE<sup>-/-</sup> mice from the salt pre-treated and control group. AAA was judged as 1.5-fold increase in the diameter of the aorta. Diameter measurements of the aorta were obtained from MRI 1H rare scans. Pie chart represents the total number of mice which had AAA in control and salt pre-treated group respectively. Control n=29, Salt n=21. \*P<0.05, by log-rank test

### Salt pre-treatment exacerbated the pathological status of AAA

To further investigate the effect of salt pre-treatment on the development of the Ang II-induced AAA, the maximum area of the AAA thrombi in the salt pre-treated and control mice was measured. The evaluation of the area of the thrombi was done by <sup>1</sup>H anatomical MRI scans. Salt pre-treated mice have significantly larger thrombi compared to the control mice (figure 32).

Figure 32

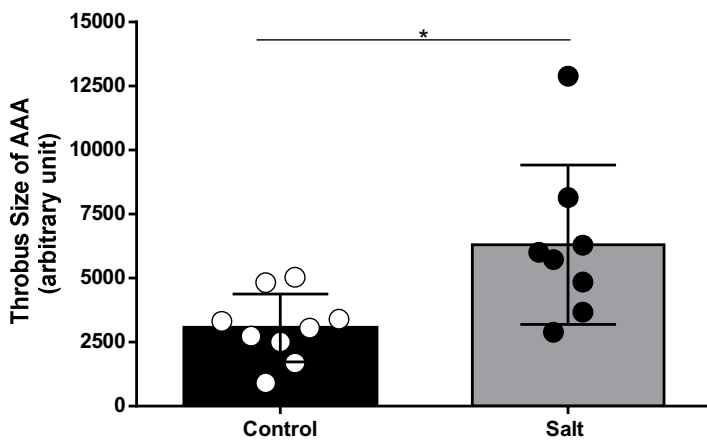
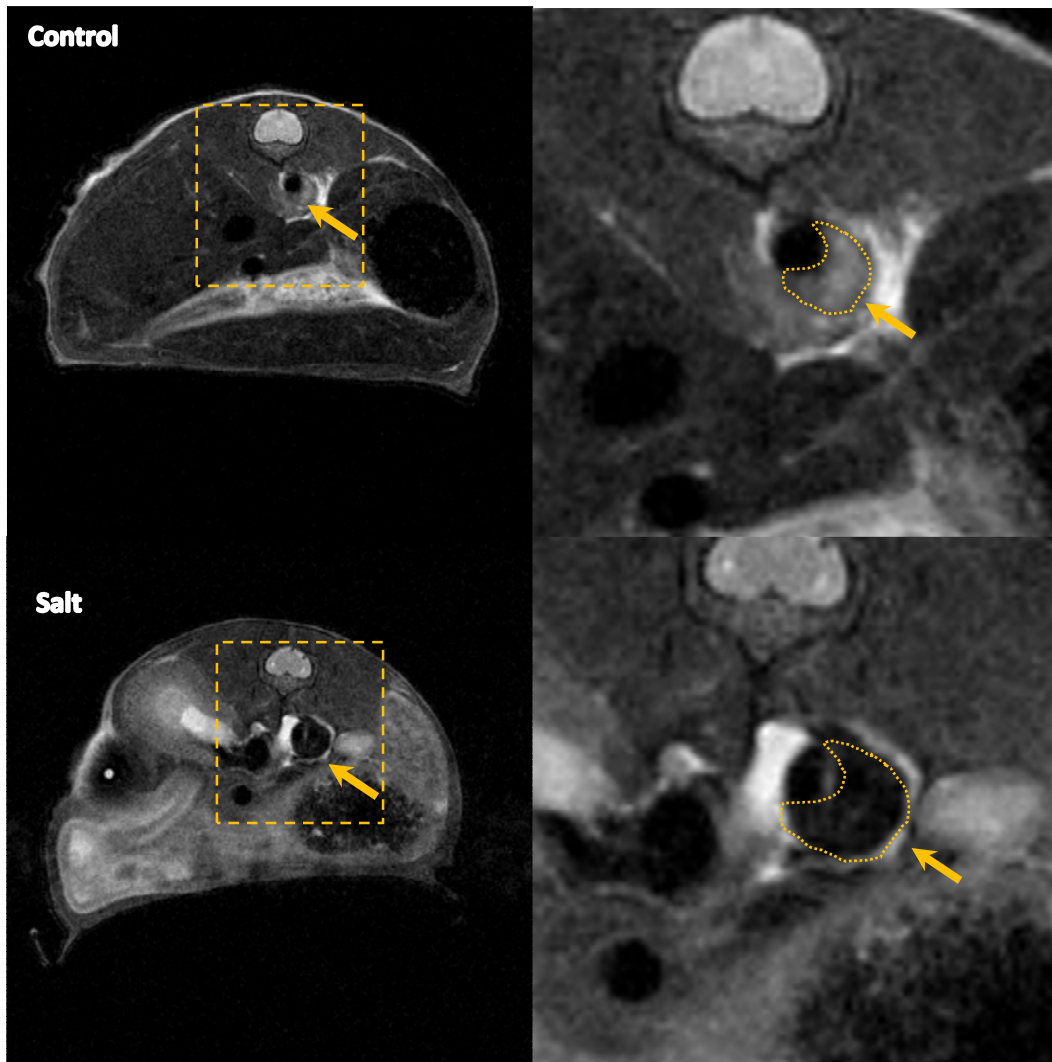


Fig. 32: Above: Representative images of the thrombi in the ApoE<sup>-/-</sup> mice which had AAA from the Salt pre-treated and control group. Below: Quantification of the maximum size of thrombi of salt pretreated and control mice which had AAA assessed at day 10 after Ang II infusion. Control n=9, Salt n=8. \*P<0.05, by 1-tailed t test.

**ApoE<sup>-/-</sup> mice which had an aneurysm in the salt pre-treated group showed higher <sup>19</sup>F signal than the corresponding mice in the control group**

In order to measure vascular inflammation in vivo, <sup>19</sup>F RARE scans were carried out after intravenous injection of Perfluorocarbons (PFCs). To assure that the <sup>19</sup>F signal corresponds to inflammation, a correlation between the <sup>19</sup>F signal-to-noise ratio and the macrophages count was done. The macrophage count was assessed by flow cytometry performed on the abdominal aorta after euthanizing the ApoE<sup>-/-</sup> mice later. A direct proportional correlation ( $R^2=0.95$ ) was observed between the <sup>19</sup>F signal-to-noise ratio and the macrophages count as shown in figure 33. The correlation validates that perfluorocarbons were engulfed by macrophages after I.V. injection and were detectable by using the <sup>19</sup>F scans. Moreover, the <sup>19</sup>F signal-to-noise ratio analogizes with the number of macrophages and thus inflammation.

Figure 33

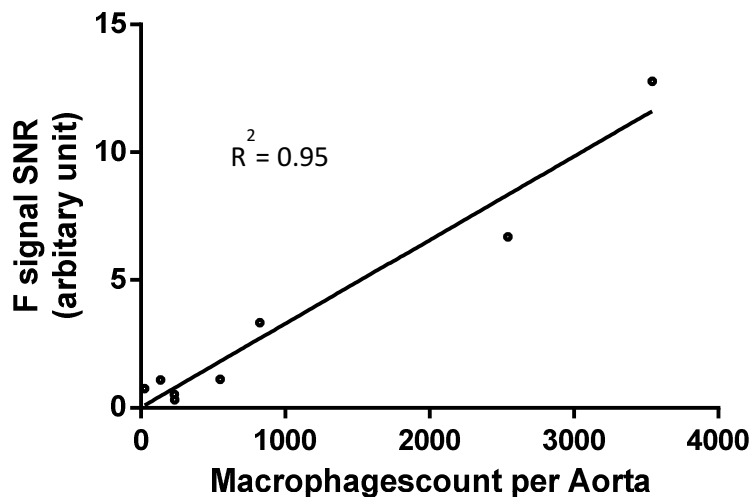


Fig. 33: Plotting the signal to noise ratio of the F-signal against the number of macrophages infiltrated in the aortic tissue revealed a positive correlation validating the engulfment of macrophages to the PFCs. n=8

To assess vascular inflammation in the Ang II infused ApoE<sup>-/-</sup> mice from the salt pre-treated and control group, <sup>19</sup>F signals were recorded for 10 days. We observed that the <sup>19</sup>F signal obtained from the salt pre-treated mice was significantly higher than the <sup>19</sup>F signal obtained from the control mice (figure 34)

**Figure 34**

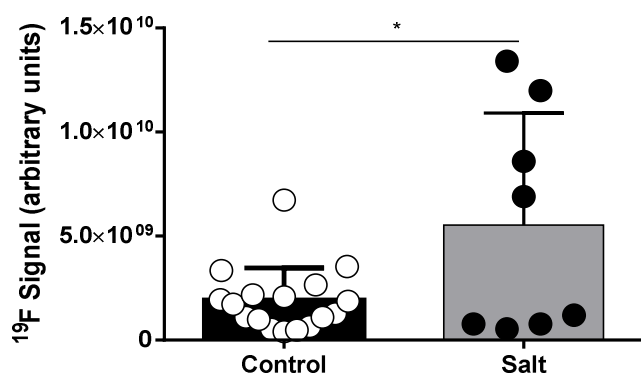


Fig. 34: F-signal obtained from MRI <sup>19</sup>F rare scans which correlated to the prevalence of phagocytes at the site of injury. F-signal rose in the salt pre-treated mice after Ang II infusion. Control n=17, Salt n=8. \*P<0.05, by 1-tailed t test.

### Salt pre-treatment increased the inflammatory cytokines in the aortic tissue

To characterize the salt mediated vascular inflammation, assessment of inflammatory cytokines in the aortic tissue of the Ang II infused mice from the salt pre-treated and control group was carried out. The relative abundance of the pro-inflammatory cytokines; TNF $\alpha$ , TGF $\beta$ , and IFN $\gamma$  were significantly higher in the aortas of the salt pre-treated group compared to the control group. The anti-inflammatory cytokine IL10 was higher in the aortas of the salt pre-treated as well. No significant change was observed in IL6, IL1 $\beta$  or IL17a. Moreover, iNOS (one of the markers of M1 macrophages) was significantly higher in the aortic tissue of the salt pre-treated mice. The elevation of the inflammatory cytokines in the aorta of the salt pre-treated mice (figure 35) suggests an increased vascular inflammatory response in mice pre-treated with salt.

**Figure 35**

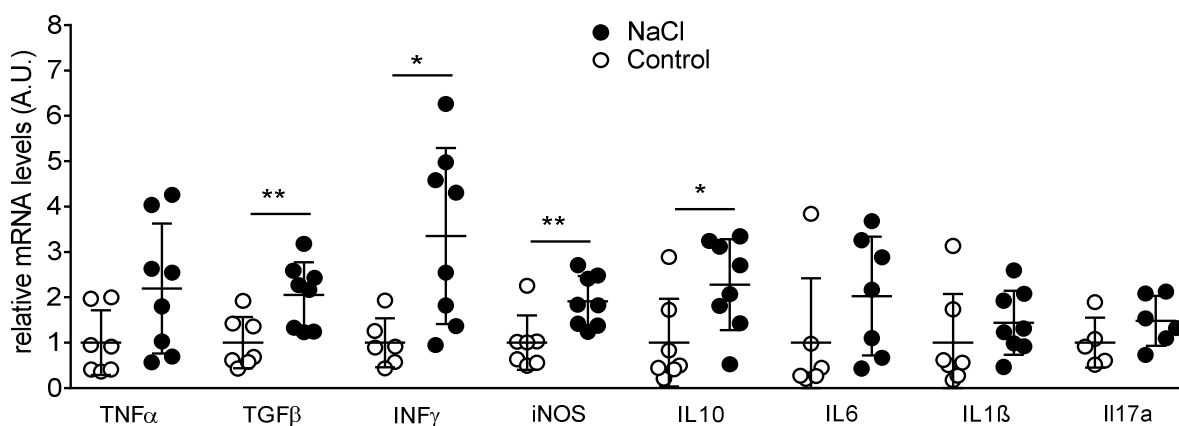


Fig. 35: The relative abundance of mRNA of inflammatory cytokines in the aortic tissue of the ApoE<sup>-/-</sup> mice of salt pre-treated and control group. Control n=9, Salt n=8. \*P<0.05, \*\*P<0.01 by 1-tailed t test

## **Salt pre-treatment increased the number of T-cells embedded in the aortic tissue and the surrounding Perivascular adipose tissue (PVAT)**

Cytokines production is crucial for CD4 and CD8 T- cells activity (Sasiain et al. 1998. Clin Exp Immunol). Since the relative expression of IFN $\gamma$  and TNF $\alpha$  was higher in the aortic tissues of the salt pre-treated mice, we assumed a higher abundance of T-cells in the aortas of the salt pre-treated mice compared to the control mice. To test this hypothesis, we performed flow cytometry on aortic tissue of the Ang II infused mice from the salt pre-treated and control group. Flow cytometric analysis showed significantly higher total numbers of CD4 $^{+}$  T helper and CD8 cytotoxic T-cells infiltrated in the aortas of salt pre-treated mice compared to control mice (figure 36). Furthermore, we evaluated the subpopulations of aortic CD4 $^{+}$  and CD8 $^{+}$  T-cells in both groups. The aortas of the salt pre-treated mice have higher numbers of CD4 effector memory (CD4+CD44+CD62L $^{-}$ ), CD4 central memory (CD4+CD44+CD62L $^{-}$ ) and early activated CD4 $^{+}$  T-cells (CD4+CD69 $^{+}$ ) (figure 36). Moreover, the numbers of CD8 effector memory (CD8+CD44+CD62L $^{-}$ ), as well as CD8 central memory (CD8+CD44+CD62L $^{+}$ ), were higher in the aortas of the salt pre-treated mice compared to the control mice.

Figure 36

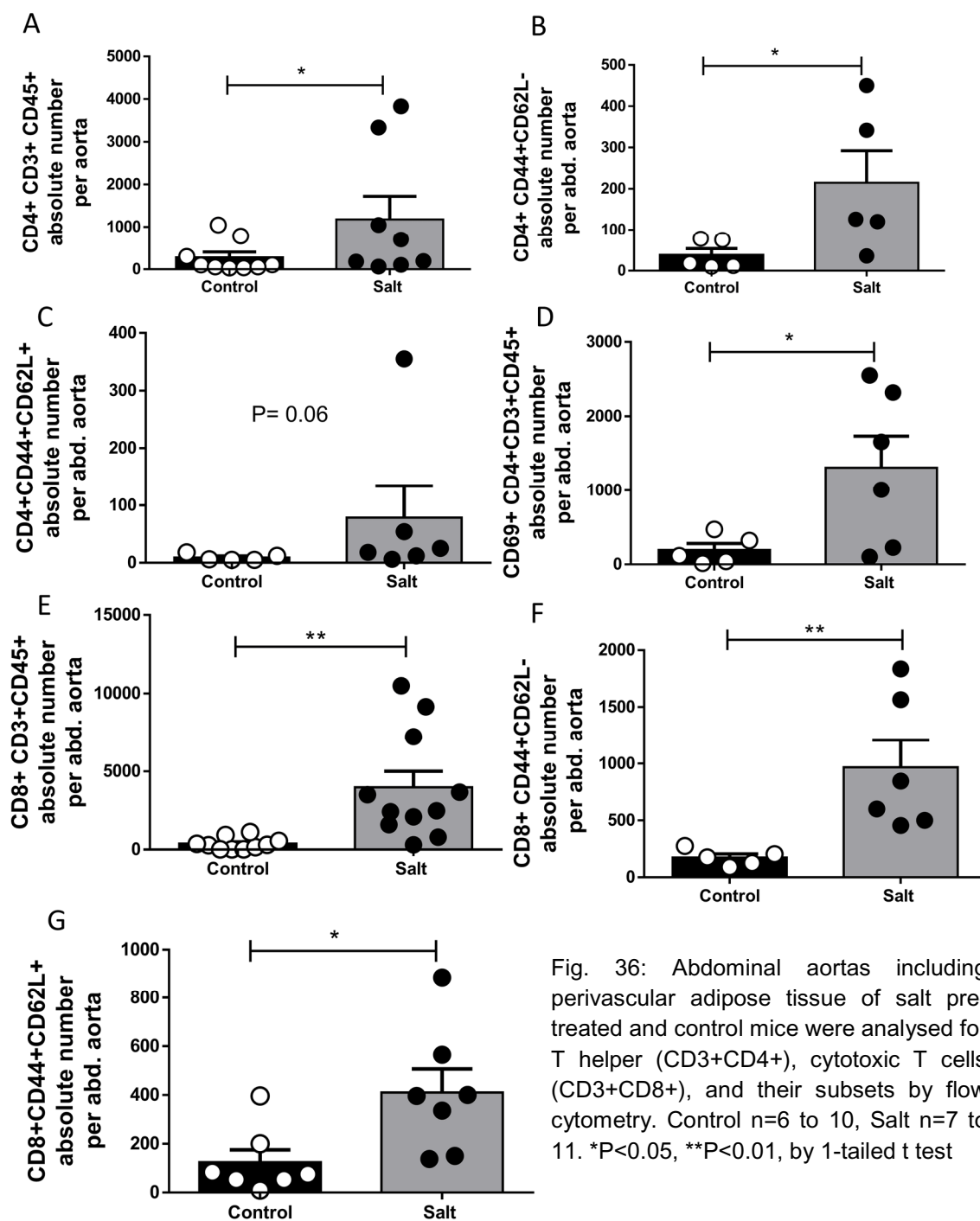


Fig. 36: Abdominal aortas including perivascular adipose tissue of salt pre-treated and control mice were analysed for T helper (CD3+CD4+), cytotoxic T cells (CD3+CD8+), and their subsets by flow cytometry. Control n=6 to 10, Salt n=7 to 11. \* $P < 0.05$ , \*\* $P < 0.01$ , by 1-tailed t test

## Salt pre-treatment increased the number of splenic IL17/INF $\gamma$ double producing CD8 T-cells in vivo but not other T-cells in the salt pre-treated mice

To get more insights on how salt mediates T-cell priming in the abdominal aortic aneurysm model, we evaluated the T-cells subsets in the spleen of the Ang II infused mice from the salt pre-treated and control group. No differences were observed in the proportions of CD4 or CD8 T-cells in the two groups. In addition, further analysis of splenic T-cells subsets revealed no difference in the population of Th17 (CD4+ IL17+) or Th1 (CD4+INF $\gamma$ +TNF $\alpha$ +) between the two groups. In contrast, the proportion of splenic IL17/INF $\gamma$  double producing CD8 T-cells (CD8+IL17+INF $\gamma$ +) was significantly higher in the salt pre-treated mice compared to the control mice (figure 37) suggesting that effector CD8 T-cells (CD8+IL17+INF $\gamma$ +) play a role in the salt mediated vascular injury.

Figure 37

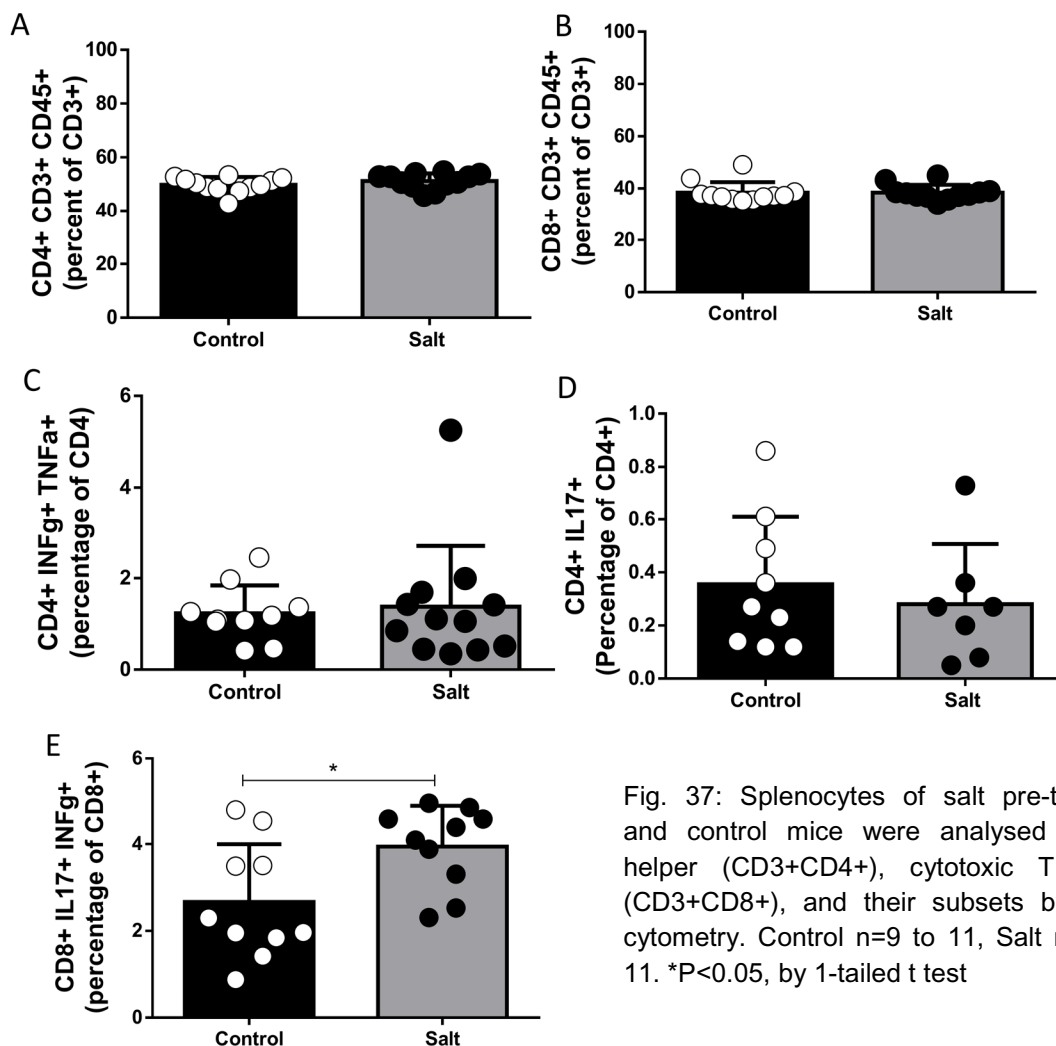


Fig. 37: Splenocytes of salt pre-treated and control mice were analysed for T helper (CD3+CD4+), cytotoxic T cells (CD3+CD8+), and their subsets by flow cytometry. Control n=9 to 11, Salt n=7 to 11. \*P<0.05, by 1-tailed t test

## Salt pre-treatment induced polarization of splenic CD8 naïve T-cells *in vitro*

To confirm the effect of high salt on the differentiation of CD8 T-cells, we carried out *in vitro* experiments in which naïve CD8 T-cells from C56BL/6 mice were differentiated into effector CD8 in the presence or absence of high salt. The supernatant of CD8 T-cells from the two culture conditions was collected after 4 days and INF $\gamma$  concentration was measured. INF $\gamma$  concentration was used as a marker for the proportion of naïve CD8 T-cells which was differentiated into effector CD8 T-cells.

The concentration of INF $\gamma$  in the supernatant of the cells which were polarized under high salt conditions (180 mM Na) were significantly higher compared to normal salt conditions (140 mM Na) (figure 38). These results show that high salt drives CD8 differentiation.

Figure 38

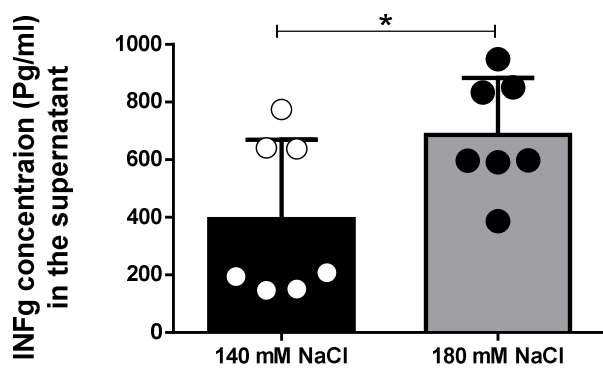


Fig. 38: *In vitro* analysis of splenic naïve CD8 cells triggered to differentiate by CD3 and CD28 antibodies under high or normal salt condition. High salt condition increased the portion of naïve CD8 cells which polarized into effector cells. The assessment was done by measuring the concentration of INF $\gamma$  in the supernatant of the cell medium. \*P<0.05, by 1-tailed t test

## The abdominal aortas of the salt pre-treated mice had a higher number of macrophages compared to the control group.

Since iNOS relative expression was higher in the abdominal aortas of the salt pre-treated mice and iNOS is one of the expression marker for M1 macrophages, we investigated the frequencies of macrophages in the abdominal aortas (with the accompanying PVAT) of the ApoE<sup>-/-</sup> mice of the salt pre-treated and control group after 10 days of Ang II infusion via flow cytometric analysis. Flow cytometric analysis revealed a higher number of infiltrated macrophages in the aortas of salt pre-treated mice compared to control mice (figure 39)

Figure 39

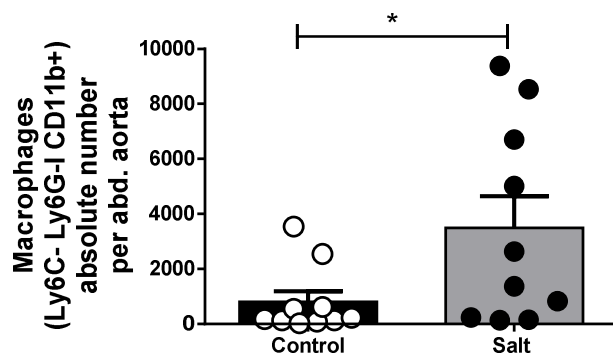


Fig. 39: Quantification of macrophages by flow cytometric analysis of the abdominal aortas including perivascular adipose tissue of salt pre-treated and control mice. Control n=10, Salt n=10. \*P<0.05, by 1-tailed t test

### Salt pre-treatment increased the number of neutrophils infiltrated in the abdominal aorta of salt pre-treated mice

Since neutrophils play a role in the AAA pathogenesis (Eliason et al. 2005. Circulation), we wanted to investigate the abundance of neutrophils. In order to assess neutrophils in our model, we performed further flow cytometric analysis on the abdominal aortas of the ApoE<sup>-/-</sup> mice of the salt pre-treated and control group after 10 days of Ang II infusion. A higher number of neutrophils was observed in the aortas of the salt pre-treated mice compared to the control mice suggesting the recruitment of neutrophils during salt mediated AAA development.

Figure 40

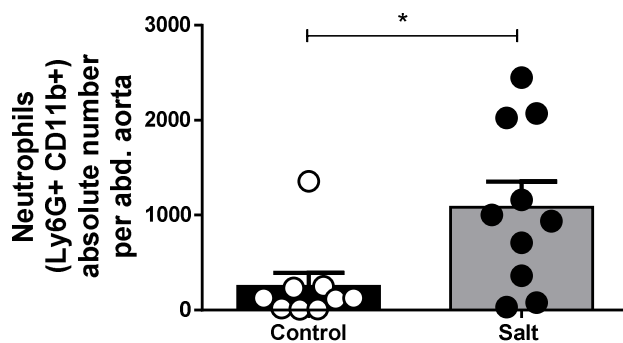


Fig. 40: Abdominal aortas including perivascular adipose tissue of salt pre-treated and control mice were analysed for neutrophils by flow cytometry. Control n=9, Salt n=10. \*P<0.05, by 1-tailed t test

### Neutrophil elastase but not metalloprotease relative expression was higher in the aortas of the salt pre-treated mice

Neutrophils contribute to the development of AAA via metalloproteases 2 and 9 (MMP2 and 9) (Longo et al. 2002. J Clin Invest) and neutrophil elastase (Weissmann

et al. 1980. N Engl J Med). To characterize the role of neutrophils in the salt mediated vascular injury, we measured the relative expression of MMP2, MMP9, and neutrophil elastase mRNA in the aortas of the salt pre-treated and control mice after Ang II infusion. Neutrophil elastase relative expression was significantly higher in the aortas of the salt pre-treated mice compared to the control mice while no difference was observed in the relative expression of MMP2 or MMP9 between the two groups (figure 41).

**Figure 41**

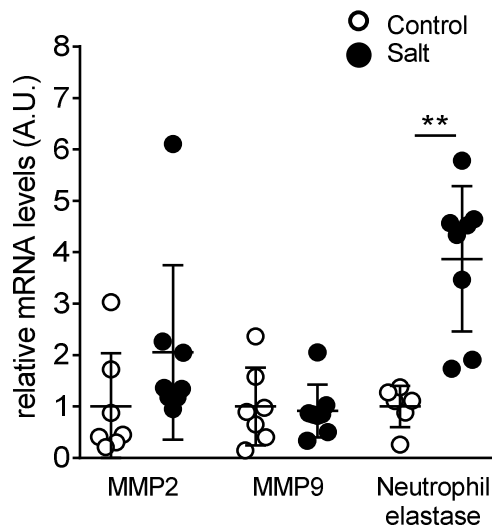


Fig. 41: The relative abundance of mRNA of MMP2, MMP9 and neutrophil elastase in the aortic tissue of the ApoE<sup>-/-</sup> mice of Salt pre-treated and control group. Control n=7, Salt n=7. \*\*P<0.01 by 1-tailed t test

### **Salt pre-treatment increased the breakdown of the elastic fibers in the aorta**

The neutrophil elastase activity is mediated by breaking elastic fibers of the intima-media of the aortas. Thus, we evaluated the number of breakdowns in aortas of salt pre-treated and control mice. Salt pre-treatment showed an increase in the number of elastic breakdowns in the aorta, as shown in figure 42. The higher number of breakdowns in the aortas of the salt pre-treated mice suggests that salt pre-treatment affects neutrophil function and aggravates neutrophil-mediated vascular damage.

Figure 42

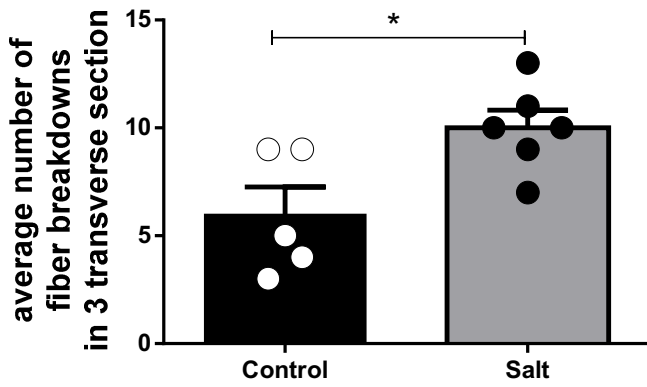
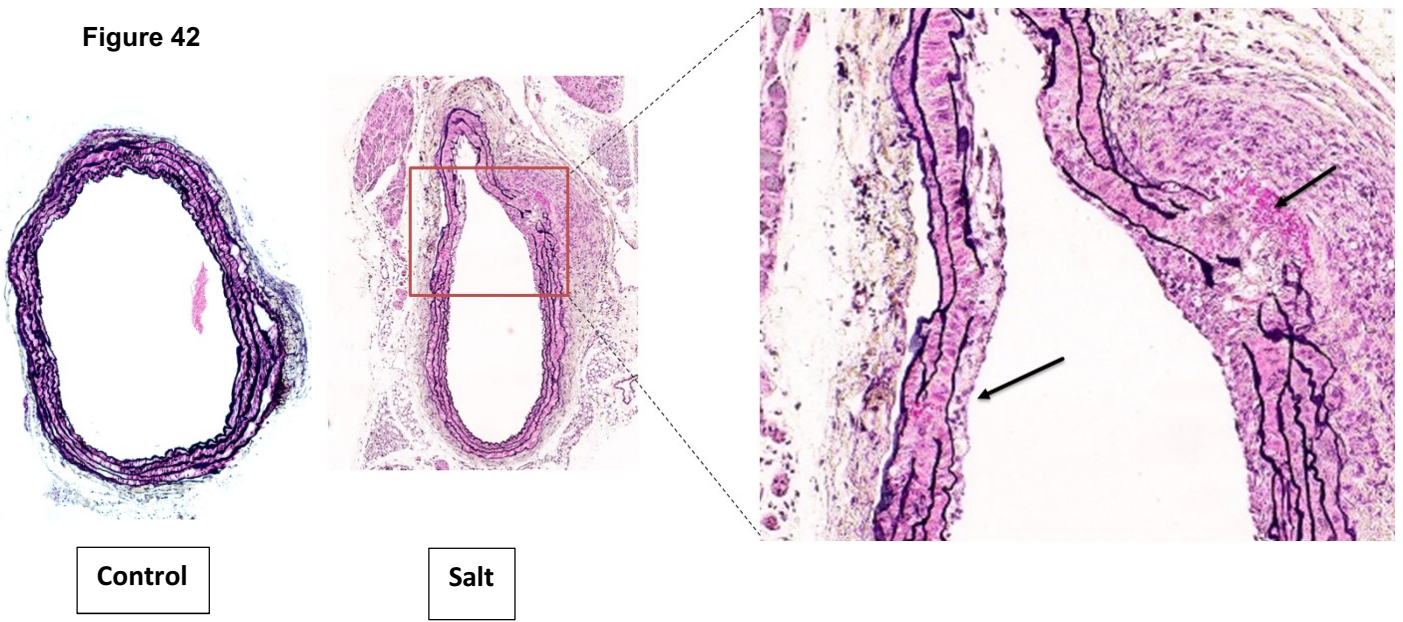


Fig. 42: Above: Assessment of average breakdown in the elastic fibers in the aortas of the Salt pre-treated and control mice by Movat staining. Below: Quantification of breakdowns. Control n=5, Salt n=6. \*P<0.05, by 1-tailed t test

## 5 Discussion

### **Part I: Effect of short chain fatty acids on Atherosclerosis**

In the present study, we aimed to define the role of propionate, one of the most important short chain fatty acids (SCFA) in atherosclerosis. In order to study the effect of C3 on atherosclerosis, we designed a model in which hypertensive ApoE<sup>-/-</sup> mice infused chronically with Ang II were either treated with sodium propionate (C3; 200mM) or sodium chloride (NaCl; 200 mM) in the drinking water.

The main risk factors for atherosclerosis are hypertension and hyperlipidemia (Kannel. 1989. J Cardiovasc Pharmacol). In our model, we infused mice with Ang II to induce hypertension (Weir *et al.* 1999. Am J Hypertens) while hyperlipidemia was achieved by performing the experiments on ApoE<sup>-/-</sup> mice. ApoE protein is crucial for lipid metabolism (Bu G. 2009. Nat Rev Neurosci) and knocking down the ApoE gene causes inefficient lipid metabolism and thus hyperlipidemia.

Our data demonstrate that chronic administration of C3 ameliorates Ang II-induced atherosclerosis. The reduction of atherosclerosis was illustrated by the assessment of atherosclerotic plaques in the whole aorta, as well as the assessment of stenosis in the brachiocephalic artery. Li *et al.* (Li *et al.* 2016. Eur Rev Med Pharmacol Sci) did a comparative study between the brachiocephalic artery and coronary artery in terms of assessment of atherosclerosis and inflammatory responses. They found that the brachiocephalic artery is better to represent atherosclerosis progression, supporting our selection of the brachiocephalic artery in our model.

The anti-atherosclerotic activity was not due to lipid concentration in the serum of the mice since there was no difference in the lipid profile of the mice of the C3 treated and control groups. This observation implies that the anti-atherosclerotic effects of C3 are not mediated by changes in lipid metabolism.

Studies performed in mouse models of autoimmune disease suggested that chronic administration of SCFA modifies the degree of disease through an immune cell-mediated mechanism (Haghikia *et al.* 2015. Immunity). And indeed, in the present study, we demonstrate that the anti-atherosclerotic effect of C3 is immune-mediated. Atherosclerosis is a chronic inflammatory disease of the vasculature in which many immune cells such as macrophages and T-cells take part (Gisterå *et al.* 2017. Nat Rev Nephrol). Moreover, Ang II amplifies vascular inflammation in ApoE<sup>-/-</sup> mice (Mazzolai *et al.* 2004. Hypertension). More specifically, there are multiple evidences that Th17 exaggerates the progression of atherosclerosis (Erbel *et al.* 2009. J Immunol). On the other hand, several studies show that regulatory T-cells (T<sub>reg</sub>) counterbalance Th17 and exhibit an anti-atherosclerotic effect (Xie *et al.* 2010. Cytokine; Didion *et al.* 2009. Hypertension). Considering those findings, it was

necessary to assess the immune cell signature in Ang II-infused mice from the C3 treated and control group. Histochemical and flow cytometric analysis performed on the aortas revealed a lower number of macrophages (F4/80+) and T-cells (CD3+, CD4+ or CD8+) infiltrated in the aortas of the C3 treated mice compared to the control mice. The reduction of the infiltrated macrophages and the total number of T-cells in the aortas of the C3 treated mice confirms our suggestion that C3 exerts the anti-atherosclerotic activity via immune cells down-modulation.

In order to get more insights into the type of T-cell subsets that were affected after C3 treatment and to characterize the C3 mediated modulation of inflammation, further flow cytometric analysis was carried out on the aortas and the spleens of the mice from the C3 treated and control group. Due to the limited number of immune cells in the aorta, the possibility to assess all T-cell subsets was limited. Therefore, we have also investigated the T cell signature in the spleen of our mice. We found a lower number of effector memory CD4 T-cells and Th17 T-cells and a higher number of naïve CD4 T-cells in the aortas and spleens of the C3 treated mice compared to the control mice. Since CD4 effector memory and Th17 T-cells are a sign of pro-inflammatory conditions (Cronkite *et al.* 2018. J Immunol Res), reduction of these T cell types in C3 treated mice highlights the anti-inflammatory effect of C3 in the development of atherosclerosis. In addition, the higher proportion of splenic naïve CD4 T-cells, representing non-active and non-stimulated T cells, in C3 treated mice compared to control mice confirms the anti-inflammatory impact of C3. Bartolomaeus and co-workers have observed the same pattern of splenic T-cells signature of reduced CD4 effector memory and Th17, as well as increased naïve CD4 T-cells in Ang II-treated wild-type mice (Bartolomaeus *et al.* 2019. Circulation). These findings confirm our data regarding the C3 mediated effect on effector memory CD4 T-cells, Th17 and CD4 naïve T-cells differentiation. Furthermore, other studies confirmed the effect of SCFA on the reduction of Th17 in different non-cardiovascular diseases. Luu *et al.* showed that pantoate suppressed the production of IL17 and Th17 in experimental mouse models of colitis and multiple sclerosis (Luu *et al.* Nat Commun. 2019). Haghikia *et al.* showed that C3 decreased the differentiation of human naïve T-cells into Th17 in vitro (Haghikia *et al.* 2015. Immunity), supporting our findings.

Since we observed a reduction in the Th17 frequencies in the C3 treated mice and we know that Th17 cells counteract T<sub>reg</sub> population (Xie *et al.* 2010. Cytokine), we evaluated the abundance of T<sub>reg</sub> in the C3 treated mice. Surprisingly, no differences in the splenic T<sub>reg</sub> population between the C3 treated and control mice were noticed. In contrast to our data, multiple studies showed that C3 influenced T<sub>reg</sub> populations. Arpaia *et al.* (Arpaia *et al.* 2013. Nature) showed that C3 promotes T<sub>reg</sub> generation and function. Smith *et al.* (Smith *et al.* 2013. Science) demonstrated that in germ-free mice, T<sub>reg</sub> numbers in the colon were reduced and could be restored by C3 administration in the drinking water. Furthermore, in vitro studies performed by Haghikia *et al.* (Haghikia *et al.* 2015. Immunity) showed that C3 induces T<sub>reg</sub> differentiation. These studies highlight that C3 promotes an anti-inflammatory effect

via T<sub>reg</sub>. We hypothesize that we did not see the difference in the splenic T<sub>reg</sub> frequencies between the C3 treated and control group in our model due to a compensatory response after 28 days of chronic Ang II infusion. We suggest that splenic T<sub>reg</sub> were already upregulated in the control mice to balance the increased Th17 in the control mice compared to the C3 treated mice. This suggestion is supported by a study showing increased plasma levels of the anti-inflammatory cytokine IL10 in AngII-infused mice (Barhoumi *et al.* 2011. Hypertension). IL10 signaling is crucial for T<sub>reg</sub> to suppress Th17 (Chaudhry *et al.* 2011. Immunity). Besides T<sub>reg</sub>, other T-cell populations like CD4 central memory, Th1, and all CD8 subpopulations, were found unaffected with C3 treatment in our study. The different responses of different immune cell subpopulations to C3 treatment is suggesting the specific action of C3 action on immune cells. The specificity of C3 could be due to the availability or absence of C3 receptors such as GPR41 and GPR43 on the surface of the immune cells (Brown *et al.* 2003. J Biol Chem).

Considering all the evidence, we demonstrate that C3 exhibits an anti-atherosclerotic effect. This anti-atherosclerotic effect is mediated by inhibiting T-cells from differentiating into pro-inflammatory phenotype. The main mechanism of C3 mediated anti-atherosclerotic effect is namely the reduction of Th17 differentiation attenuating the progression atherosclerotic plaques in hypercholesteremic ApoE<sup>-/-</sup> mice. The modulation of immune cells by SCFA was described in different studies and different models. For instance, Luu *et al.* (Luu *et al.* 2019. Nat Commun) showed that SCFA suppressed autoimmunity by modulation of immune cells and suppression of IL-17A production while it did not impact T<sub>reg</sub> production. Moreover, the beneficial effect of butyrate (one of the SCFA) on Crohn's disease and inflammatory bowel disease was reported by Silva *et al.* (Silva *et al.* 2018. Curr Pharm Des). In contrast, some studies showed a systemic pro-inflammatory effect of SCFA, contradicting our data. The pro-inflammatory effect of SCFA was shown via the activation of MAPK, phosphoinositide 3-kinase (PI3K) or rapamycin (mTOR) signaling pathways (Seljeset *et al.* 2012. J Recept Signal Transduct Res). In other studies, both pro- and anti-inflammatory co-effects of SCFA are suggestive (Li *et al.* 2018. Eur J Pharmacol). In our model, we noticed only the anti-inflammatory effect of C3 which was reflected by a reduced atherosclerotic progression.

In addition to the anti-atherosclerotic effect of C3, our results suggest that C3 has a beneficial outcome on the heart. Here we showed that C3 ameliorates cardiac fibrosis and cardiac hypertrophy. Reduction of cardiac hypertrophy was confirmed by assessing the relative expression of  $\beta$ MHC mRNA in the cardiac tissue which was found to be expressed less in the hearts of the C3 treated mice compared to the control mice.  $\beta$ MHC is a marker that is re-expressed as a result of cardiac hypertrophy (Pandya *et al.* 2011. Circ Res). Furthermore, we found that the relative expression of ANP and BNP were significantly lower in the hearts of the C3 treated mice compared to the control hearts. ANP and BNP are markers for heart functions and their higher expression is an indicator for heart insufficiency (Kerkelä *et al.* 2015.

J Am Heart Assoc). The lower expression of ANP and BNP in the C3 treated hearts suggests improved cardiac functions as a result of C3 treatment. Bartolomaeus *et al.* found that C3 reduced cardiac hypertrophy, cardiac fibrosis and reduced susceptibility to ventricular arrhythmia. Moreover, they found less expression of BNP and  $\beta$ MHC mRNA in the hearts of the C3 treated mice, confirming our outcome. SCFA were shown to attenuate myocardial infarction in the ischemia-reperfusion model in rats (Lim *et al.* 2010. J. Korean Soc. Appl. Biol. Chem). Taken together, C3 is suggestive to have a protective effect against Ang II-induced cardiac damage. Kee *et al.* (Kee *et al.* 2006. Circulation) showed that the inhibition of histone deacetylases (HDAC) class II leads to blocking of Ang II-induced cardiac hypertrophy. Since SCFA is known to inhibit the activity of HDAC (Waldecker *et al.* 2008. J Nutr Biochem; Davie. 2003. J Nutr), it is possible that C3 ameliorates Ang II-induced cardiac damage via the inhibition of HDAC. However, Bartolomaeus *et al.* did not find an effect of propionate treatment on HDAC expression in the heart. Therefore, it is more likely that improvement in heart structure and function was also mediated through an immune cell-mediated mechanism. In this regard, Kvakan *et al.* (Kvakan H. 2009. Circulation) illustrated the beneficial effect of adoptive transfer of T<sub>reg</sub> in Ang II-induced cardiac damage. Additionally, Bartolomaeus *et al.* found that depletion of T<sub>reg</sub> by injecting anti-CD25 antibody intraperitoneally abolished cardiac damage.

Besides the immune cell-mediated effect of C3 on vascular inflammation and cardiac health, we also investigate whether the positive impact of C3 is mediated by other factors. One potential factor is blood pressure. We observed that C3 has a mild blood pressure-lowering effect. Several studies (Pluznick. 2014 Gut Microbes; Marques *et al.* 2017. Circulation; Natarajan *et al.* 2016 Physiol Genomics; Bartolomaeus *et al.* 2019. Circulation; Poll *et al.* 2019. FASEB) reported the blood pressure-lowering effect of SCFA, confirming our data. It is possible that the blood pressure-lowering effect of C3 contributes to the improvement in atherosclerosis and cardiac damage. However, the mice which were not treated with C3 (control mice) had slightly high systolic blood pressure (149.7 mmHg  $\pm$  9) but they have exaggerated atherosclerosis and cardiac damage status. Thus, we believe that the improvement of atherosclerosis and cardiac damage is more likely to be immune-mediated rather than blood pressure-dependent. Not only the blood pressure was affected by C3, but also other vascular functions were improved. The improved vascular functions were illustrated by improved vasorelaxation (shown in the isolated perfused kidneys of the Ang II-infused mice from C3 treated group) and improved aortic vascular stiffness measured by atomic force microscopy. Taken together, C3 ameliorates cardiovascular damage not only via immune cells but also through a direct mechanism. It was shown previously that GPR41 and GPR43 are localized in the vascular endothelium (Pluznick. 2014 Gut Microbes; Natarajan *et al.* 2016 Physiol Genomics). Since GPR41 and GPR43 are specific receptors for SCFA (Priyadarshini *et al.* 2018. Compr Physiol; Le Poul *et al.* 2003. J Biol Chem), we suggest that the direct effect of C3 on blood pressure and vascular functions is likely to be mediated by GPR41 and GPR43.

Meta-analysis studies linking fiber intake and cardiovascular outcomes (Streppel *et al.* Arch Intern Med. 2005; McRae 2017. J Chiropr Med) suggest the beneficial outcome of fiber intake on blood pressure and preventing cardiovascular diseases. The exact mechanism of the beneficial effect of fibers on cardiovascular diseases is still unknown. Since C3, as well as other SCFA, are metabolites produced by the gut microbiota through the digestion of fibers (Topping *et al.* 2001. Physiol Rev), it seems plausible that SCFA are the linkage to the beneficial outcome of fiber intake on the cardiovascular system. In addition to our study showing robust evidence of the beneficial effects of SCFA on cardiovascular damage, the concept of the SCFA-mediated effect of fibers on the cardiovascular system was confirmed by Kaye *et al.* (Kaye *et al.* 2020. Circulation). Kaye and colleagues showed that the lack of fibers in diet predisposed the mice to hypertension and cardiac remodeling, and when they reintroduced SCFA to the fiber depleted fed mice they mice had protective effects on the development of hypertension, cardiac hypertrophy, and fibrosis, confirming our hypothesis.

In conclusion, C3 and other SCFA were shown to exert a beneficial and protective effect on the cardiovascular system, directly and via an immune cell-mediated mechanism. Our data suggest that C3 has an anti-atherosclerotic effect and improves cardiac damage mainly through the reduction of CD4 effector memory and Th17 T-cells. In addition to the immune-mediated effects, we suggest that part of the beneficial effects of C3 was mediated through C3-induced improvement of blood pressure-lowering and vascular function. Finally, the protective effect of C3 in our model was shown by the evaluation of the survival rate of the C3 treated mice and the control mice after Ang II infusion. More than 60 % of the control mice died while interestingly, none of the mice which were treated with C3 died through the end of the experiment. C3 and other SCFA are non-expensive supplements that can be augmented within the diet and can be a great approach to enhance the prevalence of cardiovascular diseases.

## **Part II: Effect of high salt intake on Abdominal Aortic Aneurysm**

In the second part of the present study, we aimed to investigate the immune-mediated effect of salt on abdominal aortic aneurysm (AAA) as a model for vascular damage. To test this hypothesis, we treated ApoE<sup>-/-</sup> mice with high salt only for 2 weeks followed by one-week washout period. To induce AAA, minipumps filled with Ang II were implanted after 1 week of salt discontinuation, and then AAA was assessed by MRI over the course of 10 days. We stopped the high salt treatment one week before we implanted Ang II containing minipumps to induce AAA. This design was chosen to eliminate the direct effect of salt on hypertension which plays a role in the pathogenesis of AAA (Cornuz *et al.* 2004. Eur J Public Health) and to investigate exclusively the immune-mediated effect. We hypothesize that pre-treatment with high salt initiates immune cell priming before inducing the development of an abdominal aortic aneurysm (AAA) via Ang II.

Here, <sup>1</sup>H MRI scans showed a higher incidence of the Ang II-induced AAA in the salt pre-treated mice (62% in the salt pre-treated group versus 31% in the control group). Recently, we and others have shown that (Stegbauer *et al.* 2019. J Vasc Surg; Coa *et al.* 2010. Front Pharmacol) around 40% of ApoE<sup>-/-</sup> mice infused with Ang II (1000 ng/kg/min) develop AAA confirming the AAA incidence in the control group of the present study. Moreover, chronic high salt intake has been shown to exaggerate the incidence of AAA (Nishijo *et al.* 1998. Lab Invest) in hypertensive Tsukuba mice. Hypertensive Tsukuba mice produce excessively Ang II, making them more susceptible to AAA (Shimokama *et al.* 1998. Virchows Arch). In accordance to the present study, the authors noticed that mice which were treated with salt suffered more frequently from internal hemorrhage as a result of thoracic and abdominal aneurysm. In our study, only 2 weeks of salt pre-treatment revealed the same outcome of AAA incidence. Moreover, a human study (Golledge *et al.* 2014. PLoS One) found out that reported high salt intake is significantly correlated with AAA prevalence in older men, confirming our findings.

Of note, the Ang II induced AAA model is rather a model for abdominal aortic dissection than dilation. Thus, in contrast to the elastase model (Lu *et al.* 2017. J Vasc Surg), the Ang II induced AAA model is an ideal model for investigating immune cell mediated acute vascular inflammation (Peshkova *et al.* 2016. FEBS J). Based on this assumption, one purpose of the present study was to investigate whether vascular inflammation triggers dissection or whether vascular inflammation develops concomitantly with the dissection. For this purpose, we measured vascular inflammation of the abdominal aorta via <sup>19</sup>F MRI in vivo for 10 days. In some mice, dissections of the abdominal aorta were formed already after 2 days of Ang II infusion. On the other side, abdominal aortic inflammation was detected in mice which did not develop abdominal aortic dissection or aneurysm, when we compared abdominal aortic inflammation in the two groups using <sup>19</sup>F MRI scans. We demonstrated that salt pre-treated mice showed a higher F signal. Higher F signal reflects the higher number of phagocytes infiltrated in the aorta and thus higher

vascular inflammation. Based on these results, we can conclude that salt pre-treatment promotes both the formation of abdominal aortic dissection and vascular inflammation. However, it is still debatable which step initiates vascular injury. We propose that in most cases, vascular inflammation precedes the formation of dissection and results in immune-mediated vascular tissue remodeling. Based on this new imaging technique, we can track vascular inflammation and changes in aortic wall structure. However, we can still not affirm the exact mechanism why dissection or aneurysm occur only in a certain part of our experimental mice. It is well described that AAA is mediated by remodeling in the aortic tissue and extracellular matrix components such as switching of vascular smooth muscle cells (VSMC), and degradation of elastin and collagen (Ailawadi *et al.* 2009. J Thorac Cardiovasc Surg; Tsamis *et al.* 2013. J R Soc Interface). Some studies demonstrated the role of immune cells in the remodeling of aortic tissue and extracellular matrix. For instance, neutrophils were shown to contribute to the development of AAA via the release of neutrophil elastase (Weissmann *et al.* 1980. N Engl J Med) which in turn disrupt the elastic fibers in the aortic tissue. Moreover, it was shown that macrophages induce apoptosis in the VSMC (Imanishi *et al.* 2002. Atherosclerosis). Likewise, it has been shown that T-cells modulate the ECM components such as collagen content in cardiac tissue in mice (Yu *et al.* 2006. Hypertension). Taken altogether, it more likely that salt-induced vascular inflammation which in turn leads to remodeling in the vascular tissue and the extracellular matrix and eventually causes dissection form of AAA.

Next, to characterize the salt mediated vascular inflammation, we evaluated the abundance of cytokines and immune cells in the abdominal aorta and perivascular adipose tissue (PVAT). We included the PVAT in the assessment of the abdominal aorta since PVAT was shown to harbor immune cells such as T-cells, macrophages and neutrophils, and contributes to the formation of Ang II-dependent AAA (Police *et al.* 2009. Arterioscler Thromb Vasc Biol). In our study, we observed the accelerated expression of TNF $\alpha$  and IFN $\gamma$  in the aortas of salt pre-treated mice compared to the control mice. TNF $\alpha$  and IFN $\gamma$  is mainly produce by macrophages and T-cells (Holtmann *et al.* 1995. Naturwissenschaften). The pathophysiological role of these cytokines was confirmed in several human and animal studies. Thus, elevated expression levels of TNF $\alpha$  and INF $\gamma$  were detected in aortic aneurysm or in the serum of patients with AAA (Sato *et al.* 2004. Clin Sci; Szekanecz *et al.* 1994. Agents Actions; Juvonen *et al.* 1997. Arterioscler Thromb Vasc Biol). Moreover, defective IFN $\gamma$  production was found to abrogate AAA in mice (Zhou *et al.* 2013. J Immunol). In one systemic review of studies examining inflammation associated cytokines in abdominal aortic aneurysm samples, it was suggested that TNF $\alpha$  and IFN $\gamma$  are the most consistently upregulated cytokines in large AAAs (Golledge *et al.* 2009. Dis Markers). These findings verify the concept that salt pre-treatment exaggerates AAA via an immune cell-mediated mechanism. Besides TNF $\alpha$  and IFN $\gamma$ , TGF $\beta$  was also significantly upregulated in aortas of salt pretreated mice compared to the control mice. TGF $\beta$  is a multifunctional cytokine and its role in AAA

is still not clear. Thus, it has been reported that TGF $\beta$  exacerbates the development of AAA possible by inducing apoptosis (Chaouchi *et al.* 1995 Oncogene) a hallmark in the pathogenesis of AAA (Wang *et al.* 2013. Cardiovasc Pathol). On the other hand, TGF $\beta$  regulates regulatory T-cell (T<sub>reg</sub>) growth and development (Wahl. 1994. J Exp Med; Fu *et al.* 2004. Am J Transplant). T<sub>reg</sub> performs immunosuppressive functions and controls pro-inflammatory Th17 (Xie *et al.* 2010. Cytokine) and thereby seems to reduce AAA formation (Ait-Oufella *et al.* 2013. Arterioscler Thromb Vasc Biol). Here, we cannot name the exact role of the elevated TGF $\beta$  in the aortas in the salt pre-treated mice. Surprisingly, we found the expression of the anti-inflammatory IL10 higher in the aortas of the salt pre-treated mice. We suggest the higher expression of IL10 is due to a compensatory mechanism to balance the exaggerated pro-inflammatory condition caused by salt pre-treatment. In line with this assumption, several studies observed increased levels of IL10 as a result of compensatory action. For example, Barhoumi and colleagues (Barhoumi *et al.* 2011. Hypertension) reported an increase in the plasma levels of IL10 in Ang II-infused mice. Furthermore, Mallat and colleagues found that IL10 was expressed in human atherosclerotic plaques (Mallat *et al.* 1999. Arterioscler Thromb Vasc Biol). Furthermore, the elevation of IL10 in our model could be due to the high relative expression of TGF $\beta$  which in turn induces the activation of T<sub>reg</sub> as a part of a compensatory mechanism (Rubtsov *et al.* 2008. Immunity).

Since TNF $\alpha$  and IFN $\gamma$  are produced predominantly by T-cells, we investigated the T-cell signature in the aortas of the salt pre-treated and control mice. We found that salt pre-treatment increased the total number of CD4 and CD8 T-cells in the aorta. These findings suggest the contribution of T-cells in salt-mediated vascular injury. Likewise, the abundance of central memory and effector memory of CD4 and CD8 T-cells was significantly higher in the aortas of the salt pre-treated mice compared to the control mice. Furthermore, CD69 CD4 T-cell frequency was higher in the aortas of the salt pre-treated mice as well. CD69 is an early activation marker (Ziegler *et al.* 1994. Stem Cells). The elevation of central memory, effector memory and CD69 CD4 T-cells in the salt pre-treated mice demonstrates the activation of T-cells and their differentiation into pro-inflammatory phenotype as a result of salt pre-treatment. Due to the limit number of immune cells in the aorta and to further investigate the roles of effector T-cells in salt-mediated vascular injury, we carried out flow cytometric analysis on splenic T cells. Splenic effector CD8 (Tc1) subpopulation was found to be more abundant in the salt pre-treated mice compared to the control group. Splenic Tc1 CD8 T cells which are producing both IL17 and IFN $\gamma$  are known as a cytotoxic subpopulation of CD8 effector T-cells (Tajima *et al.* 2011. Int Immunol). The higher abundance of the systemic Tc1 CD8 T-cells in the salt pre-treated mice suggests the key role of Tc1 CD8 T-cells in the salt-mediated vascular injury in the AAA. This observation is supported by other studies showing the effect of Tc1 CD8 T-cells on the vascular injury. Maga *et al.* demonstrated that Tc1 CD8+ T-cells adhere to the injured vessels and are involved in vascular injury in humans (Maga *et al.* 2018. Clin Immunol). In addition, Tc1 was shown to induce AAA via

extracellular matrix remodeling (Zhou *et al.* 2013. J Immunol). To validate the role of salt on the differentiation of CD8 T-cells, we carried out *in vitro* experiments in which we cultured splenic naïve CD8 T-cells in a medium that has a sodium concentration of 140 mM or 180 mM. The cell culture medium which has 140 mM Na represents normal physiological blood conditions. While the medium with 180 mM Na represents the high salt effect. Interestingly, a higher number of naïve CD8 T-cells were differentiated into Tc1 CD8 cells high salt medium (180 mM Na) compared to the normal salt medium (140 mM Na), verifying the effect of high salt on CD8 differentiation.

Interestingly, we could not see any effects of salt pre-treatment on Th17 frequencies. This observation contrasts with several studies showing the elevation of Th17 subpopulation as a result of high salt treatment. Kleinewietfeld *et al.* reported the role of salt in the development of experimental autoimmune encephalomyelitis via the induction of murine and human Th17 T-cells (Kleinewietfeld *et al.* 2013. Nature). Wei *et al.* showed that high salt intake induces the development of gut Th17 and thus exacerbates colitis in mice (Wei *et al.* 2017. Ocotarget). The upregulation of Th17 in the salt mediated lupus nephritis was shown by Yang *et al.* (Yang *et al.* 2015. Int Immunopharmacol). Furthermore, Wilck *et al.* (Wilck *et al.* 2017. Nature) verified the effect of high salt diet in the development of gut Th17. There are several reasons for this discrepancy. First, the time point; in the present study, mice were pre-treated with salt before the induction of AAA in our study, while in all other studies T cells were analyzed directly after high salt treatment. Second, the model design; we infused the mice with a high dose of Ang II to induce vascular injury. In other studies, different inflammatory stimuli were applied to induce different diseases (Kleinewietfeld *et al.* 2013. Nature).

Alongside the effect of salt on T-cells, our study spotlights the impact of salt pre-treatment on the macrophage's abundance in the aorta. Flow cytometric analysis showed that the aortas of the salt pre-treated mice had a higher number of macrophages compared to the control mice. Moreover, the higher expression of iNOS in the aortas of the salt pre-treated mice indicates the higher abundance of M1 macrophages rather than M2 macrophages. M1 macrophages are a pro-inflammatory subset of macrophages (Mills *et al.* 2000. J Immunol). The higher abundance of M1 macrophages in the aortas of the salt pre-treated mice supports the salt-mediated effect on driving immune cells into a pro-inflammatory phenotype in the vascular injury. The effect of salt on priming macrophages in the M1 direction was already shown in other studies (Müller *et al.* 2013. PLoS One; Zhang *et al.* 2015. Cell Res; Binger *et al.* 2015. J Clin Invest), supporting our results. In the context of AAA development and progression, Raffort *et al.* showed that macrophages take part in AAA development by inducing extracellular matrix degradation (matrix metalloproteases), inflammation (production of cytokines), and finally tissue healing and repair mechanisms (Raffort *et al.* 2017. Nat Rev Cardiol). IFN $\gamma$  polarizes macrophages into M1 macrophages (Mills *et al.* 2000. J Immunol).

IFN $\gamma$  is also a product of Tc1 CD8 T-cells. In the present study, the number of Tc1 CD8 T-cells were significantly increased in salt pre-treated mice, confirming the hypothesis that salt-pretreatment drives immune cells in a pro-inflammatory phenotype and thereby contribute to accelerate vascular damage. Nishimura and colleagues have shown that CD8 effector T-cells play a crucial role in the recruitment of macrophages (Nishimura *et al.* 2009. Nat Med). Moreover, they reported that depletion of CD8 T-cells reduces the infiltration of M1 macrophages in the adipose tissue. These pieces of evidence prove the contribution of M1 macrophages in the salt-mediated vascular injury, most likely via a stimulation of activated CD8 Tc1 T-cells.

Neutrophils play a crucial role in the development of vascular damage. It was demonstrated that the depletion of neutrophils inhibits the formation of abdominal aortic aneurysm (Eliason *et al.* 2005. Circulation). To characterize the role of neutrophils in our experimental model, we assessed the infiltration of neutrophils in aortas of ApoE<sup>-/-</sup> mice from the salt pre-treated and control group. The higher abundance of infiltrated neutrophils in abdominal aortas of salt pre-treated mice was confirmed by flow cytometry. In addition, higher expression of neutrophil elastase in the aortas of salt pre-treated mice confirms the higher abundance of neutrophils. Furthermore, elevated neutrophil elastase expression in the salt pre-treated mice was validated by the assessment of breakdowns in the aortic elastic fibers. The excessive breakdowns of elastic fibers in the aortas of the salt pre-treated mice indicate the higher activity and abundance of neutrophil elastase and thus neutrophils. These findings confirm the role of neutrophils in the salt-mediated vascular injury in our model. In line with this assumption, multiple studies suggest a key role of neutrophils in vascular inflammation (Gómez-Moreno *et al.* 2018. Eur J Clin Invest). Thus, Meher *et al.* showed that neutrophils promoted the AAA formation via IL1 $\beta$ -mediated neutrophil extracellular trap formation (Meher *et al.* 2018. Arterioscler Thromb Vasc Biol).

The metalloproteases, MMP2 and MMP9 are secreted mainly from macrophages and neutrophils and have been associated with cardiovascular disorders (Hu *et al.* 2007. Nat Rev Drug Discov). We did not see significant differences in the relative expression of MMP2 and MMP9 in the aortas between the salt pre-treated and control mice. However, there was a tendency for MMP2 and MMP9 to be higher in the salt pre-treated mice.

In summary, in the second part of our study, we showed that only 2 weeks of salt pre-treatment exacerbated the incidence and prevalence of Ang II-induced AAA. Salt pre-treatment was demonstrated to aggravate the vascular inflammation and prime immune cells into a pro-inflammatory phenotype. We suggest that, vascular inflammation induces vascular remodeling and changes in extracellular matrix leading to structural vascular damage and finally to the dissection of the abdominal aorta. The present study revealed an important role of salt pre-treatment on CD8 differentiation and function in vascular disease. T-cells, macrophages, and

neutrophils were demonstrated to be the key players in the salt-mediated vascular injury. Reducing salt and changing lifestyle is necessary to avoid related cardiovascular disease and should be considered as one of the first cost-effective measurements to taken.

## 6 Conclusion

In our study, we demonstrated nutrition factors like SCFAs and salt have a great impact on vascular disease. This effect was mainly immune cell-mediated. Chronic C3 treatment shifted the immune cell response into an anti-inflammatory phenotype and thereby attenuates the development of atherosclerosis. In contrast, salt pre-treatment exaggerated the pro-inflammatory response and aggravates the incidence and outcome of AAA compared to control mice. Treatment with C3 or salt shifted the balance between the anti-inflammatory and pro-inflammatory immune cells. Dysbalance between the anti-inflammatory and pro-inflammatory immune cells mediates a protective or aggravating effect on vascular injury. The effect of C3 and salt on immune cells was reflected in the degree of vascular injury. Beside the immune-mediated effect, we cannot rule out direct effects of C3 and salt on atherosclerosis and AAA. In particular, chronic C3 treatment improved vascular function and attenuated blood pressure response to Ang II. C3, as well as other SCFA, are produced by the gut microbiome through the fermentation process of indigestible fibers. Both fibers and salt are main nutrition components, nevertheless, each has a distinctive effect on immune response and in turn affects cardiovascular status differently. Results from the study support present guidelines recommending an increased fiber intake and a reduced salt intake. Moreover, the present studies give new insights into how food habits influence cardiovascular disease, which still the leading cause of death.

## 7 References

### A

Afsar B, Kuwabara M, Ortiz A, et al. Salt Intake and Immunity. 2018. *Hypertension*. 72(1):19–23.

Ailawadi G, Moehle CW, Pei H, Walton SP, Yang Z, Kron IL, Lau CL, Owens GK. Smooth muscle phenotypic modulation is an early event in aortic aneurysms. 2009. *J Thorac Cardiovasc Surg*. 138(6):1392-9.

Ait-Oufella H, Wang Y, Herbin O, Bourcier S, Potteaux S, Joffre J, Loyer X, Ponnuswamy P, Esposito B, Dalloz M, Laurans L, Tedgui A, Mallat Z. Natural regulatory T cells limit angiotensin II-induced aneurysm formation and rupture in mice. 2013. *Arterioscler Thromb Vasc Biol*. 33(10):2374-9.

Arpaia N, Campbell C, Fan X, Dikiy S, van der Veeken J, deRoos P, Liu H, Cross JR, Pfeffer K, Coffey PJ, Rudenski AY. Metabolites produced by commensal bacteria promote peripheral regulatory T-cell generation. 2013. *Nature*. 504:451–455.

Arpaia N, Campbell C, Fan X, et al. Metabolites produced by commensal bacteria promote peripheral regulatory T-cell generation. 2013. *Nature*. 504(7480):451–455.

### B

Barhoumi T, Kasal DA, Li MW, Shbat L, Laurant P, Neves MF, Paradis P, Schiffrin EL. T regulatory lymphocytes prevent angiotensin II-induced hypertension and vascular injury. 2011. *Hypertension*. Mar;57(3):469-76.

Bergheanu SC, Bodde MC, Jukema JW. Pathophysiology and treatment of atherosclerosis : Current view and future perspective on lipoprotein modification treatment. 2017. *Neth Heart J*. 25(4):231–242.

Bibbins-Domingo K, Chertow GM, Coxson PG, Moran A, Lightwood JM, Pletcher MJ, and Goldman L. Projected effect of dietary salt reductions on future cardiovascular disease. 2010. *N Engl J Med*. 362(7):590-9.

Binger KJ, Gebhardt M, Heinig M, et al. High salt reduces the activation of IL-4- and IL-13-stimulated macrophages. 2015. *J Clin Invest*. 125(11):4223–4238.

Binger KJ, Gebhardt M, Heinig M, Rintisch C, Schroeder A, Neuhofer W, Hilgers K, Manzel A, Schwartz C, Kleinewietfeld M, Voelkl J, Schatz V, Linker RA, Lang F, Voehringer D, Wright MD, Hubner N, Dechend R, Jantsch J, Titze J, Müller DN. High salt reduces the activation of IL-4- and IL-13-stimulated macrophages. 2015. *J Clin Invest*. 125(11):4223-38.

Brestoff JR, Artis D. Commensal bacteria at the interface of host metabolism and the immune system. 2013. *Nat Immunol*. 14(7):676–684.

Brown AJ, Goldsworthy SM, Barnes AA, Eilert MM, Tcheang L, Daniels D, Muir AI, Wigglesworth MJ, Kinghorn I, Fraser NJ, Pike NB, Strum JC, Steplewski KM, Murdock PR, Holder JC, Marshall FH, Szekeres PG, Wilson S, Ignar DM, Foord SM, Wise A, Dowell SJ. The Orphan G protein-coupled receptors GPR41 and GPR43 are activated by propionate and other short chain carboxylic acids. 2003. *J Biol Chem*. 278(13):11312-9.

Bu G. Apolipoprotein E and its receptors in Alzheimer's disease: pathways, pathogenesis and therapy. 2009. *Nat Rev Neurosci*. 10(5):333–344.

Bugaut M. Occurrence, absorption and metabolism of short chain fatty acids in the digestive tract of mammals. 1987. *Comp Biochem Physiol B*. 86(3):439–472.

Burnier M, Brunner HR. Angiotensin II receptor antagonists. 2000. *Lancet*. 355(9204):637-45.

Busuttill RW, Rinderbriecht H, Flesher A, Carmack C. Elastase activity: the role of elastase in aortic aneurysm formation. 1982. *J Surg Res*. 32(3):214-7.

Butcher, M.J., et al., Flow cytometry analysis of immune cells within murine aortas. *J Vis Exp*, 2011(53).

## C

Cao RY, Amand T, Ford MD, Piomelli U, Funk CD. The Murine Angiotensin II-Induced Abdominal Aortic Aneurysm Model: Rupture Risk and Inflammatory Progression Patterns. 2010. *Front Pharmacol*. 1:9.

Castellano JM, Kovacic JC, Sanz J, Fuster V. Are we ignoring the dilated thoracic aorta? 2012. *Ann N Y Acad Sci*. 1254:164–174.

Cavaillon JM. Pro- versus anti-inflammatory cytokines: myth or reality. 2001. *Cell Mol Biol (Noisy-le-grand)*. 47(4):695–702.

Chang Y, Wei W. Angiotensin II in inflammation, immunity and rheumatoid arthritis. 2015. *Clin Exp Immunol.* 179(2):137–145.

Chaouchi N, Arvanitakis L, Auffredou MT, Blanchard DA, Vazquez A, Sharma S. Characterization of transforming growth factor-beta 1 induced apoptosis in normal human B cells and lymphoma B cell lines. 1995. *Oncogene.* 11(8):1615-22.

Chaplin DD. 1. Overview of the human immune response. 2006. *J Allergy Clin Immunol.* 117(2 Suppl Mini-Primer):S430–S435.

Chaudhry A, Samstein RM, Treuting P, Liang Y, Pils MC, Heinrich JM, Jack RS, Wunderlich FT, Brüning JC, Müller W, Rudensky AY. Interleukin-10 signaling in regulatory T cells is required for suppression of Th17 cell-mediated inflammation. 2011. *Immunity.*;34(4):566-78.

Childs CE, Calder PC, Miles EA. Diet and Immune Function. 2019. *Nutrients.*11(8):1933.

Chistiakov DA, Bobryshev YV, Nikiforov NG, Elizova NV, Sobenin IA, Orekhov AN. Macrophage phenotypic plasticity in atherosclerosis: The associated features and the peculiarities of the expression of inflammatory genes. 2015. *Int J Cardiol.* 184:436-45.

Cochain C, Zerneck A. Macrophages in vascular inflammation and atherosclerosis. 2017. *Pflugers Arch.* 469(3-4):485-499.

Cohen JR, Keegan L, Sarfati I, Danna D, Ilardi C, Wise L. Neutrophil chemotaxis and neutrophil elastase in the aortic wall in patients with abdominal aortic aneurysms. 1991. *J Invest Surg.* 4(4):423-30.

Cornuz J, Sidoti Pinto C, Tevaearai H, Egger M. Risk factors for asymptomatic abdominal aortic aneurysm: systematic review and meta-analysis of population-based screening studies. 2004. *Eur J Public Health.* 14(4):343–349.

Cronkite DA, Strutt TM. The Regulation of Inflammation by Innate and Adaptive Lymphocytes. *J 2018. Immunol Res.* 2018:1467538.

## **D**

Davie JR. Inhibition of histone deacetylase activity by butyrate. 2003. *J Nutr.* 133(7 Suppl):2485S–2493S.

Davis FM, Rateri DL, Daugherty A. Abdominal aortic aneurysm: novel mechanisms and therapies. 2015. *Curr Opin Cardiol.* 30(6):566–573.

Dayton S, Pearce ML. Prevention of Coronary Heart Disease and other complications of Atherosclerosis by Modified Diet. 1969. *Am J Med*. Vol. 46.

Didion SP, Kinzenbaw DA, Schrader LI, Chu Y, Faraci FM. Endogenous interleukin-10 inhibits angiotensin II-induced vascular dysfunction. 2009. *Hypertension*. 54(3):619-24.

Dimayuga PC, Chyu KY, Cercek B. Immune responses regulating the response to vascular injury. 2010. *Curr Opin Lipidol*. 21(5):416–421.

Dimmeler S. Cardiovascular disease review series. 2011. *EMBO Mol Med*. 3(12): 697.

## E

Eliason JL, Hannawa KK, Ailawadi G, et al. Neutrophil depletion inhibits experimental abdominal aortic aneurysm formation. 2005. *Circulation*. 112(2):232–240.

Erbel C, Chen L, Bea F, Wangler S, Celik S, Lasitschka F, Wang Y, Böckler D, Katus HA, Dengler TJ. Inhibition of IL-17A attenuates atherosclerotic lesion development in apoE-deficient mice. 2009. *J Immunol*. 183(12):8167-75.

Erkkilä AT, Lichtenstein AH. Fiber and cardiovascular disease risk: how strong is the evidence? 2006. *J Cardiovasc Nurs*. 21(1):3–8.

## F

Fernández-Alfonso MS, Somoza B, Tsvetkov D, Kuczmanski A, Dashwood M, Gil-Ortega M. Role of Perivascular Adipose Tissue in Health and Disease. 2017. *Compr Physiol*. 8(1):23–59.

Fernández-Ruiz, I. Immune system and cardiovascular disease. 2016. *Nat Rev Cardiol*. 13, 503

Fiuza-Luces C, Santos-Lozano A, Joyner M, Carrera-Bastos P, Picazo O, Zugaza JL, Izquierdo M, Ruilope LM, Lucia A. Exercise benefits in cardiovascular disease: beyond attenuation of traditional risk factors. 2018. *Nat Rev Cardiol*. 15(12):731-743.

Flegal KM, Kruszon-Moran D, Carroll MD, Fryar CD, Ogden CL. Trends in Obesity Among Adults in the United States, 2005 to 2014. 2016. *JAMA*. 315(21):2284-91.

Fleming SE, Choi SY, Fitch MD. Absorption of short-chain fatty acids from the rat cecum in vivo. 1991. *J Nutr.* 121(11):1787–1797.

Forsdahl SH, Singh K, Solberg S, Jacobsen BK. Risk factors for abdominal aortic aneurysms: a 7-year prospective study: the Tromsø Study, 1994-2001. 2009. *Circulation.*119(16):2202–2208.

Frančula-Zaninović S, Nola IA. Management of Measurable Variable Cardiovascular Disease' Risk Factors. 2018. *Curr Cardiol Rev.* 14(3): 153–163.

Frisoli TM, Schmieder RE, Grodzicki T, Messerli FH. Salt and hypertension: is salt dietary reduction worth the effort? 2012. *Am J Med.* 2012;125(5):433–439.

Fu S, Zhang N, Yopp AC, Chen D, Mao M, Chen D, Zhang H, Ding Y, Bromberg JS. TGF-beta induces Foxp3 + T-regulatory cells from CD4 + CD25 - precursors. 2004. *Am J Transplant.* 4(10):1614-27.

## G

Garg N, Muduli SK, Kapoor A, Tewari S, Kumar S, Khanna R, Goel PK. Comparison of different cardiovascular risk score calculators for cardiovascular risk prediction and guideline recommended statin uses. 2017. *Indian Heart J.* 69(4): 458–463.

George KP & Green DJ. Historical perspectives in the assessment of cardiovascular structure and function. 2018. *Eur J Appl Physiol.* 118: 1079.

Getz GS, Reardon CA. Animal models of atherosclerosis. 2012 *Arterioscler Thromb Vasc Biol.* 32(5):1104–1115.

Gill PA, van Zelm MC, Muir JG, Gibson PR. Review article: short chain fatty acids as potential therapeutic agents in human gastrointestinal and inflammatory disorders. 2018. *Aliment Pharmacol Ther.* 48(1):15–34.

Ginhoux F, Jung S. Monocytes and macrophages: developmental pathways and tissue homeostasis. 2014. *Nat Rev Immunol.* (6):392-404.

Gisterå A, Hansson GK. The immunology of atherosclerosis. 2017. *Nat Rev Nephrol.* 13(6):368-380.

Golledge AL, Walker P, Norman PE, Golledge J. A systematic review of studies examining inflammation associated cytokines in human abdominal aortic aneurysm samples. 2009. *Dis Markers.* 26(4):181-8.

Golledge J, Hankey GJ, Yeap BB, Almeida OP, Flicker L, Norman PE. Reported high salt intake is associated with increased prevalence of abdominal aortic aneurysm and larger aortic diameter in older men. 2014. *PLoS One*.9(7):e102578. doi: 10.1371/journal.pone.0102578. PMID: 25036037; PMCID: PMC4103816.

Gómez-Moreno D, Adrover JM, Hidalgo A. Neutrophils as effectors of vascular inflammation. 2018. *Eur J Clin Invest*. 48 Suppl 2:e12940.

Güden-Silber T, Temme S, Jacoby C, Flögel U. Biomedical 19F MRI Using Perfluorocarbons. 2018. *Methods Mol Biol*.1718:235–257

Guo DC, Papke CL, He R, Milewicz DM. Pathogenesis of thoracic and abdominal aortic aneurysms. 2006. *Ann N Y Acad Sci*.1085:339–352.

Guzik TJ, Hoch NE, Brown KA, McCann LA, Rahman A, Dikalov S, Goronzy J, Weyand C, Harrison DG. Role of the T cell in the genesis of angiotensin II induced hypertension and vascular dysfunction. 2007. *J Exp Med*.204(10):2449-60.

Guzik TJ, Skiba DS, Touyz RM, Harrison DG. The role of infiltrating immune cells in dysfunctional adipose tissue. *Cardiovasc Res*. 2017;113(9):1009–1023.

## H

Haghikia A, Jorg S, Duscha A, Berg J, Manzel A, Waschbisch A, Hammer A, Lee DH, May C, Wilck N, Balogh A, Ostermann AI, Schebb NH, Akkad DA, Grohme DA, Kleinewietfeld M, Kempa S, Thone J, Demir S, Muller DN, Gold R, Linker RA. Dietary fatty acids directly impact central nervous system autoimmunity via the small intestine. 2015. *Immunity*. 43:817-829

Hartley L, May MD, Loveman E, Colquitt JL, Rees K. Dietary fibre for the primary prevention of cardiovascular disease. 2016. *Cochrane Database Syst Rev*. (1):CD011472.

Hashmat S, Rudemiller N, Lund H, Abais-Battad JM, Van Why S, Mattson DL. Interleukin-6 inhibition attenuates hypertension and associated renal damage in Dahl salt-sensitive rats. 2016. *Am J Physiol Renal Physiol*. 311:F555–F561

He FJ, MacGregor GA. Effect of modest salt reduction on blood pressure: a meta-analysis of randomized trials. Implications for public health. 2002 *J Hum Hypertens*. 16(11):761–770.

Henrichot E, Juge-Aubry CE, Pernin A, et al. Production of chemokines by perivascular adipose tissue: a role in the pathogenesis of atherosclerosis? 2005. *Arterioscler Thromb Vasc Biol.* 25(12):2594–2599.

Hernandez AL, Kitz A, Wu C, et al. Sodium chloride inhibits the suppressive function of FOXP3+ regulatory T cells. 2015. *J Clin Invest.* 125(11):4212–4222.

Herring N, Kalla M, Paterson DJ. The autonomic nervous system and cardiac arrhythmias: current concepts and emerging therapies. 2019. *Nat Rev Cardiol.* [Epub ahead of print]

Herrington W, Lacey B, Sherliker P, Armitage J, Lewington S. Epidemiology of Atherosclerosis and the Potential to Reduce the Global Burden of Atherothrombotic Disease. 2016. *Circ Res.* 118(4):535–546.

High salt reduces the activation of IL-4- and IL-13-stimulated macrophages. 2015. *J Clin Invest.* 125(11):4223–4238.

Holtmann H, Resch K. Cytokines. 1995. *Naturwissenschaften.* 82(4):178–187.

Honda, K., Littman, D. The microbiota in adaptive immune homeostasis and disease. 2016. *Nature.* 535, 75–84.

## I

Imanishi T, Han DK, Hofstra L, Hano T, Nishio I, Liles WC, Gown AM, Schwartz SM. Apoptosis of vascular smooth muscle cells is induced by Fas ligand derived from monocytes/macrophage. 2002. *Atherosclerosis.* 161(1):143-51.

Insull W Jr. The pathology of atherosclerosis: plaque development and plaque responses to medical treatment. 2009. *Am J Med.* 122(1 Suppl):S3–S14.

## J

Jacobs DR Jr, Tapsell LC. What an anticardiovascular diet should be in 2015. 2015. *Curr Opin Lipidol.* 26(4):270–275.

Jörg S, Kissel J, Manzel A, Kleinewietfeld M, Haghikia A, Gold R, Müller DN, Linker RA. High salt drives Th17 responses in experimental autoimmune encephalomyelitis without impacting myeloid dendritic cells. 2016. *Exp Neurol.* 279:212-222.

Juvonen J, Surcel HM, Satta J, Teppo AM, Bloigu A, Syrjälä H, Airaksinen J, Leinonen M, Saikku P, Juvonen T. Elevated circulating levels of inflammatory cytokines in patients with abdominal aortic aneurysm. 1997. *Arterioscler Thromb Vasc Biol.* 17(11):2843-7.

## K

Kannel WB. Risk factors in hypertension. 1989. *J Cardiovasc Pharmacol.* 13 Suppl 1:S4–S10

Kaye DM, Shihata W, Jama HA, Tsyganov K, Ziemann M, Kiriazis H, Horlock D, Vijay A, Giam B, Vinh A, Johnson C, Fiedler A, Donner D, Snelson M, Coughlan MT, Phillips S, Du XJ, El-Osta A, Drummond G, Lambert GW, Spector T, Valdes AM, Mackay CR, Marques FZ. Deficiency of Prebiotic Fibre and Insufficient Signalling Through Gut Metabolite Sensing Receptors Leads to Cardiovascular Disease. 2020. *Circulation.*

Kee HJ, Sohn IS, Nam KI, Park JE, Qian YR, Yin Z, Ahn Y, Jeong MH, Bang YJ, Kim N, Kim JK, Kim KK, Epstein JA, Kook H. Inhibition of histone deacetylation blocks cardiac hypertrophy induced by angiotensin II infusion and aortic banding. 2006. *Circulation.* 113(1):51-9.

Kerkelä R, Ulvila J, Magga J. Natriuretic Peptides in the Regulation of Cardiovascular Physiology and Metabolic Events. 2015. *J Am Heart Assoc.* 4(10):e002423.

Kim Y, Je Y. Dietary fibre intake and mortality from cardiovascular disease and all cancers: A meta-analysis of prospective cohort studies. 2016. *Arch Cardiovasc Dis.* 109(1):39–54.

Kleinewietfeld M, Manzel A, Titze J, Kvakan H, Yosef N, Linker RA, Muller DN, Hafler DA. Sodium chloride drives autoimmune disease by the induction of pathogenic TH17 cells. 2013. *Nature.* 496(7446):518-22.

Koh A, De Vadder F, Kovatcheva-Datchary P, Bäckhed F. From Dietary Fiber to Host Physiology: Short-Chain Fatty Acids as Key Bacterial Metabolites. 2016. *Cell.* 165(6):1332-1345.

Kostyk AG, Dahl KM, Wynes MW, Whittaker LA, Weiss DJ, Loi R, Riches DW. Regulation of chemokine expression by NaCl occurs independently of cystic fibrosis transmembrane conductance regulator in macrophages. 2006. *Am J Pathol.* 169(1):12-20

Kvakan H, Kleinewietfeld M, Qadri F, Park JK, Fischer R, Schwarz I, Rahn HP, Plehm R, Wellner M, Elitok S, Gratze P, Dechend R, Luft FC, Muller DN. Regulatory T cells ameliorate angiotensin II-induced cardiac damage. 2009. *Circulation.* 119(22):2904-12.

Kyaw T, Winship A, Tay C, et al. Cytotoxic and proinflammatory CD8<sup>+</sup> T lymphocytes promote development of vulnerable atherosclerotic plaques in apoE-deficient mice. 2013. *Circulation*. 127(9):1028–1039.

Kyaw T, Winship A, Tay C, Kanellakis P, Hosseini H, Cao A, Li P, Tipping P, Bobik A, Toh BH. Cytotoxic and proinflammatory CD8<sup>+</sup> T lymphocytes promote development of vulnerable atherosclerotic plaques in apoE-deficient mice. 2013. *Circulation*. 127(9):1028-39.

## L

Lavie CJ, Arena R, Alpert MA, Milani RV, Ventura HO. Management of cardiovascular diseases in patients with obesity. 2018. *Nat Rev Cardiol*. 15(1):45-56.

Le Poul E, Loison C, Struyf S, Springael JY, Lannoy V, Decobecq ME, Brezillon S, Dupriez V, Vassart G, Van Damme J, Parmentier M, Detheux M. Functional characterization of human receptors for short chain fatty acids and their role in polymorphonuclear cell activation. 2003. *J Biol Chem*. 278(28):25481-9.

Leigh JA, Alvarez M, Rodriguez CJ. Ethnic Minorities and Coronary Heart Disease: an Update and Future Directions. 2016. *Curr Atheroscler Rep*. 2016;18(2):9.

Li M, van Esch BCAM, Wagenaar GTM, Garszen J, Folkerts G, Henricks PAJ. Pro- and anti-inflammatory effects of short chain fatty acids on immune and endothelial cells. 2018. *Eur J Pharmacol*. 831:52–59.

Lim SH, Song K, Lee J. Butyrate and propionate, short chain fatty acids, attenuate myocardial damages by inhibition of apoptosis in a rat model of ischemia-reperfusion. 2010. *J. Korean Soc. Appl. Biol. Chem*. 53, 570–577.

Li Y, G Zhang C, Wang XH, Liu DH. Progression of atherosclerosis in ApoE-knockout mice fed on a high-fat diet. 2016. *Eur Rev Med Pharmacol Sci*. 20(18):3863-3867.

Lintermans LL, Stegeman CA, Heeringa P, Abdulahad WH. T cells in vascular inflammatory diseases. 2014. *Front Immunol*. 5:504.

Longo GM, Xiong W, Greiner TC, Zhao Y, Fiotti N, Baxter BT. Matrix metalloproteinases 2 and 9 work in concert to produce aortic aneurysms. 2002. *J Clin Invest*. 110(5):625-32.

Lozano R, Naghavi M, Foreman K, Lim S, Shibuya K, Aboyans V, Abraham J, Adair T, Aggarwal R, Ahn SY, Alvarado M, Anderson HR, Anderson LM, Andrews KG, Atkinson C, Baddour LM, Barker-Collo S, Bartels DH, Bell ML, Benjamin EJ, Bennett D, Bhalla

K, Bikbov B, Bin Abdulhak A, Birbeck G, Blyth F, Bolliger I, Boufous S, Bucello C, Burch M, Burney P, Carapetis J, Chen H, Chou D, Chugh SS, Coffeng LE, Colan SD, Colquhoun S, Colson KE, Condon J, Connor MD, Cooper LT, Corriere M, Cortinovis M, de Vaccaro KC, Couser W, Cowie BC, Criqui MH, Cross M, Dabhadkar KC, Dahodwala N, De Leo D, Degenhardt L, Delossantos A, Denenberg J, Des Jarlais DC, Dharmaratne SD, Dorsey ER, Driscoll T, Duber H, Ebel B, Erwin PJ, Espindola P, Ezzati M, Feigin V, Flaxman AD, Forouzanfar MH, Fowkes FG, Franklin R, Fransen M, Freeman MK, Gabriel SE, Gakidou E, Gaspari F, Gillum RF, Gonzalez-Medina D, Halasa YA, Haring D, Harrison JE, Havmoeller R, Hay RJ, Hoen B, Hotez PJ, Hoy D, Jacobsen KH, James SL, Jasrasaria R, Jayaraman S, Johns N, Karthikeyan G, Kassebaum N, Keren A, Khoo JP, Knowlton LM, Kobusingye O, Koranteng A, Krishnamurthi R, Lipnick M, Lipshultz SE, Ohno SL, Mabweijano J, MacIntyre MF, Mallinger L, March L, Marks GB, Marks R, Matsumori A, Matzopoulos R, Mayosi BM, McAnulty JH, McDermott MM, McGrath J, Mensah GA, Merriman TR, Michaud C, Miller M, Miller TR, Mock C, Mocumbi AO, Mokdad AA, Moran A, Mulholland K, Nair MN, Naldi L, Narayan KM, Nasseri K, Norman P, O'Donnell M, Omer SB, Ortblad K, Osborne R, Ozgediz D, Pahari B, Pandian JD, Rivero AP, Padilla RP, Perez-Ruiz F, Perico N, Phillips D, Pierce K, Pope CA 3rd, Porrini E, Pourmalek F, Raju M, Ranganathan D, Rehm JT, Rein DB, Remuzzi G, Rivara FP, Roberts T, De León FR, Rosenfeld LC, Rushton L, Sacco RL, Salomon JA, Sampson U, Sanman E, Schwebel DC, Segui-Gomez M, Shepard DS, Singh D, Singleton J, Sliwa K, Smith E, Steer A, Taylor JA, Thomas B, Tleyjeh IM, Towbin JA, Truelsen T, Undurraga EA, Venketasubramanian N, Vijayakumar L, Vos T, Wagner GR, Wang M, Wang W, Watt K, Weinstock MA, Weintraub R, Wilkinson JD, Woolf AD, Wulf S, Yeh PH, Yip P, Zabetian A, Zheng ZJ, Lopez AD, Murray CJ, AlMazroa MA, Memish ZA. Global and regional mortality from 235 causes of death for 20 age groups in 1990 and 2010: a systematic analysis for the Global Burden of Disease Study 2010. 2012. *Lancet*. 380(9859):2095-128.

Lu G, Su G, Davis JP, Schaheen B, Downs E, Roy RJ, Ailawadi G, Upchurch GR Jr. A novel chronic advanced stage abdominal aortic aneurysm murine model. 2017. *J Vasc Surg*. 66(1):232-242.e4.

Lu H, Daugherty A. Recent Highlights of ATVB Atherosclerosis. 2016. *Arterioscler Thromb Vasc Biol*. 2015;35(3):485–491.

Luu M, Pautz S, Kohl V, Singh R, Romero R, Lucas S, Hofmann J, Raifer H, Vachharajani N, Carrascosa LC, Lamp B, Nist A, Stiewe T, Shaul Y, Adhikary T, Zaiss MM, Lauth M, Steinhoff U, Visekruna A. The short-chain fatty acid pentanoate suppresses autoimmunity by modulating the metabolic-epigenetic crosstalk in lymphocytes. 2019. *Nat Commun*. 10(1):760.

Luu M, Pautz S, Kohl V, Singh R, Romero R, Lucas S, Hofmann J, Raifer H, Vachharajani N, Carrascosa LC, Lamp B, Nist A, Stiewe T, Shaul Y, Adhikary T, Zaiss MM, Lauth M, Steinhoff U, Visekruna A. The short-chain fatty acid pentanoate suppresses autoimmunity

by modulating the metabolic-epigenetic crosstalk in lymphocytes. 2019. *Nat Commun.*10(1):760.

## **M**

Maas AHEM, Appelman YEA. Gender differences in coronary heart disease. 2010. *Neth Heart J.* 18(12): 598–602.

Madhur MS, Lob HE, McCann LA, et al. Interleukin 17 promotes angiotensin II-induced hypertension and vascular dysfunction. 2010. *Hypertension.* 55(2):500–507.

Maga P, Mikolajczyk TP, Partyka L, Siedlinski M, Maga M, Krzanowski M, Malinowski K, Luc K, Nizankowski R, Bhatt DL, Guzik TJ. Involvement of CD8<sup>+</sup> T cell subsets in early response to vascular injury in patients with peripheral artery disease in vivo. 2018. *Clin Immunol.* 194:26-33.

Mallat Z, Heymes C, Ohan J, Faggini E, Lesèche G, Tedgui A. Expression of interleukin-10 in advanced human atherosclerotic plaques: relation to inducible nitric oxide synthase expression and cell death. 1999. *Arterioscler Thromb Vasc Biol.*19(3):611-6.

Marchesi C, Paradis P, Schiffrin EL. Role of the renin–angiotensin system in vascular inflammation. 2008. *Trends Pharmacol Sci.* 29:367–374.

Marques FZ, Nelson E, Chu PY, Horlock D, Fiedler A, Ziemann M, Tan JK, Kuruppu S, Rajapakse NW, El-Osta A, Mackay CR, Kaye DM. High-Fiber Diet and Acetate Supplementation Change the Gut Microbiota and Prevent the Development of Hypertension and Heart Failure in Hypertensive Mice. 2017. *Circulation.* 135(10):964-977.

McNabney SM, Henagan TM. Short Chain Fatty Acids in the Colon and Peripheral Tissues: A Focus on Butyrate, Colon Cancer, Obesity and Insulin Resistance. 2017. *Nutrients.* 9(12):1348.

McRae MP. Dietary Fiber Is Beneficial for the Prevention of Cardiovascular Disease: An Umbrella Review of Meta-analyses. 2017. *J Chiropr Med.* 16(4):289–299.

Meher AK, Spinosa M, Davis JP, Pope N, Laubach VE, Su G, Serbulea V, Leitinger N, Ailawadi G, Upchurch GR Jr. Novel Role of IL (Interleukin)-1 $\beta$  in Neutrophil Extracellular Trap Formation and Abdominal Aortic Aneurysms. 2018. *Arterioscler Thromb Vasc Biol.* 38(4):843-853.

Mills CD, Kincaid K, Alt JM, Heilman MJ, Hill AM. M-1/M-2 macrophages and the Th1/Th2 paradigm. 2000. *J Immunol.* 164(12):6166-73.

Mittrücker HW, Visekruna A, Huber M. Heterogeneity in the differentiation and function of CD8<sup>+</sup> T cells. 2014. Arch Immunol Ther Exp (Warsz). 62(6):449–458.

Movat HZ. Demonstration of all connective tissue elements in a single section; pentachrome stains. 1955. AMA Arch Pathol. 60(3):289-95.

Müller S, Quast T, Schröder A, Hucke S, Klotz L, Jantsch J, Gerzer R, Hemmersbach R, Kolanus W. Salt-dependent chemotaxis of macrophages. 2013. PLoS One. 8(9):e73439.

Nagai M, Hoshida S, Kario K. Sleep Duration as a Risk Factor for Cardiovascular Disease—a Review of the Recent Literature. 2010. Curr Cardiol Rev. 6(1): 54–61.

Natarajan N, Hori D, Flavahan S, et al. Microbial short chain fatty acid metabolites lower blood pressure via endothelial G protein-coupled receptor 41. 2016. Physiol Genomics. 48(11):826–834.

## N

Natarajan N, Hori D, Flavahan S, Steppan J, Flavahan NA, Berkowitz DE, Pluznick JL. Microbial short chain fatty acid metabolites lower blood pressure via endothelial G protein-coupled receptor 41. 2016. Physiol Genomics. 48(11):826-834.

National Research Council (US) Committee on Diet and Health. Diet and Health: Implications for Reducing Chronic Disease Risk. Washington (DC): National Academies Press (US). 1989. 19, Atherosclerotic Cardiovascular Diseases.

Nishijo N, Sugiyama F, Kimoto K, Taniguchi K, Murakami K, Suzuki S, Fukamizu A, Yagami K. Salt-sensitive aortic aneurysm and rupture in hypertensive transgenic mice that overproduce angiotensin II. 1998. Lab Invest. 78(9):1059-66.

Nishimura S, Manabe I, Nagasaki M, Eto K, Yamashita H, Ohsugi M, Otsu M, Hara K, Ueki K, Sugiura S, Yoshimura K, Kadowaki T, Nagai R. CD8<sup>+</sup> effector T cells contribute to macrophage recruitment and adipose tissue inflammation in obesity. 2009. Nat Med. 15(8):914-20.

Nosalski R, Guzik TJ. Perivascular adipose tissue inflammation in vascular disease. 2017. Br J Pharmacol. 174(20):3496-3513.

## O

Owen L, Corfe B. The role of diet and nutrition on mental health and wellbeing. 2017. Proc Nutr Soc. 76(4):425–426.

Ozen G, Daci A, Norel X, Topal G. Human perivascular adipose tissue dysfunction as a cause of vascular disease: Focus on vascular tone and wall remodelling. 2015. *Eur J Pharmacol.* 766:16–24.

## **P**

Park J, Kim M, Kang SG, Jannasch AH, Cooper B, Patterson J, Kim CH. Short-chain fatty acids induce both effector and regulatory t cells by suppression of histone deacetylases and regulation of the mtor-s6k pathway. 2015. *Mucosal immunology.* 8:80-93

Peshkova IO, Schaefer G, Koltsova EK. Atherosclerosis and aortic aneurysm - is inflammation a common denominator? 2016. *FEBS J.* 283(9):1636-52.

Peters SG, Pomare EW, Fisher CA. Portal and peripheral blood short chain fatty acid concentrations after caecal lactulose instillation at surgery. 1992. *Gut.* 33(9):1249–1252.

Pieters M, de Maat MP. Diet and haemostasis - a comprehensive overview. 2015. *Blood Rev.* 29(4):231–241.

Pluznick J. A novel SCFA receptor, the microbiota, and blood pressure regulation. 2014. *Gut Microbes.* 5(2):202–207.

Pluznick JL. Gut microbiota in renal physiology: focus on short-chain fatty acids and their receptors. 2016. *Kidney Int.* 90(6):1191–1198.

Pluznick JL. Microbial Short-Chain Fatty Acids and Blood Pressure Regulation. 2017. *Curr Hypertens Rep.* 19(4):25.

Priyadarshini M, Kotlo KU, Dudeja PK, Layden BT. Role of Short Chain Fatty Acid Receptors in Intestinal Physiology and Pathophysiology. 2018. *Compr Physiol.* 8(3):1091–1115.

## **R**

Rader DJ, Daugherty A. Translating molecular discoveries into new therapies for atherosclerosis. 2008. *Nature.* 451(7181):904–913.

Raffort J, Lareyre F, Clément M, Hassen-Khodja R, Chinetti G, Mallat Z. Monocytes and macrophages in abdominal aortic aneurysm. 2017. *Nat Rev Cardiol.* 14(8):457-471.

Robertson L, Atallah E, Stansby G. Pharmacological treatment of vascular risk factors for reducing mortality and cardiovascular events in patients with abdominal aortic aneurysm. 2017. *Cochrane Database Syst Rev*.1(1):CD010447.

Ross R. The pathogenesis of atherosclerosis: a perspective for the 1990s. 1993. *Nature*. 362(6423):801–809.

Rubtsov YP, Rasmussen JP, Chi EY, Fontenot J, Castelli L, Ye X, Treuting P, Siewe L, Roers A, Henderson WR Jr, Muller W, Rudensky AY. Regulatory T cell-derived interleukin-10 limits inflammation at environmental interfaces. 2008. *Immunity*. 28(4):546-58.

Ruiz-Ortega M, Lorenzo O, Egido J. Angiotensin III increases MCP-1 and activates NF-kappaB and AP-1 in cultured mesangial and mononuclear cells. 2000. *Kidney Int*. 57(6):2285-98.

## S

Safar ME. Arterial stiffness as a risk factor for clinical hypertension.2018. *Nat Rev Cardiol*. 15(2):97-105.

Sakalihasan N, Michel JB, Katsargyris A, Kuivaniemi H, Defraigne JO, Nchimi A, Powell JT, Yoshimura K, Hultgren R. Abdominal aortic aneurysms. 2018. *Nat Rev Dis Primers*. 4(1):34.

Sasiain MC, de la Barrera S, Fink S, Finiasz M, Alemán M, Fariña MH, Pizzariello G, Valdez R. Interferon-gamma (IFN-gamma) and tumour necrosis factor-alpha (TNF-alpha) are necessary in the early stages of induction of CD4 and CD8 cytotoxic T cells by *Mycobacterium leprae* heat shock protein (hsp) 65 kD. 1998. *Clin Exp Immunol*. 114(2):196-203.

Satoh H, Nakamura M, Satoh M, Nakajima T, Izumoto H, Maesawa C, Kawazoe K, Masuda T, Hiramori K. Expression and localization of tumour necrosis factor-alpha and its converting enzyme in human abdominal aortic aneurysm. 2004. *Clin Sci (Lond)*.106(3):301-6

Sawicka K, Szczyrek M, Jastrzębska I, Prasał M, Zwolak A, Daniluk J. Hypertension – The Silent Killer. 2011. *J Pre Clin Clin Res*. 5(2):43-46.

Schierke F, Wyrwoll MJ, Wisdorf M, et al. Nanomechanics of the endothelial glycocalyx contribute to Na<sup>+</sup>-induced vascular inflammation. 2017. *Sci Rep*. 7:46476.

Schneider, C. A.; Rasband, W. S. & Eliceiri, K. W. (2012), "NIH Image to ImageJ: 25 years of image analysis", *Nature methods* 9(7): 671-675.

Seljeset S, Siehler S. Receptor-specific regulation of ERK1/2 activation by members of the "free fatty acid receptor" family. 2012. *J Recept Signal Transduct Res.* 32(4):196-201.

Shimokama T, Haraoka S, Horiguchi H, Sugiyama F, Murakami K, Watanabe T. The Tsukuba hypertensive mouse (transgenic mouse carrying human genes for both renin and angiotensinogen) as a model of human malignant hypertension: development of lesions and morphometric analysis. 1998. *Virchows Arch.* 432(2):169-75.

Silva JPB, Navegantes-Lima KC, Oliveira ALB, Rodrigues DVS, Gaspar SLF, Monteiro VVS, Moura DP, Monteiro MC. Protective Mechanisms of Butyrate on Inflammatory Bowel Disease. 2018. *Curr Pharm Des.* (35):4154-4166.

Silvestre-Roig C, Braster Q, Ortega-Gomez A. et al. Neutrophils as regulators of cardiovascular inflammation. 2020. *Nat Rev Cardiol.*

Sivaprakasam S, Prasad PD, Singh N. Benefits of short-chain fatty acids and their receptors in inflammation and carcinogenesis. 2016. *Pharmacol Ther.* 164:144–151.

Smith PM, Howitt MR, Panikov N, Michaud M, Gallini CA, Bohlooly YM, Glickman JN, Garrett WS. The microbial metabolites, short-chain fatty acids, regulate colonic treg cell homeostasis. 2013. *Science.* 341:569-573.

Smith PM, Howitt MR, Panikov N, Michaud M, Gallini CA, Bohlooly-Y M, Glickman JN, Garrett WS. The microbial metabolites, short-chain fatty acids, regulate colonic Treg cell homeostasis. 2013. *Science.* 341:569–573.

Stearns ME, Wang M, Hu Y, Garcia FU, Rhim J. Interleukin 10 blocks matrix metalloproteinase-2 and membrane type 1-matrix metalloproteinase synthesis in primary human prostate tumor lines. 2003. *Clin Cancer Res.* 9(3):1191-9.

Stegbauer J, Chen D, Herrera M, Sparks MA, Yang T, Königshausen E, Gurley SB, Coffman TM. Resistance to hypertension mediated by intercalated cells of the collecting duct. 2017. *JCI Insight.* 2(7):e92720.

Stegbauer J, Thatcher SE, Yang G, Bottermann K, Rump LC, Daugherty A, Cassis LA. Mas receptor deficiency augments angiotensin II-induced atherosclerosis and aortic aneurysm ruptures in hypercholesterolemic male mice. 2019. *J Vasc Surg.* 70(5):1658-1668.e1.

Stewart J, Manmathan G, Wilkinson P. Primary prevention of cardiovascular disease: A review of contemporary guidance and literature. 2017. *JRSM Cardiovasc Dis.* 6:2048004016687211.

Strazzullo P, D'Elia L, Kandala NB, Cappuccio FP. Salt intake, stroke, and cardiovascular disease: meta-analysis of prospective studies. 2009. *BMJ.* 339:b4567.

Streppel MT, Arends LR, van 't Veer P, Grobbee DE, Geleijnse JM. Dietary fiber and blood pressure: a meta-analysis of randomized placebo-controlled trials. 2005. *Arch Intern Med.* 165(2):150–156.

Strohm D, Boeing H, LeschikBonnet E, Heseker H, Arens-Azevêdo U, Bechthold A, Knorpp L, Kroke A for the German Nutrition Society (DGE) Salt intake in Germany, health consequences, and resulting recommendations for action. A scientific statement from the German Nutrition Society (DGE). 2016. *Ernahrungs Umschau* 63(03): 62–70

Szekanecz Z, Shah MR, Pearce WH, Koch AE. Human atherosclerotic abdominal aortic aneurysms produce interleukin (IL)-6 and interferon-gamma but not IL-2 and IL-4: the possible role for IL-6 and interferon-gamma in vascular inflammation. 1994. *Agents Actions.* 42(3-4):159-62.

## T

Tajima M, Wakita D, Satoh T, Kitamura H, Nishimura T. IL-17/IFN- $\gamma$  double producing CD8<sup>+</sup> T (Tc17/IFN- $\gamma$ ) cells: a novel cytotoxic T-cell subset converted from Tc17 cells by IL-12. 2011. *Int Immunol.* 23(12):751-9.

Taleb S, Tedgui A, Mallat Z. IL-17 and Th17 cells in atherosclerosis: subtle and contextual roles. 2015. *Arterioscler Thromb Vasc Biol.* 35(2):258-64.

Temme S, Grapentin C, Quast C, Jacoby C, Grandoch M, Ding Z, Owenier C, Mayenfels F, Fischer JW, Schubert R, Schrader J, Flögel U. Noninvasive Imaging of Early Venous Thrombosis by <sup>19</sup>F Magnetic Resonance Imaging With Targeted Perfluorocarbon Nanoemulsions. 2015. *Circulation.* 131(16):1405-14.

Téo FH, de Oliveira RTD, Villarejos L, Mamoni RL, Altemani A, Menezes FH, Blotta MHSL. Characterization of CD4<sup>+</sup> T Cell Subsets in Patients with Abdominal Aortic Aneurysms. 2018. *Mediators Inflamm.* 2018:6967310.

Thaulow E, Erikssen J, Sandvik L, Erikssen G, Jorgensen L, Cohn PF. Initial clinical presentation of cardiac disease in asymptomatic men with silent myocardial ischemia and

angiographically documented coronary artery disease (the Oslo Ischemia Study). 1993. *Am J Cardiol.* 72(9):629-33

Threapleton DE, Greenwood DC, Evans CE, Cleghorn CL, Nykjaer C, Woodhead C, Cade JE, Gale CP, Burley VJ. Dietary fibre intake and risk of cardiovascular disease: systematic review and meta-analysis. 2013. Version 2. *BMJ.* 347:f6879.

Topping DL, Clifton PM. Short-chain fatty acids and human colonic function: roles of resistant starch and nonstarch polysaccharides. 2001, *Physiol Rev.* 81(3):1031–1064.

Touyz RM. Molecular and cellular mechanisms in vascular injury in hypertension: role of angiotensin II. 2005. *Curr Opin Nephrol Hypertens.* 14(2):125-31.

Tsamis A, Krawiec JT, Vorp DA. Elastin and collagen fibre microstructure of the human aorta in ageing and disease: a review. 2013. *J R Soc Interface.*10(83):20121004.

Tse K, Tse H, Sidney J, Sette A, Ley K. T cells in atherosclerosis. 2013. *Int Immunol.* 25(11):615-22.

## **U**

Underhill DM, Bassetti M, Rudensky A, Aderem A. Dynamic interactions of macrophages with T cells during antigen presentation. 1999. *J Exp Med.* 190(12):1909-14.

## **V**

van Beek SC, Conijn AP, Koelemay MJ, Balm R. Editor's Choice - Endovascular aneurysm repair versus open repair for patients with a ruptured abdominal aortic aneurysm: a systematic review and meta-analysis of short-term survival. 2014. *Eur J Vasc Endovasc Surg.* 47(6):593–602.

Vinolo MA, Rodrigues HG, Nachbar RT, Curi R. Regulation of inflammation by short chain fatty acids. 2011. *Nutrients.* 3(10):858–876.

## **W**

Wahl SM. Transforming growth factor beta: the good, the bad, and the ugly. 1994. *J Exp Med.* 180(5):1587-90.

Waldecker M, Kautenburger T, Daumann H, Busch C, Schrenk D. Inhibition of histone-deacetylase activity by short-chain fatty acids and some polyphenol metabolites formed in the colon. 2008. *J Nutr Biochem*. 19(9):587-93.

Wallace ML, Ricco LA, Barrett B. Screening Strategies for Cardiovascular Disease in Asymptomatic Adults. 2014. *Prim Care*. 41(2): 371–397.

Wang Y, Krishna S, Walker PJ, Norman P, Golledge J. Transforming growth factor- $\beta$  and abdominal aortic aneurysms. 2013. *Cardiovasc Pathol*. 22(2):126-32.

Wei Y, Lu C, Chen J, Cui G, Wang L, Yu T, Yang Y, Wu W, Ding Y, Li L, Uede T, Chen Z, Diao H. High salt diet stimulates gut Th17 response and exacerbates TNBS-induced colitis in mice. 2017. *Oncotarget*. 8(1):70-82.

Weir MR, Dzau VJ. The renin-angiotensin-aldosterone system: a specific target for hypertension management. 1999. *Am J Hypertens*. 12(12 Pt 3):205S-213S.

Weiss D, Sorescu D, Taylor WR. Angiotensin II and atherosclerosis. 2001. *Am J Cardiol*. 87(8A):25C–32C.

Weissmann G, Smolen JE, Korchak HM. Release of inflammatory mediators from stimulated neutrophils. 1980. *N Engl J Med*. 303(1):27–34.

Wenzel UO, Bode M, Kurts C, and Ehmke H. Salt, inflammation, IL-17 and hypertension. *Br J Pharmacol*. 2019.

WHO: Salt reduction: <https://www.who.int/news-room/fact-sheets/detail/salt-reduction>

Wilck N, Matus MG, Kearney SM, Olesen SW, Forslund K, Bartolomeus H, Haase S, Mähler A, Balogh A, Markó L, Vvedenskaya O, Kleiner FH, Tsvetkov D, Klug L, Costea PI, Sunagawa S, Maier L, Rakova N, Schatz V, Neubert P, Frätzer C, Krannich A, Gollasch M, Grohme DA, Côte-Real BF, Gerlach RG, Basic M, Typas A, Wu C, Titze JM, Jantsch J, Boschmann M, Dechend R, Kleinewietfeld M, Kempa S, Bork P, Linker RA, Alm EJ, Müller DN. Salt-responsive gut commensal modulates TH17 axis and disease. 2017. *Nature*. 551(7682):585-589.

Williams CM, Lovegrove JA, Griffin BA. Dietary patterns and cardiovascular disease. 2013. *Proc Nutr Soc*. 72(4):407-11.

## X

Xie JJ, Wang J, Tang TT, Chen J, Gao XL, Yuan J, Zhou ZH, Liao MY, Yao R, Yu X, Wang D, Cheng Y, Liao YH, Cheng X. 2010. The Th17/Treg functional imbalance during atherogenesis in ApoE(-/-) mice. *Cytokine*. 49(2):185-93.

## Y

Yang G, Istas G, Hoges S, Yakoub M, Hendgen-Cotta U, Rassaf T, Rodriguez-Mateos A, Hering L, Grandoch M, Mergia E, Rump LC, Stegbauer J. Angiotensin-(1-7)-induced mas receptor activation attenuates atherosclerosis through a nitric oxide-dependent mechanism in apolipoproteine-ko mice. 2018. *Pflugers Arch*. 470:661-667.

Yang X, Yao G, Chen W, Tang X, Feng X, Sun L. Exacerbation of lupus nephritis by high sodium chloride related to activation of SGK1 pathway. 2015. *Int Immunopharmacol*. 29(2):568-573.

Yu Q, Horak K, Larson DF. Role of T lymphocytes in hypertension-induced cardiac extracellular matrix remodeling. 2006. *Hypertension*. 48(1):98-104.

## Z

Zeng H, Horie K, Madisen L, et al. An inducible and reversible mouse genetic rescue system. 2008. *PLoS Genet*. 4(5):e1000069.

Zhang MZ, Yao B, Wang Y, et al. Inhibition of cyclooxygenase-2 in hematopoietic cells results in salt-sensitive hypertension. 2015. *J Clin Invest*. 125(11):4281–4294.

Zhang WC, Zheng XJ, Du LJ, Sun JY, Shen ZX, Shi C, Sun S, Zhang Z, Chen XQ, Qin M, Liu X, Tao J, Jia L, Fan HY, Zhou B, Yu Y, Ying H, Hui L, Liu X, Yi X, Liu X, Zhang L, Duan SZ. High salt primes a specific activation state of macrophages, M(Na). 2015. *Cell Res*. 25(8):893-910.

Zhou HF, Yan H, Cannon JL, Springer LE, Green JM, Pham CT. CD43-mediated IFN- $\gamma$  production by CD8<sup>+</sup> T cells promotes abdominal aortic aneurysm in mice. *J Immunol*. 2013;190(10):5078–5085.

Zhou X, Nicoletti A, Elhage R, Hansson GK. Transfer of CD4(+) T cells aggravates atherosclerosis in immunodeficient apolipoprotein E knockout mice. 2000. *Circulation*.;102(24):2919-22.

**Annex: One part of my doctoral thesis is published in the following paper:**

Bartolomaeus H, Balogh A, **Yakoub M**, Homann S, Markó L, Höges S, Tsvetkov D, Krannich A, Wundersitz S, Avery EG, Haase N, Kräker K, Hering L, Maase M, Kusche-Vihrog K, Grandoch M, Fielitz J, Kempa S, Gollasch M, Zhumadilov Z, Kozhakhmetov S, Kushugulova A, Eckardt KU, Dechend R, Rump LC, Forslund SK, Müller DN, Stegbauer J, Wilck N. Short-Chain Fatty Acid Propionate Protects From Hypertensive Cardiovascular Damage. *Circulation*. 2019 Mar 12;139(11):1407-1421. doi: 10.1161/CIRCULATIONAHA.118.036652. PMID: 30586752; PMCID: PMC6416008.

My contribution in this paper is performing the experiments done in ApoE<sup>-/-</sup> mice and contributing to writing the manuscript.

Similarities between the thesis and the mentioned paper are as the following:

- Figure 14 in the thesis is similar to figure 2B in the paper.
- Figure 15 in the thesis is similar to supplemental figure S1 F in the paper.
- Table 1 in the thesis is similar to supplemental table 1 in the paper.
- Figure 16 in the thesis is similar to figure 3E in the paper.
- Figure 17 in the thesis is similar to figure 2F in the paper.
- Part of figure 18 in the thesis is similar to figure 3D in the paper.
- Part of figure 19 in the thesis is similar to figure 3C in the paper.
- Parts of figure 20 in the thesis is similar to figure 3A and 3B in the paper.
- Parts of figure 21 in the thesis is similar to figure 1C in the paper.
- Parts of figure 22 in the thesis is similar to figure 1D in the paper.
- Part of figure 24 in the thesis is similar to figure 3H in the paper.
- Figure 26 in the thesis is similar to figure S6 A in the paper.
- Figure 27 in the thesis is similar to figure S6 C in the paper.

## 8 Acknowledgment

First and foremost, I would like to show my full gratitude and appreciation to PD Dr **Johannes Stegbauer**, who has been always supportive through all the steps of my doctoral research. I have learned a lot from him. Despite his huge responsibilities, he was never bothered by me asking for advice at any time. He encouraged me to learn many techniques, attend conferences and courses. Without his guidance, nothing could have been accomplished.

IRTG 1902 has been a great opportunity for my profession by offering an international exchange phase as well as several training courses and lectures. I would like to sincerely thank Prof Dr **Axel Gödecke** for leading IRTG 1902 and for his support for me to attend overseas conferences. I would like to express my special thanks to Dr **Sandra Berger**. Her door was always open for me. She always helped and supported me with any problem I faced during my doctoral studies.

My profound gratitude goes to Ms **Christina Schwandt**, Ms **Blanka Duvnjak**, and Ms **Nicola Kuhr** for their outstanding technical support. I am extremely grateful to all my colleagues in the laboratory, especially, Dr **Lydia Hering**, Dr **Guang Yang**, Mr **Masudur Rahman**, Dr **Sacha Höges**, Mr **Doron Argov**, Mr **Tobias Hofebauer**, and Ms **Denada Arifaj**. I had a great time with them.

I would like to extend my thanks to Dr **Sebastian Temme** and everyone in his team for the MRI experiments. He was always patient and welcoming whenever I have a question.

My exchange phase in the USA was a great experience. I appreciate the support of Dr **Morgan Salmon**, Prof Dr **Gorav Ailawadi**, Dr **Julian Dahl**, and Dr **Eric Scott**.

Finally, I would like to thank my mentor Prof Dr **Jürgen Scheller** and Prof Dr **Lars Christian Rump** for their counselling.